University of Strathclyde

Strathclyde Institute of Pharmacy & Biomedical Sciences

Peroral delivery of paclitaxel aided by biodegradable nanoparticles: *in vitro* and *in vivo* evaluation

by

Vivekanand Bhardwaj

A thesis presented in fulfilment of the requirements for the degree of Doctor of Philosophy

2010

Copyright statement

Acknowledgment

Table of Contents

Abstract

Paclitaxel is an anticancer drug approved for treatment of a wide range of cancers. Due to its low solubility and poor permeability across the gastrointestinal barrier it is administered in an injectable micellar formulation (Taxol®). Cremophor EL, which is an excipient in this marketed formulation, can cause hypersensitivity reactions and requires premedication of patients. The study was envisaged to prepare a non-toxic stable dosage form for the drug that could be orally administered to improve patient compliance. The biodegradable biocompatible polymer PLGA was cast into nanospheres that could physically entrap paclitaxel and deliver it preferentially to cancerous tissues. A cationic surfactant was used as stabiliser to prepare positively charged nanoparticles by employing the process of emulsification-solvent diffusion-evaporation.

The prepared formulation was characterized using a gamut of techniques and a freeze-dried product was developed. It was subjected to *in vitro* cell culture studies to establish the safety of the delivery system and efficacy of paclitaxel. Since the drug is a substrate of efflux pumps that contribute to drug resistance, studies were carried out to explore if the formulation can circumvent these mechanisms.

The product was used to assess the pre-clinical efficacy in three cancer models in rodents whereby it was established that nanoparticles not only enable the oral delivery of paclitaxel, but also increase its efficacy. The uptake of the orally administered nanoparticles and the disposition of the drug was shown by a tissue distribution study carried out using radiolabeled drug. The developed formulation presents a strong case of improving drug delivery using polymeric nanoparticles.

List of abbreviations

AFM	atomic force microscopy
ANOVA	analysis of variance
Apx	Appendix
ATCC	American type cell culture
BCL-2	B cell lymphoma
BCS	biopharmaceutics classification system
Calcein-AM	calcein acetoxy-methyl ester
CCNSC	Cancer Chemotherapy National Service Centre
CDER	Centre for Drug Evaluation and Research
CMC	critical micellar concentration
CSF	cerebrospinal fluid
DEHP	di(2-ethylhexyl)phthalate
DLS	dynamic light scattering
DMAB	didodecyldimethylammonium bromide
DMBA	7,12-dimethyl benz[a]anthracene
DMEM	Dulbecco's modified eagle medium
DMSO	dimethylsulphoxide
DNA	deoxyribose nucleic acid
EDTA	ethylene diamine tetra acetate
EPR	enhanced permeation and retention
FBS	foetal bovine serum
FS	full saturation
GIT	gastro intestinal tract
GRAS	generally recognized as safe
HBSS	Hank's buffered salt solution
HPLC	high pressure liquid chromatography
i.p.	intraperitoneal
i.v.	Intravenous
LDH	lactate dehydrogenase
MDR	multiple drug resistance/resistant

MTT	2-(4,5-dimethylthiazol-2-yl)-3,5-diphenyl-2H-tetrazol-3-ium bromide
NAD^+	oxidized nicotinamide adenine dinucleotide
NADH	reduced nicotinamide adenine dinucleotide
NCI	National Cancer Institute
NEAA	non-essential amino acids
NP	Nanoparticle
OD	Optical density
PCS	photon correlation spectroscopy
PDI	polydispersity index
PGA	Polyglycolide
Pgp	P-glycoprotein
PLA	Polylactide
PLGA	poly(lactide-co-glycolide)
PVA	polyvinyl alcohol
PVC	polyvinyl chloride
RES	reticulo-endothelial system
rpm	rotations per minute
RPMI	Roswell Park Memorial Institute
sd	standard deviation
SD	Sprague Dawley
sem	standard error of mean
SS	sub-saturation
TEER	trans epithelial electrical resistance
TPGS	d-alpha-tocopheryl polyethylene glycol 1000 succinate
TSG	tumour suppressor genes
UKCCCR	UK Co-ordinating Committee on Cancer Research
USDA	United States Department of Agriculture
USFDA	United States Food and Drug Administration
UV	Ultraviolet

List of Symbols

$	Dollar
%	Percentage
μ	Micro
μg	Microgram
μl	Microlitre
μM	Micromolar
^{o}C	degrees celsius
conc	concentration
D	coefficient of diffusion
dl	Decilitre
g	acceleration due to earth's gravity
h	hour(s)
K_B	Boltzmann constant
kcps	kilo counts per second
kJ	Kilojoule(s)
M	Molar
mBar	milliBar (pressure)
mg/m^2	milligrams per square metre
min	minute(s)
ml	Millilitre(s)
mm	Millimetre(s)
m/s	Metre(s) per second
mV	Millivolt(s)
ng	Nanogram(s)
nm	Nanometre(s)
nm.s^{-1}	Nanometre(s) per second
Ω/cm^2	Ohms per square centimetre
P_{appAB}	apparent intestinal permeability from apical to basolateral side
P_{appBA}	apparent intestinal permeability from basolateral to apical side
US$	United States dollars
v/v	volume by volume
w/v	weight by volume
w/w	weight by weight
ζ	coefficient of friction

List of Tables

List of Figures

Figures in appendices

1 Introduction

Cancer is a group of diseases in which cells exhibit an uncontrolled growth in the body. It is the leading cause of death in the modern world and the frequency and distribution of incidence is rising above the demarcations of age, sex, geographical and political boundaries and the economic status of the affected population. Cancers additionally exhibit invasion and metastasis and the tumours promote angiogenesis. Cancers are caused by aberrations in that part of the genetic code of cells that programs their differentiation, multiplication and life span. These abnormalities may arise under the influence of ionising radiation, certain chemicals, and even some viruses. All types of cells and tissues can develop cancers and different cancers grow at varying rates, depending on the type of cells affected and show different rates of metastasis and relapse.

The discovery of the cytotoxic effects of chemical warfare agent nitrogen mustard by Louis S. Goodman and Alfred Gilman paved the way for modern chemotherapy. The ongoing vigorous research in this field has succeeded in coming up with some very effective drugs. The current cancer treatment strategies revolve around surgical removal of the affected tissue, destroying the tumour cells by radiation and anticancer drug therapy. The anticancer drug therapy includes biological therapies like monoclonal antibodies, cancer vaccines, anti-angiogenic compounds, cancer growth factor (e.g. tyrosine kinases) inhibitors, interferons, interleukins, gene therapy, and hormone therapy. Although also used in conjunction, chemotherapy is the only option when the cancer has metastasized or surgery and radiation therapy are not possible to remove the cancer from the body. The aim is to wipe out the cancer because even a few neoplastic cells surviving can multiply and result in relapse.

The physiology of solid tumours is different from the normal tissues in 4 major ways: angiogenesis, leaky vasculature, poor lymphatic drainage and microenvironment in the interior regions. All these have been explored for targeting anticancer drugs to the tumours (Brown and Giaccia 1998).

Anticancer agents kill cells by inhibiting the cell replication process (mitosis) of rapidly multiplying cells. Due to their very nature, these drugs kill even normal cells and their effectiveness usually relies on the markedly higher activity in the cancer cells vis-à-vis the non-cancerous ones. As an implying caveat, slowly multiplying cancers do not respond to chemotherapy as much as the fast multiplying ones. On the other hand, the most significant side effects of anticancer drugs are seen in the rapidly multiplying normal cells like the epithelial cells, hair follicles and bone-marrow cells. The primary objective in drug discovery today is to design drugs that would kill only the cancerous cells. Scientists have attained success in this quest with drugs like imatinib and trastuzumab by targeting the therapy. Imatinib is directed against a particular tyrosine kinase exclusively limited to certain cancers like gastrointestinal stromal tumours and chronic myelogenous leukemia. This strain arises out of a faulty chromosome that gives rise to such malignancies. Trastuzumab is a monoclonal antibody based product that helps in regulating the HER2 receptor mediated uncontrolled growth in breast cancers. There are various other drugs in development based on gene targeting. However, with the currently available spectrum of drugs wherein most agents do not have this specificity, it is a challenge for the pharmaceutical scientist to devise mechanisms to deliver the drug directly and selectively to the target cells.

Another big hurdle in cancer treatment is the access of systemically circulating drugs to the cancerous cells. Solid tumours pose a significant

challenge for drug delivery of anticancer drugs because of the differential blood supply in various parts of the tumour. The inner parts of the tumours can have seriously impaired circulation and the peripheries generally have a very rich blood supply due to stimulated angiogenesis. Thus it is very difficult to transport the anticancer drug to the core of a tumour. Further, cells can recruit and over-express a class of transporters that flush the drug out of the cells (efflux pumps). This results in resistance towards the substrate and often cross-resistance to other drugs is also produced. Thus, an ideal anticancer treatment should kill only the cancerous cells, make the drug reach the target areas and allow the drug to act on the neoplastic cells for a sufficiently long period of time.

1.1 Paclitaxel

During the early attempts in finding treatment for cancer, in addition to the chemical warfare agents and antimetabolites, both of which were of synthetic origin, there was a parallel interest in mitotic poisons from plant origin, primarily inspired by colchicine as early as 1930s. Together with podophyllin and its main constituent podophyllotoxin, colchicine was screened for anticancer activity, but was dropped due to its severe toxicity. The United States National Cancer Institute (NCI) initiated a systematic study to assess biological activity of plants in early 1950s through its Laboratory of Chemical Pharmacology. The NCI had established the Cancer Chemotherapy National Service Centre (CCNSC) in 1955 for screening new compounds for anticancer activity, including botanical samples. Meanwhile, vinblastine was isolated by University of Ontario in 1957 and vincristine by Eli Lilly in 1961 from *Vinca rosea*. These two compounds went on to be clinically approved for chemotherapy. Notably the University of Ontario group expressed the view while reporting their results in 1958, that discovery of their compounds was

accidental since the plant was originally studied for antidiabetic use. In the background of chance discovery of *Vinca* alkaloids, it was decided that the screening was to be exhaustive, and not to be restricted to those plants that are claimed in folklore or traditional medicine to be possessing medicinal properties—anticancer or otherwise. In 1960, the plant screening program was launched by NCI with help from the United States Department of Agriculture (USDA) to screen at least 1000 species annually. From 1960 to its end in 1981, the plant screening program evaluated an estimated 15000 species and around 114,000 plant extracts. Paclitaxel was the only compound from the entire program that went on to receive clinical approval. Paclitaxel is one of the most promising molecules for the treatment of various solid tumours and its use is steadily increasing.

Paclitaxel was originally obtained from bark of the Western yew tree (*Taxus brevifolia).* As per the NCI screening protocol, the activity of stembark extract was discovered in an *in vitro* screen in KB cell culture on 22nd of May 1964 at Microbiological Associates in Bethesda, Maryland, USA. The *in vivo* screening was carried out on three types of tumours/cancers transplanted in laboratory mice. The extracts were inactive in Dunning leukaemia model and the P1798 lymphosarcoma, but showed activity at one out of two doses in L1210 model (a lymphoid leukaemia) (Goodman and Walsh 2001). The conflicting results prompted rescreening in KB culture, which yielded reproducible activity. The extract was then found active in P-388 (leukaemia), W256 (carcinosarcoma) and P1434 (leukaemia) model that has been used in the discovery of the *Vinca* alkaloids. By the end of 1965, chemists potentiated the activity 1000 times in a chloroform extract. Because of the complicated ring system, the structure elucidation itself took several years (Wani et al. 1971). The structure of paclitaxel was discovered to be a complex diterpine

taxane (Figure 1.1) and its chemical synthesis is not economically viable. Although it was discovered by government agencies, the development was carried out by Bristol Myers Squibb following an open proposal by NCI, partly due to the concerns regarding ecological implications of harvesting the bark of yew tree (the yield was 0.004% w/w of stembark, and the tree was destroyed in the process). Today almost all the paclitaxel is produced using plant tissue culture. The company marketed it under the trade name Taxol® as a micellar formulation for intravenous administration.
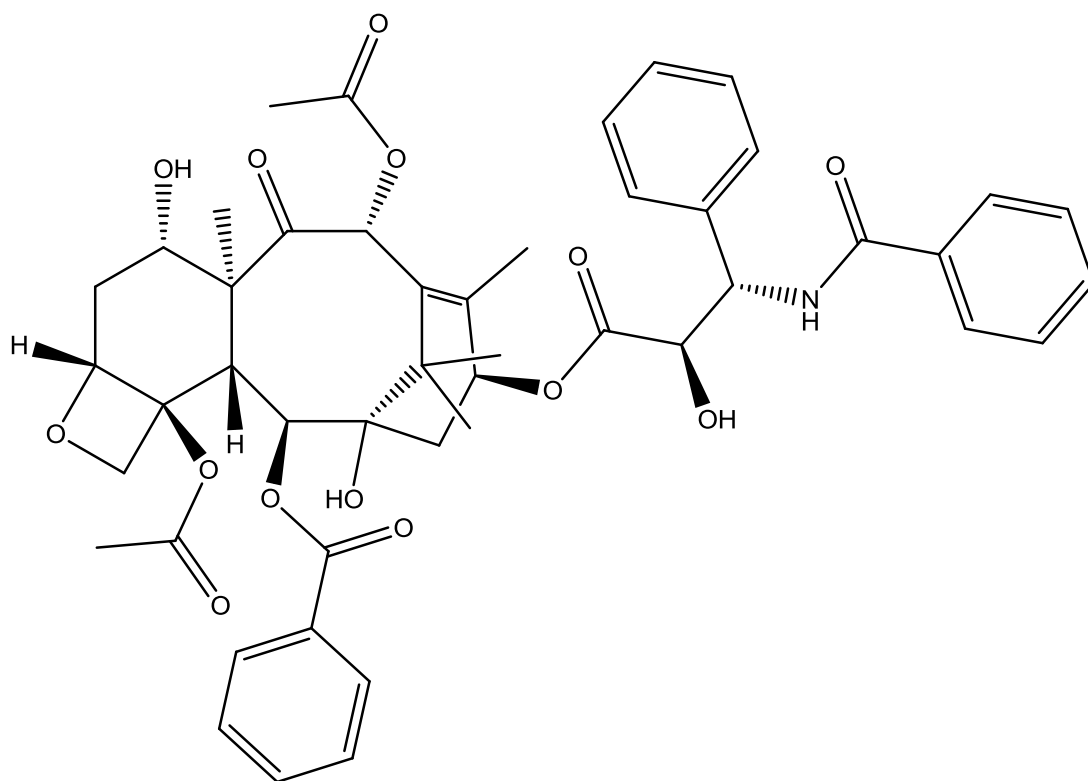
Figure 1.1: Chemical structure of paclitaxel

1.1.1 Mechanism of action

Interestingly, paclitaxel was discovered to act by a unique mechanism of action. In a study with human HeLa and mouse fibroblast cell replication, it blocked cells in the G2 and M phase of the cell cycle and stabilized cytoplasmic microtubules (Schiff and Horwitz 1980). Microtubules are cytoskeletal structures and are involved in various cellular functions such as

spindle formation during cell division, movement, phagocytosis, defining the shape of cells and sensory transduction (Rowinsky et al. 1990). They are 25nm in diameter and the length can vary from 0.2-25 μm. Paclitaxel promotes assembly of microtubules, stabilizes them against depolymerization and inhibits cell replication (Schiff et al. 1979; Kumar 1981). It binds to the β subunit of the polymerized tubulin in microtubules, but does not bind to tubulin heterodimers with high affinity. This binding is reversible and stoichiometric, but the saturation of paclitaxel binding occurs at 0.78 mol paclitaxel/mol of tubulin (Parness and Horwitz 1981). This fact has profound implications in understanding the activity and biodistribution of paclitaxel in the body.

The clinical success of paclitaxel is partly related to its other mechanism of action in which it binds to the Bcl-2 (name derived from B cell lymphoma) protein which acts like an anti-apoptotic gene. This binding prevents the anti-apoptotic action of Bcl-2 and thus induces apoptosis (programmed cell death) in the treated cells (Haldar et al. 1995). This observation was corroborated by the fact that paclitaxel resistant cells had exhibited down regulation of Bcl-2 (Haldar et al. 1996).

For a drug to have more than one mechanisms of action is advantageous in chemotherapy because cells are known to develop resistance. This is the very basis of routinely using multi-drug regimen in cancer treatment, and probably explains the clinical efficacy of paclitaxel. Though Horwitz and co-workers had reported that the binding of paclitaxel to the monomers and dimers was a not a high-affinity phenomenon, another recent report claims that paclitaxel, if crystallized within the cells could sequester free tubulin available in cytoplasm and induce a "depleted infrastructure linked cytotoxicity" (Foss et al. 2008). Paclitaxel has very low water solubility and

the doses used for chemotherapy are rather high. In addition to killing the cancer cells, such high concentrations can potentially precipitate the drug within the blood cells resulting in progressive construction of asters and bundles.

1.1.2 Approved indications

Paclitaxel was approved in December 1992 for metastatic ovarian carcinoma and in April 1994, for breast carcinoma after failure of first line chemotherapy and relapse cases (www.fda.gov). In June 1998, the United States Food and Drug Administration (USFDA) approved paclitaxel for use in combination with cisplatin, for the first-line treatment of non-small cell lung cancer in patients who are not candidates for potentially curative surgery and/or radiation therapy. Additionally, paclitaxel was approved for use in stents to prevent restenosis. The approved indications for paclitaxel are summarized in Table 1.1.

Table 1.1: List of approvals of paclitaxel indications

Trade Name	Approved Use	Manufacturer/ Distributor	Approval Date
Taxol®	Treatment of patients with metastatic carcinoma of the ovary after failure of first-line or subsequent chemotherapy.	Bristol-Myers Squibb	29.12.1992
Taxol®	Treatment of breast cancer after failure of combination chemotherapy for metastatic disease or relapse within 6 months of adjuvant chemotherapy. Prior therapy should have included an anthracycline unless clinically contraindicated.	Bristol-Myers Squibb	13.04.1994
Taxol®	New dosing regimen for patients who have failed initial or subsequent chemotherapy for metastatic carcinoma of the ovary	Bristol-Myers Squibb	22.06.1994
Taxol®	Second line therapy for AIDS related Kaposi's sarcoma.	Bristol-Myers Squibb	04.08.1997

Trade Name	Approved Use	Manufacturer/ Distributor	Approval Date
Paxene™	Treatment of advanced AIDS-related Kaposi's sarcoma after failure of first line or subsequent systemic chemotherapy	Baker Norton Pharmaceuticals, Inc	24.12.1997
Taxol®	First-line therapy for the treatment of advanced carcinoma of the ovary in combination with cisplatin.	Bristol-Myers Squibb	09.04.1998
Taxol®	For use in combination with cisplatin, for the first-line treatment of non-small cell lung cancer in patients who are not candidates for potentially curative surgery and/or radiation therapy.	Bristol-Myers Squibb	30.06.1998
Taxol®	For the adjuvant treatment of node-positive breast cancer administered sequentially to standard doxorubicin-containing combination therapy.	Bristol-Myers Squibb	25.10.1999
Taxol®	First line ovarian cancer with 3 hour infusion.	Bristol-Myers Squibb	20.06.2000
Taxus® Express®	For improving luminal diameter for the treatment of de novo lesions < 28 mm in length in native coronary arteries > 2.5 to < 3.75 mm in diameter.	Boston Scientific Corporation	04.03.2004
Abraxane®	For the treatment of breast cancer after failure of combination chemotherapy for metastatic disease or relapse within 6 months of adjuvant chemotherapy. Prior therapy should have included an anthracycline unless clinically contraindicated	AM Bioscience	07.01.2005
Source: USFDA, Centre for Drug Evaluation and Research (CDER)			

1.1.3 Taxol®

The first marketed formulation of paclitaxel was administered emulsified in cremophor EL (a 50:50 mixture of polyoxyethylated castor oil and alcohol) as an intravenous infusion over 3-24 hours. Each ml of the marketed Taxol® contains 6mg paclitaxel, 527mg cremophor EL, 49.7% v/v ethanol and citric acid anhydrous qs. Chemically, cremophor EL is macrogol glycerol ricinoleate (polyoxyl castor oil). In addition to Taxol®, it is used in three other

marketed formulations: (a) cyclosporine A injection (Sandimmune®), (b) teniposide (Vumon®) and (c) Valrubicin (Valstar®).

The cremophor EL, however, can cause anaphylactoid reactions and also produces vasodilation, laboured breathing, lethargy, hypotension, hyperlipidaemia, abnormal lipoprotein patterns, aggregation of erythrocytes,and peripheral neuropathy (Dye and Watkins 1980; Strachan 1981; Weiss et al. 1990; Gelderblom et al. 2001). As a result, Taxol® therapy has to be often preceded by administration of premedication, especially corticosteroids like dexamethasone and anti-inflammatory agents like antihistamines (clemastine or ranitidine). Cremophor EL has also been implicated in leaching of plasticizers like di(2-ethylhexyl)phthalate (DEHP), from the plastic PVC (polyvinyl chloride) tubing used for administration of intravenous fluids (Waugh et al. 1991; Mass et al. 1996). Moreover, the physical stability of paclitaxel in cremophor EL and ethanol system is a concern. Even at room temperature, paclitaxel solutions in the mixture of cremophor EL and ethanol, when diluted with saline or other intravenous fluids, turn milky white indicating precipitation of paclitaxel. Following exposure to aqueous media, the preparations should be used preferably within 3 hours or maximum up to 24 hours (Waugh et al. 1991). This particular aspect of this formulation has not been discussed in detail in literature although it has potential implications on the performance of the formulation as well as the drug.

1.1.4 Pharmacokinetics

Paclitaxel exhibits a two phase clearance following intravenous administration when given with cremophor EL. The first phase ($T_{1/2\alpha}$= 0.27-0.32 hours) represents combined effect of initial rapid distribution to the peripheral compartment and metabolic excretion of the drug. The second

phase ($T_{1/2}\beta$= 1.3-8.6 hours) represents combined effect of slow clearance from the peripheral compartment and metabolic excretion of the drug (Rowinsky et al. 1990). Pharmacokinetic parameters of paclitaxel following 3- and 24-hour infusions of marketed formulation Taxol® at dose levels of 135 and 175 mg/m² in ovarian cancer patients are summarized in Table 1.2 (Source: Taxol® product insert).

Like many other anticancer drugs, paclitaxel is incompletely absorbed following oral administration (Peltier et al. 2006; Khandavilli and Panchagnula 2007) owing majorly to the active efflux in the intestine (Sparreboom et al. 1997). It is a substrate for the P-glycoprotein (Pgp) efflux transporters that flush out the drug from the basolateral side to the lumen of the intestine. These efflux pumps can be inhibited to increase the oral bioavailability of paclitaxel (Varma and Panchagnula 2005).

Table 1.2: Pharmacokinetic parameters of marketed paclitaxel (Taxol®)

Dose	Infusion	n	C_{max}	AUC $_{(0-\infty)}$	$T_{1/2}$	Cl_T
(mg/m²)	Duration (h)	(patients)	(ng/ml)	(ng.h/ml)	(h)	(l/h/m²)
135	24	2	195	6300	52.7	21.7
175	24	4	365	7993	15.7	23.8
135	3	7	2170	7952	13.1	17.7
175	3	5	3650	15007	20.2	12.2
C_{max} = Maximum plasma concentration						
$AUC_{(0-\infty)}$ = Area under the plasma concentration-time curve from time 0 to infinity						
$T_{1/2}$ = Plasma half life						
Cl_T = Total body clearance						
h = hour						

An *in vitro* study done with paclitaxel concentrations ranging from 0.1 to 50 µg/ml, indicated that between 89-98% of drug is bound to human serum proteins, and was not displaced from the protein binding sites by most of the other protein bound drugs (Source: Taxol® product insert). In some clinical trials 95-98% binding has been reported (Wiernik et al. 1987). Another study

estimated 7.6-12.4% unbound drug in plasma. The drug slowly partitions into cerebrospinal fluid (CSF) and after 24 h, CSF levels can reach 10% of the plasma levels (Gelderblom et al. 2003). Also, the drug is extensively bound to the erythrocytes. The drug partitions heavily in the peripheral compartment especially in tissues like liver, spleen, heart, lung and muscle (Lesser et al. 1995).

In vitro studies performed on liver microsomes and tissue slices showed that paclitaxel was metabolized by the cytochrome P450 group of enzymes. The subtype CYP2C8 converts it to the major metabolite 6α-hydroxypaclitaxel; and CYP3A4 converts to minor metabolites, 3'-p-hydroxypaclitaxel and 6α, 3'-p-dihydroxypaclitaxel (Source: Taxol® product insert).

Paclitaxel is primarily excreted via non-renal routes irrespective of duration of infusion. After 1, 6 and 24 hour intravenous infusions of 15-275 mg/m^2 doses of Taxol®, only 1.2-13.6% of the drug was collected in urine. Of a 3 hour radioactivity labelled Taxol® infusion administered at a 225 or 250 mg/m^2 dose, 71% of paclitaxel or its metabolites were excreted in the faeces over 5 days, and 14% were recovered in the urine. Only 5% of the drug was excreted unchanged in the fraction recovered in the faeces, 6α-hydroxypaclitaxel being the primary metabolite (Source: Taxol® product insert).

1.1.5 Problems with delivery of paclitaxel: Poor biopharmaceutics

Till date, paclitaxel is administered only by the parenteral route via slow intravenous injection. The biggest challenges in development of an orally deliverable formulation of paclitaxel are its very low water solubility and poor intestinal permeability.

The molecular weight of the drug is high and it has a large number of hydrogen bond acceptors, which is expected to decrease its drug-likeliness

according to the rule of 5 (Lipinski et al. 1997). Additionally, it is extensively pumped out by the Pgp pump (Roy and Horwitz 1985) in the intestine. Due to these reasons, the drug shows poor bioavailability when administered orally (Choi and Jo 2004; Varma and Panchagnula 2005). The low solubility and permeability of paclitaxel make it a Class IV drug as per the Biopharmaceutic Classification System (BCS) (Amidon et al. 1995).

The physicochemical properties of paclitaxel explain some reasons behind the difficulties in drug delivery. Paclitaxel is obtained as a white crystalline powder, practically insoluble in water. It is highly lipophilic and dissolves in majority of organic solvents. Being non-ionizable, pH modulation does not yield any help in solubilising the compound. The compound degrades in acidic as well as basic media, exhibiting maximum stability between pH values 4 and 5 (Jiaher and Valentino 2009). Its properties are listed in Table 1.3 (Pubchem).

The implications of poor solubility of paclitaxel manifested long before it was considered as a candidate for drug development. An interesting aspect of paclitaxel delivery is the possible role of its poor water solubility in the outcome of various *in vitro* as well as *in vivo* screening tests. One of the major challenges, even after the clinical approvals of paclitaxel is keeping it in solution form with all the help of different solublizers and solvents. As a result, there might have been instances where the absence of efficacy might have been false negatives since the drug was not in solution to be able to act on the target cells.

1.1.6 Drug delivery approaches for paclitaxel

Various means have been tried to achieve the delivery of paclitaxel in the body including co-solvency (Tarr and Yalkowsky 1987), emulsification (Lunberg 1997; Khandavilli and Panchagnula 2007), micellization (Varma

and Panchagnula 2005), liposomes (Crosasso et al. 2000; Treat et al. 2000; Soepenberg et al. 2004), nanoparticles (Kim et al. 2005; Zhang and Feng 2006), cyclodextrins (Alcaro et al. 2002; Hamada et al. 2006) and local delivery approaches like pastes (Winternitz et al. 1996; Zhang et al. 1996; Dordunoo et al. 1997) and implants (Walter et al. 1994; Panchagnula et al. 2006). The majority of these approaches were focussed on removing the need of cremophor EL, and a few were also directed towards attaining oral delivery. Attempts of oral delivery of paclitaxel are discussed in a later section.

Table 1.3: Physicochemical and biopharmaceutical properties of paclitaxel

Property	Value/Description
Melting point	216-217°C.
Molecular weight	853.9
Molecular formula	$C_{47}H_{51}NO_{14}$
LogP	3.5
clogP	4.73
Water solubility	Practically insoluble
Hydrogen bond donors	4
Hydrogen bond acceptors	14
Rotatable bonds	14
P_{appAB} (nm.s^{-1})	1.3
P_{appBA} (nm.s^{-1})	135.0
Efflux ratio	108.0
Topological polar surface area	221
Intestinal absorption	1.5-6%

1.1.7 Commercial background

In early 2005, USFDA approved a nanoparticulate formulation of paclitaxel (Abraxane®) composed of a dispersion of micronized drug coated with albumin in aqueous medium. Another formulation Nanoxel™ is marketed in

India and undergoing clinical trials in USA. Although both these formulations do not use cremophor EL, they are approved for intravenous use only and there is no product of paclitaxel that can be administered orally. Today, paclitaxel is a leading drug in the battle against cancer. It constitutes about 22% of all major cancer chemotherapy drugs on the world market and is the only chemotherapeutic agent to have sales over US$ 1 billion, so called "blockbuster molecules". Since the first sale of paclitaxel in 1993, worldwide sales of paclitaxel have escalated to US$ 1.6 billion in 2000 and to US$ 9 billion by 2005. Abraxane®, the nanoparticulate formulation of paclitaxel has received approval by the USFDA in January 2005 for the treatment of breast cancer and its recorded sales of US$ 134 million in its first eleven months on the market. However, the market response is below expectation, primarily due to the fact that there are no significant benefits apparent over Taxol®. Furthermore, newer applications of paclitaxel are being discovered at a rapid pace making it a more versatile therapeutic agent, where oral delivery of paclitaxel is going to be of immense importance.

One of the factors that have limited the use of paclitaxel is the lack of effective formulations. Paclitaxel is also used as an anti-proliferative agent for the prevention of restenosis (recurrent narrowing) of coronary stents; locally delivered to the wall of the coronary artery, a paclitaxel coating limits the growth of neointima (scar tissue) within stents (USFDA).

The oral administration of paclitaxel can significantly reduce the hospital expenditure associated with chemotherapy. An oral formulation shall facilitate other and new uses of paclitaxel like in multiple sclerosis (Cao et al. 2000), Alzheimer's disease (Holzgrabe 2005), rheumatoid arthritis (Brahn et al. 1994; Liggins et al. 2004), polycystic kidney syndrome (Woo et al. 1997), psoriasis (Ehrlich et al. 2004) and Parkinson's disease (www.angiotech.com,

(Zhang et al. 2005; Jiang et al. 2006)).

There are big incentives for development of a formulation that can be administered by alternate routes. The following section reviews the reasons, incentives and progress of exploring oral administration.

1.2   Paclitaxel: a case for oral chemotherapy

Paclitaxel acts on cancers via more than one mechanism and among the other chemotherapeutic agents has comparatively fewer side effects of its own. For the intravenous chemotherapy with paclitaxel that can last from 3-24 hours, the patient is required to be hospitalized. In addition to causing physical and emotional distress, this increases the costs involved in treatment. Besides, the conventional formulation utilizes the toxic excipient in significantly higher concentration compared to other marketed formulations. Even at such high level, cremophor EL is hardly able to keep the diluted paclitaxel in solution for 24 hours. Though two new formulations of paclitaxel have entered the market, both of them are for intravenous administration. Considering the clinical efficacy of paclitaxel, it is a very attractive and deserving candidate for a pursuit to achieve oral deliverability.

1.2.1   Advantages of oral drug delivery

Depending on the affected tissue, the drugs can be applied or administered to the body from various routes and are chiefly classified into three classes-peroral, parenteral and topical. The topical route is often used to localize the therapy and minimize body burden of the drug and directly target the affected area or tissue. Parenteral route is preferred and restricted for those applications in which the drug is required urgently or when it is either unstable in the gastrointestinal tract (GIT) or is not absorbed through it.

Despite the better understanding and success of drug absorption from other routes, oral route retains the focus and preference for drug delivery. The GIT is the nature's intended mode of uptake of foreign matter (food) and is anatomically and physiologically adapted for it. Therapeutic interventions are   routinely   applied   from   alternate   routes,   but   the   advantage   is

16

physiologically heavily inclined in favour of oral drug delivery.

Advantages of oral drug delivery in comparison to parenteral can be summarized as

(a) Convenient

(b) Higher patient compliance

(c) Can be administered without trained supervision

(d) No requirement of sterilization of dosage form

(e) Cheaper

(f) Longer shelf-life of product

(g) Solids as well as liquids can be administered

(h) The release of the drug can be more easily delayed or controlled.

(i) Best approach for local treatment of diseases of the GIT.

1.2.2 Oral chemotherapy

Most of the anticancer drugs show low oral absorption due to poor aqueous solubility, poor permeability across the gastrointestinal membrane, and chemical instability in the GIT due to pH and/or enzymes.

The pre-clinical success of a lot of drug candidates is not matched in human body due to the factors affecting absorption, distribution, metabolism and excretion. The use of drug delivery systems addresses one or more of the following questions related to the drug (Allen and Cullis 2004)

(a) physicochemical or physiological instability

(b) poor aqueous solubility or permeability

(c) insufficient drug concentration in target tissue

(d) high volume of distribution

(e) non-target organ toxicity

(f) rapid clearance from body

Diverse formulation strategies can be employed to tackle these challenges,

depending on the design of delivery system, chemical properties of the carrier, and altered conditions in cancerous tissue.

Almost 80% of the approved indications of anticancer drugs are for formulations that are administered by the non-oral routes (Table 1.4) and one of the objectives of developing novel drug delivery systems is to be able to administer them orally.

Table 1.4: Dosage forms for USFDA approved anticancer drugs in 2007

Dosage form	No. of approved indications	
	Non-oral	oral
Aerosol	1	
Capsule		13
Gel	2	
Implant	2	
Intramuscular injection	8	
Intrathecal injection	1	
Intravenous injection	140	
Intravesical instillation	1	
Powder for injection	1	
Subcutaneous injection	9	
Tablet		28
Total	**165**	**41**
(Source: USFDA, CDER, Oncology tools)		

Principally, an anticancer drug is administered at the maximum tolerated dose to attain highest cell kill of cancer cells. This is followed by a drug free interval during which the body can recover from the side effects in the non-target cells. This model is best supported by parenteral delivery of drugs. For this reason, the concept of chemotherapy has been fundamentally built on the concept of parenteral administration. This applies to both operational as

well as financial considerations for oncology establishments (Weingart et al. 2008).

However, many drug therapies today are cytostatic, and require chronic administration of the chemotherapeutic agents. These daily low-dose schedules can have fewer and less severe dose-limiting adverse effects (Carney 1991) that warrant therapy cessation for bone-marrow revival. Oral administration provides a better alternative to parenteral therapy for this model.

Another incentive in USA for development of oral anticancer drugs is their inclusion in part D of the Medicare programme. Drugs administered by the physician (as in a chemotherapy infusion) are covered under part B, whereas an oral self-administered anticancer drug can be covered under part D as a prescription product. This has provided a stimulus to the pharmaceutical industry and it is expected that almost one-fourth of the anticancer drugs under development are for oral use (Weingart et al. 2008).

But it is important that measures are taken to optimize adherence protocols because failure to do so might result in ineffective treatment (Partridge et al. 2002; Patton 2008). When efficacy is not compromised, patients tend to prefer oral over intravenous medication (Liu et al. 1997). However, a lot of chemotherapy regimens involve more than one agent and in such circumstances, patients prefer to have all of them by the same route- either oral or parenteral. Thus in addition to discovery of new drugs that are orally bioavailable, it is important that oral formulations are developed for existing parenterally administered drugs. This would allow more patients to be brought under the cover of oral formulations.

Considering the advantages of oral administration and the incidence of adverse effects associated with parenteral delivery, the healthcare fraternity

is continuously devising strategies to increase oral bioavailability. Drugs are being discovered to possess pleiotropic activities. This would allow exploitation of their full therapeutic potential in high benefit to risk ratio indications also.

1.2.3 Oral delivery of paclitaxel

As mentioned previously, paclitaxel is incompletely absorbed from the GIT. Clinical trials are being carried out to use it orally (Koolen et al. 2009). While cremophor EL causes adverse systemic reactions on intravenous administration, the oral use is expected to limit the side effects to the GIT. However, when paclitaxel was given orally with cremophor EL, the absorption of former was decreased (Malingre et al. 2001; Bardelmeijer et al. 2002). The excipient is itself not absorbed from intestine and because it solubilises paclitaxel, it impedes its absorption.

Since one of the contributors of limited oral bioavailability of paclitaxel is drug efflux, it has been co-administered with known inhibitors like the immunosuppressant drug cyclosporin A (Meerum Terwogt et al. 1999; Malingré et al. 2001). Cyclosporin A and verapamil (another efflux pump inhibitor) have been used with other micellar preparations of paclitaxel in Pluronic® polyethers and poly(acrylic acid) (PAA) (Bromberg 2008). However, due to the inherent immunosuppressive effects of Cyclosporin A and cardiac side effects of verapamil, they are not attractive options. An efflux inhibitor GF120918 increased AUC of oral paclitaxel (as Taxol®) in Female wild-type FVB mice by 6.6 fold (Bardelmeijer et al. 2000). When administered in a vehicle consisting of dimethylisosorbide, Tween® 80, and *dl-α*-tocopheryl acetate at a concentration of 6 mg/ml, co-administration of an efflux inhibitor KR-30031 increased the relative oral bioavailability from 4.6% to 34.4% and the effect of KR-30041 and ketoconazole was additive (Woo et

al. 2003). Vitamin E-TPGS is another compound that has shown improved absorption of oral paclitaxel (Varma and Panchagnula 2005). Paclitaxel has been combined with PEG (polyethylene glycol) to increase its oral bioavailability (Choi and Jo 2004). It acts like a prodrug in this form and is claimed to bypass the Pgp efflux. The prodrug, 7-mPEG 5000-succinyloxymethyloxycarbonyl-paclitaxel provided a 4 fold increase in absorption from 1.6 to 6.3%. The same group has also reported increase in oral bioavailability of paclitaxel and/or the prodrug on co-administration of flavone (Choi et al. 2004a), naringin (Choi and Shin 2005), and pre-treatment of quercetin (Choi et al. 2004b).

Emulsions have been explored for improving oral bioavailability of paclitaxel (Tiwari and Amiji 2006). Increase in AUC has been observed when paclitaxel was incorporated in self-micro-emulsifying drug delivery systems (SMEDDS) (Yang et al. 2004). In another study Taxol® was reported to have a bioavailability of 2%, and a self emulsifying drug delivery system (SEDDS) provided 0.9%. A modification, termed super-saturated self emulsifying drug delivery system (S-SEDDS) that used hydroxypropylmethyl cellulose to stabilise the SEDDS improved the bioavailability to 9.5% while simultaneous use of cyclosporin A raised the value to 23% (Gao et al. 2003).

Incorporation of paclitaxel in lipid nanocapsules improved its oral bioavailability in rats and the AUC was increased by three fold in comparison to Taxol®. In comparison to Taxol®, coadministration of verapamil increased the AUC by 3 fold while lipid nanocapsules also increased the AUC, but the effect was slightly lower than with verapamil (Peltier et al. 2006). Cyclodextrins are also being explored to enable oral delivery of paclitaxel.

The net clinical efficacy of a compound is not only dictated by the desired

action, but also the relative lack of those that are undesirable. For any drug, increase in bioavailability can also increase the side effects since they too are pharmacodynamic manifestations of the drug. This distinction is even more demanding for anticancer drugs since the same fundamental activity is warranted in the target cells and to be avoided in the normal cells. The dose of anticancer drugs is titrated so as to administer the maximum tolerable dose. Any increase or decrease in systemic bioavailability of such a molecule will thus disturb the delicate equilibrium against the health of the patient. This discussion however applies to orally administered drugs. Paclitaxel being delivered only parenterally is already 100% bioavailable.

The focal point of product development studies is converging on means that impart such ability to the delivery system that can attain, even for otherwise poorly bioavailable compounds, sufficient concentrations across the intestinal barrier. The challenges for paclitaxel can be summarized as solubility, permeability and resistance/Pgp efflux. Amongst the various novel drug delivery systems, nanoparticulates have attracted significant interest in this direction. The following section reviews the basics and applications of nanoparticulate delivery.

1.3   Nanotechnology for drug delivery

The use of colloidal gold as rejuvenating medicine has been long known in ancient civilizations (Daniel and Astruc 2003). The ayurvedic system of medicine, one of the oldest, uses a preparation of colloidal gold known as "swarn bhasm" (gold ash) for a variety of therapeutic effects. The quest for exploring miniature vehicles for modern drug delivery was pioneered by Professor Peter Paul Speiser at the Federal Institute of Technology, Zurich. His group first experimented with beads (Khanna and Speiser 1969; Khanna et al. 1970) and microparticles (Merkle and Speiser 1973) and then reported a nanoparticulate product of polymerized micellar system for vaccine delivery (Birrenbach 1973; Birrenbach and Speiser 1976). Interestingly, Benacerraf and coworkers were studying interactions of the reticulo-endothelial system (RES) with carbon nanoparticles of about 25nm (Benacerraf et al. 1957) and radiolabeled albumin microaggregated particles since 1950s and their procedure was later refined by another group in the Department of Radiological Science at the Johns Hopkins Medical Institutions in Baltimore (Scheffel et al. 1973), a modification of which was used in one of the earliest attempts for drug delivery (Kramer 1974). Nanoparticles are now a major focus area in the field of drug delivery for both new and already marketed compounds.

Definition of nanoparticles: Nanoparticles for pharmaceutical purposes are defined by the Encyclopaedia of Pharmaceutical Technology as solid colloidal particles ranging in size from 1 to 1000 nm. They consist of macromolecular materials and can be used therapeutically as drug carriers, in which the active principle (drug or biologically active material) is dissolved, entrapped, or encapsulated, or to which the active principle is adsorbed or attached (Kreuter 1994).

1.3.1 Nanoparticulate drug delivery

Pharmaceutical companies and academic researchers worldwide are exploring new strategies to (i) increase the efficacy of existing drugs, (ii) reduce adverse effects (iii) and to achieve site specificity. Innovation is achieved by design (osmotic pumps, matrix or depots, gels), or use of excipients (formulation design). Since anticancer drugs are cytotoxic, the aim of effective drug delivery is to get the drug reach the target site (cancerous cells) while minimizing the distribution in non-target areas. Nanoparticles are an interesting and promising prospect in the emerging drug delivery systems. Nanoparticles can be prepared based on lipids or polymers or inorganic material like silica. Polymeric nanoparticles are the most extensively explored form, capable of incorporating a wide range of drugs of both low and high molecular weight, and varying water solubility. Solvent emulsion evaporation method provides a simple means to produce nanoparticles from preformed polymers employing simple apparatus.

Achieving drug delivery by the aid of nanotechnology is not new (Couvreur et al. 1977; Kante et al. 1980), but the last few years have seen an overwhelming research thrust in this area (Alonso 2004; Duncan 2005; Hanes 2006; Moghimi and Kissel 2006).

Small particles have been shown to be taken up through and across the biomembranes by unique mechanisms, which can address one or more of the bioavailability problems (Florence 1997; Sakuma et al. 2001). These particles can produce local effect at the site of administration and also systemic effect by entering the circulatory system.

The Peyer's patches in the small intestine are claimed to be the primary gateways of particle uptake (Eldridge et al. 1990), delivering the particles to the circulatory system through the lymphatics, with the absorption more

pronounced and rapid for smaller particles. The mucus lining the internal surface of GIT acts as a physical diffusion-barrier to drug absorption (Meaney and O'Driscoll 1999) and at the same time provides a method to increase the retention time of these delivery systems in the GIT by mucoadhesion (Lehr and Lee 1993). The larger size of pores in the tumour vasculature and reduced lymphatic drainage allows polymers, large compounds and particulate carriers to accumulate, thereby providing an opportunity to concentrate the drug in the target locales. By the well documented Enhanced Permeation and Retention (EPR) effect (Matsumura and Maeda 1986; Maeda 1992), nanoparticles can localize in the tumour (Figure 1.2).

The localization can be promoted with the use of covalently (or otherwise) conjugated cell markers with affinity for transporters and over-expressed receptors (Rosenthal et al. 2002). However, not much is conclusively known about the biodistribution and fate of these nanoparticles after absorption. Studies have shown particles releasing incorporated drug for up to 11 days after oral administration (Mittal et al. 2007). Even in absence of conclusive pharmacokinetic profiling of nanoparticulate formulations, therapeutic efficacy has been recorded (Ankola et al. 2007).

Due to its compromised biopharmaceutical properties (Panchagnula 1998) and wide spectrum of action, paclitaxel forms an ideal drug to be incorporated into nanoparticles in an attempt to increase the non-parenteral bioavailability and improvement in therapeutic efficacy.

1.3.2 Paclitaxel delivery by nanotechnology

As previously mentioned, in the last few years two nanoparticulate products of paclitaxel have been launched in the market: Abraxane® (Abraxis BioScience, Inc. and AstraZeneca) and Nanoxel™ (Dabur, India), but have to

be administered by parenteral route as sustained infusions.

Nanoxel™ is a product based on micellar solubilisation of paclitaxel in self-nano-emulsifying system. It is approved in India for marketing by Dabur and is in phase I clinical trials in USA in a study sponsored by Fresenius Kabi Oncology Ltd. The material used is pH sensitive co-polymer of N-isopropyl acrylamide (NIPAM) and vinylpyrrolidone (VP) monomers. Smooth spherical particles of 80 -100 nm showed upto three-fold higher uptake in target cancer cells as compared to cremophor paclitaxel (Singh et al. 2008).

Normal Tissues
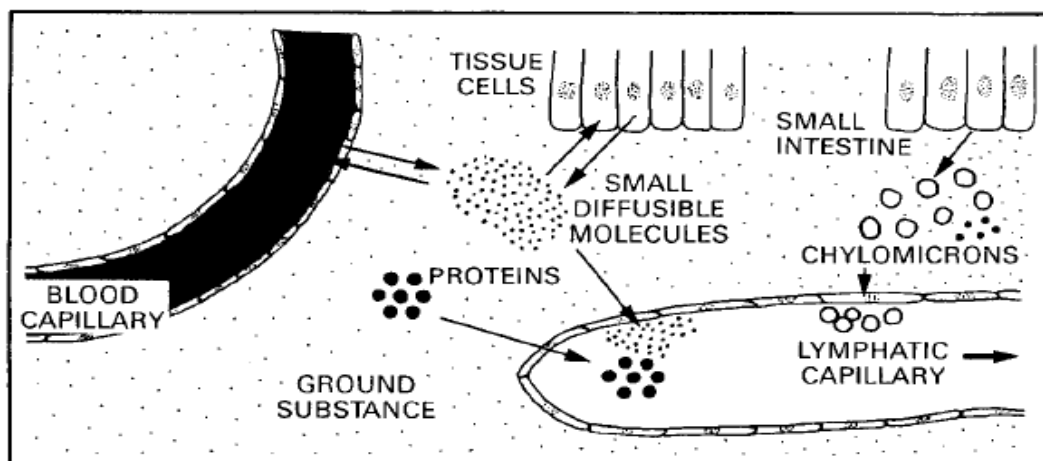
Tumor Tissues
(Hypervascularity, no lymphatic capillary)
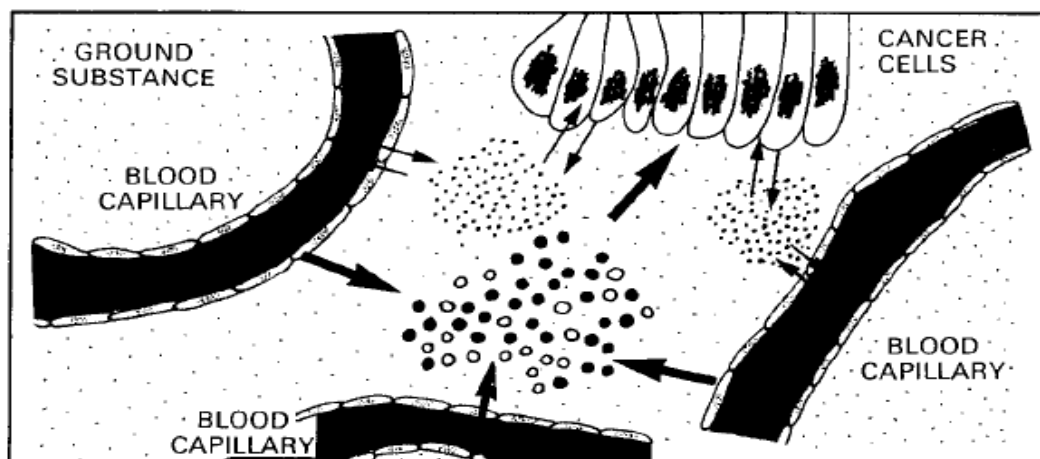
Figure 1.2: EPR effect; reproduced from (Maeda 1992)

Developed and tested as ABI-007, Abraxane® is composed of 20-400nm (US patent 6096331) albumin-bound paclitaxel. It is prepared using high pressure homogenization of paclitaxel in presence of human serum albumin and helps in increasing the maximum tolerable dose (MTD) to 300 mg/m^2 from 200-250 mg/m^2 for conventional Taxol® (Ibrahim et al. 1992).

The micronization of paclitaxel can be carried out using sonication, nanoprecipitation, spray drying and ball milling (US patents 5439686, 5498421). It is the first product in the market based on Abraxis Biosciences' nanoparticles-albumin bound (nab™) technology. The nab™ technology is a subset of a broader Protosphere™ platform based on using proteins to make nanoparticles for delivery of water insoluble drugs. The reasons behind the choice of carrier material are based on three pathways in which tumour cells feed their high growth rate. First, albumin is the most abundant protein in the body and is used by body to transport nutrients, which are utilized at a higher than normal rate by the rapidly multiplying cancer cells. Second, tumours employ gp60 pathway by which nutrients are preferentially transported across the endothelial barrier when attached to albumin (Schnitzer 1992; Desai et al. 2006).

Third, the tumours secrete a specialized protein called Secreted Protein Acidic and Rich in Cysteine (SPARC) into their interstitium that specifically binds albumin-bound nutrients and concentrates them within the tumour's interstitium to prevent their leaching. In clinical trials, it has shown greater efficacy and a reduced toxicity compared to standard paclitaxel (Gradishar et al. 2005). Other advantages over Taxol® are that less saline is required for infusion of this formulation, premedication for prevention of immune reactions is not required and there is no danger of leaching of harmful chemicals from the plastic infusion sets.

Poly-(γ-L-glutamylglutamine)–paclitaxel (PGG–PTX) is another newly reported formulation that was shown to have better activity than Abraxane® in three mouse tumour models in a once a week, three cycle treatment module (Feng et al. 2010). It should be noted that majority of systems discussed in the previous section targeted towards oral delivery of paclitaxel are in sub-micron size range (micelles, lipid nanocapsules, self-emulsifying systems).

The clinical approval of the nanoparticulate dosage forms has reinforced the potential in this non-classical delivery approach. The present study was envisaged to develop nanoparticles that would allow paclitaxel to be orally administered.

1.4 Hypothesis and objectives

A typical process of product development involves manufacture and characterization of the formulation, its testing in suitable in vitro assays followed by safety and efficacy studies in animals.

Hypothesis: The aim of this study was to test the hypothesis that a nanoparticulate formulation can circumvent the hurdles of poor biopharmaceutical properties of paclitaxel and enable its oral delivery.

To test the hypothesis, the project was envisaged with the following objectives

(a) Development of a nanoparticulate formulation of paclitaxel and measurements and analysis to characterize the product.

(b) In vitro analysis of the formulation to establish safety and efficacy in culture.

(c) Administration of the developed formulation to experimental animals by oral route and established that it has been delivered.

(d) To evaluate if incorporation of paclitaxel in nanoparticles can restore cytotoxicity in drug resistant cancer.

The overall objective of the proposed work was to check the feasibility of peroral delivery of paclitaxel using nanoparticles and evaluating therapeutic response of the developed formulation against the traditionally used formulation as control. The following chapters address the aforementioned objectives experimentally.

2 Development and characterization of paclitaxel encapsulated nanoparticles

2.1 *Introduction*

The performance of nanostructured drug delivery systems is influenced mostly by size (Mathiowitz et al. 1997; Desai et al. 2004) and/or surface properties like charge and hydrophilicity (Kreuter et al. 1997; Kreuter 2004). The solvents and stabilisers used in the preparation of nanoparticles play a significant role not only in the final product characteristics but also in the uptake, biodistribution, fate, release profile of incorporated drug (Bhardwaj et al. 2005) and hence the therapeutic efficacy *in vivo*.

2.1.1 Carrier

Besides lipidic and inorganic material, polymers are routinely used for manufacture of nanoparticles. The most important requirements from a systemically available nanostructured drug delivery vehicle are biocompatibility and biodegradability. Biodegradable polymers have been extensively used in controlled drug delivery as they have the advantage of not requiring surgical removal after they serve their intended purpose.

The bioresorbable aliphatic polyesters are the most widely used class for applications in drug delivery (Weir et al. 2004). Poly-glycolide (PGA), poly-lactide (PLA), and their copolymer poly-lactide-co-glycolide (PLGA) are the most commonly explored biodegradable polymers (Figure 2.1). PLGA has been in focus in the search for appropriate matrices for drug delivery nanoparticles due to its commercial availability, versatility, and hydrolytic degradation into resorbable harmless products. The popularity of PLGA is further explained by the fact that USFDA has approved many products

containing PLGA for a number of clinical applications (Edlund and Albertsson 2002).

PLGA is a block copolymer and several grades ranging from lactide:glycolide ratios of 50:50 to 95:5 are commercially available. PLGA is amorphous or crystalline depending on whether D,L-lactic acid or L-lactic acid, respectively is used as the monomer. The glass transition temperature (T_g) of PLGAs ranges from 45 to 55°C allowing sufficient mechanical strength for formulation above the physiological temperature.

Poly(lactide-co-glycolide)

Lactic acid   Glycolic acid
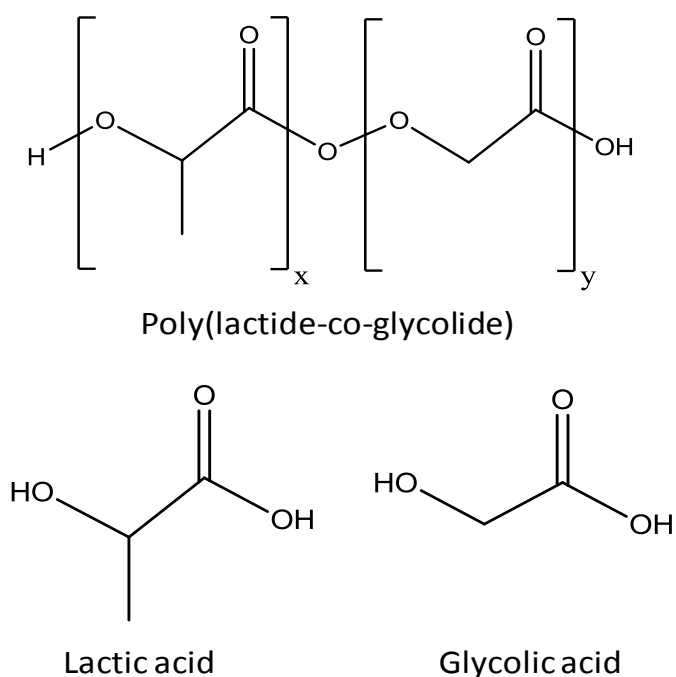
Figure 2.1 PLGA and its constituent monomers

The PLGA copolymer has been shown to be degraded in body by hydrolytic cleavage of ester linkage to lactic and glycolic acid that are formed at very slow rate and easily metabolized in the body. Vert, Visscher and Ikada have extensively worked on establishing the hydrolytic degradation pathways using microspheres (Anderson and Shive 1997). While the smaller forms like microspheres degrade in a homogenous fashion as a function of the surface area, large-scale devices made from PLGA have been shown to undergo heterogeneous degradation comprising of surface as well as bulk hydrolysis.

This degradation is greatly enhanced by the autocatalytic properties of carboxyl end groups. The degradation time is directly proportional to the lactide content, 50:50 copolymer being the fastest to degrade *in vivo* in about 50-60 days (Visscher et al. 1985; Anderson and Shive 1997). The crystalline form is more resistant to degradation than the amorphous (Jain 2000). Ravi Kumar and co-workers (Bala et al. 2004) have reviewed the use of PLGA in polymeric nanoparticles. Further support to PLGA nanoparticles for drug delivery for cancer has come from a report establishing that degradation of PLGA is faster in static conditions compared to dynamic ones (Huang et al. 2006). Thus particles in general circulation shall be relatively stable and hence release lesser drug compared to when they are trapped in the tumour. The local pH falls in the vicinity of the nanoparticles due to release of degradation products and the free carboxyl groups enhance hydrolytic degradation by autocatalysis.

Since nanoparticles can persist in the body for several weeks, they can be considered as implants. Depending on the way of administration, different fractions can be circulating or trapped in different parts of the body. For this reason, it is important to understand the response of the body to the foreign material. Various regulatory agencies have issued guidelines for assessing biocompatibility of such implanted material under the classification of medical devices. The biocompatibility studies as defined by the ISO 10993/EN 30993 recommend tests for cytotoxicity, acute systemic toxicity, sensitization, genotoxicity, skin irritation, implantation, intracutaneous reactivity, and haemocompatibility (Gad and Philip 2005). Considering the range of this testing for approval of new material, scientists prefer to employ already approved material. Considering the long history and wide range of marketed products ranging from microspheres to rod shaped implants (Decapeptyl,

Gonapeptyl depot, Leuplin, Lupron depot, Eligard, Zoladex for depot, Profact depot, Trelstar Depot) for anticancer drug delivery, PLGA became a strong candidate.

It must however be stressed that the applications of these polymers has to be balanced in view of the therapeutic target. Implants with PLGA microspheres invoke tissue response in three phases depending on their size (Anderson and Shive 1997). Since nanoparticles behave differently from microparticles, a possibility of different tissue response can not be ruled out. While any toxicity exhibited when entrapped in tumours will be desirable, there is a possibility that it might cause unwanted effects in non-target tissues.

Due to the fast degradation of 50:50 PLGA, it was chosen as the polymer for making nanoparticles. Simultaneous studies in the group using histology had proved that polymeric nanoparticles based on this grade did not exhibit inflammatory response in the rat (Hariharan et al. 2006). It readily dissolves in organic solvents like acetone, acetonitrile, ethyl acetate, halogenated solvents like chloroform and dichloromethane, but is insoluble in methanol, ethanol and tert-butyl methyl ether. It is insoluble in water, but dissolves and degrades rapidly in alkaline solutions.

2.1.2 Process

Many methods are available for manufacture of nanoparticles (Vauthier and Bouchemal 2009) from preformed polymers. For water insoluble polymers, emulsification often precedes a step of nanoprecipitation attained by solvent evaporation, diffusion, salting out or a combination of these. The choice of the organic solvent used for solubilising the polymer depends on the process employed. The method used in this project was emulsification-solvent diffusion-evaporation using ethyl acetate as the solvent for the polymer. The

energy for size reduction of emulsion globules was provided by mechanical means through a rotor in shaft type tissue homogeniser. Solvent evaporation was allowed passively as a function of vapour pressure at atmospheric pressure in a fume hood.

2.1.3 Stabiliser

A brief mention of colloidal stability is necessary to understand the process of physical stabilization of nanoparticles. Characteristics of nanoparticles can be defined on the basis of the colloidal or the particle theory. The difference in solutions and colloids, especially in the stability, arises from the element of dispersion. It provides an extra degree of freedom that result in a different kind of instability. Here a distinction needs to be made between micellar systems and suspensions based on saturation solubility (Derjaguin 1993). As time progresses, due to the differential solubilization rate of smaller and bigger particles, the former can disappear resulting in gradual decrease in 'degree of dispersion'. Micellar systems, on the other hand, do not exhibit this behaviour and are much more thermodynamically stable (Deryagin 1992). The inherent stability as well as instability of the colloidal particles are affected by the Brownian motion (Appendix A). Interfacial forces play a key role in the thermodynamic stability of emulsions and suspensions (Appendix B). At the foundation of the colloidal stability is a balance between the basic physicochemical phenomena of van der Waals attractive forces and electrostatic repulsion as explained by the DLVO theory (Appendix C). Nanoparticles can be stabilized against agglomeration by Coulombic separation or steric hindrance. The Coulombic separation can be affected by imparting a charge to the nanoparticles. Steric stabilization is achieved by the long tail like structures of surfactants and other stabilisers that get physically adsorbed on the particle surface. These protrusions prevent the particles

from coming too close and attain the primary energy minima. Here a distinction is required to be made between stabilisers that have one point of attachment and those that have many. The latter group is mostly composed of polymers like polyvinyl alcohol (PVA) and constitutes the more effective class. The reason for this observation lies in the fact that adsorption is relatively a low energy phenomenon and the stabiliser is only weakly associated with the surface. This process is reversible and the molecules keep on attaching and detaching to maintain equilibrium. Thus, single point attachment can transiently leave the surface naked, the surface being exposed for either a replacement stabiliser molecule or another particle. However, the polymeric multi-point attachments ensure that even if some of the attachments are broken, there are others that will still provide a zone of inhibition for physical approach. Thus the adsorption process of steric stabilisers is akin a non-equilibrium process. It should be noted that the Brownian motion can contribute to both the stability (by acting against gravity sedimentation) and instability (by inducing collisions or reducing the interparticle distance).

DMAB was used as a stabiliser/surfactant for preparation of nanoparticles. Our interest in this compound is because of the small size particles that it produces and the high positive surface charge provided (Hariharan et al. 2006). The molecule is a V-shaped two chain compound that readily ionises in water. Figure 2.2 and Figure 2.3 depict the energy minimised structures (Chem3D software MM2 job, Cambridgesoft) of the parent compound and the cation respectively.

It must be pointed out that since DMAB is a surfactant, it is important to keep its concentration in the final formulation below the critical micellar concentration (CMC) to prevent lysis of membranes of cells.
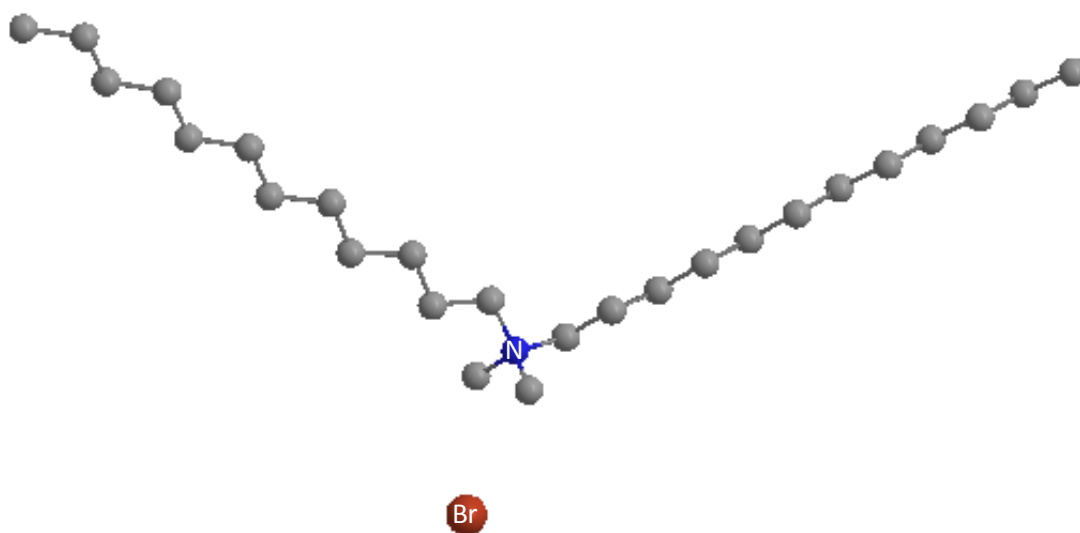
Formal Charge = 0
Connolly Accessible Area = 1008.216 Sq. Å
Connolly Molecular Area = 553.26 Sq. Å
Connolly Solvent Excluded Volume = 516.747 Cu. Å

Figure 2.2: Energy minimised structure of unionised DMAB; energy minimization carried out using MM2 job of Chem3D molecular modelling software (Cambridgesoft, UK)
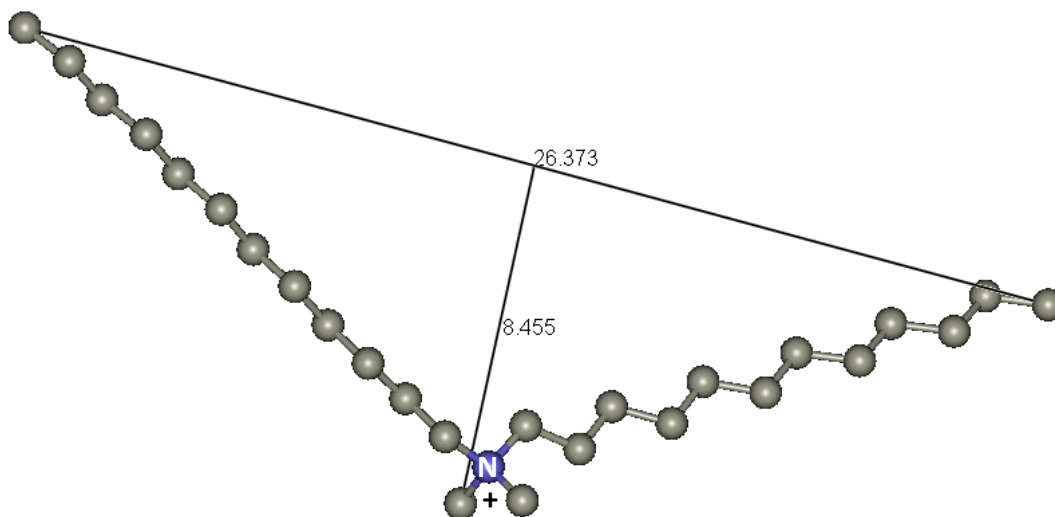
Formal Charge = 1
Connolly Accessible Area = 948.058 Sq. Å
Connolly Molecular Area = 517.157 Sq. Å
Connolly Solvent Excluded Volume = 477.007 Cu. Å

Figure 2.3: Energy minimised structure of ionised DMAB; energy minimization carried out using MM2 job of Chem3D molecular modelling software (Cambridgesoft, UK). Dimensions of the molecule are in Angstroms (Å).

DMAB belongs to the chemical class of quaternary ammonium salts that have a marked surfactant activity. DMAB forms micelles at around 20-50 μM and vesicles at higher concentrations. Aqueous solutions of concentrations higher than 3% w/v are very viscous. Some properties of DMAB are summarized in Table 2.1.

Table 2.1: Properties of DMAB

Property	Value
Molecular weight	462.64
CMC	20-50 μM
Molarity of 1.0% w/v	21.6 mM

Recent reports suggests that DMAB imparts capability to the nanoparticles to interact with a model cellular membrane and this interaction was proportional to their cellular uptake *in vitro* (Peetla and Labhasetwar 2009).

An important point to consider regarding the use of stabilisers prepared by emulsion techniques is that only a fraction of what is required for emulsification is left on the particle surface. The purpose of the stabiliser is to reduce the surface free energy in the emulsion. When emulsion globules precipitate as particles, a small fraction of stabiliser is adsorbed on the surface while unbound should be removed from the preparation to avoid any adverse effects related to the same. For drug delivery applications, nanoparticles should ideally be around 100nm in diameter. Although different tumours can have varying vasculature architecture, most of them have a lower cut-off of 200nm vessels (Hobbs et al. 1998). Thus, to be effectively targeted by the EPR effect, the particle size should be below this cut-off.

2.1.4 Characterization of nanoparticles

The foremost requirement for characterization of nanoparticles is sizing. Because of the limitation of the lenses, objects smaller than 150-200nm can not be directly seen under the optical microscope (refer to Bragg diffraction). Electron microscopy allows smaller particles to be imaged, but the techniques require skilled sample preparation.

Dynamic light scattering provides an easy way to estimate the particle size of colloids. The measurement of scatter of light incident on particles is combined with the Brownian motion on a time-scale to calculate the particle size and the size distribution of the sample. The theory of DLS for analysis of particle size is discussed in Appendix D.

Another microscopy technique useful for estimation of particle size is the atomic force microscopy (AFM). It involves moving a finely pointed cantilever on the surface of a sample wherein the change in forces as the two surfaces come close or move apart are measured. As the cantilever scans a two dimensional space, the cantilever can be made to move at a constant level of interaction with the surface. This would involve dipping of the lever in troughs and rising above raised surfaces. A laser incident on the cantilever is monitored as the scan takes place and this generates a three-dimensional topological image. Thus AFM not only provides data on size, but also helps in gathering information about the surface and is a fast emerging technique for characterization of nanoparticles.

2.1.5 Freeze-drying

Stability is one of the most important requirements of a pharmaceutical product. A nanoparticulate formulation can experience physical (aggregation) as well as chemical instability. Since polyesters undergo hydrolytic cleavage in water, storing the nanoparticles as an aqueous

suspension will lead to slow degradation of polymer and leaching of drug (Abdelwahed et al. 2006c). Removal of water by atmospheric evaporation is time consuming, will require elaborate surface area arrangements and raise issues of stability and contamination. Moreover, the redispersibility of the nanoparticles is a concern. To obtain an industrially viable stable product, the nanoparticles can be freeze dried. The resulting product can be reconstituted on demand. The process is comparatively faster, can be scaled up and extensive instrumentation is available.

There are three basic components of freeze-drying: freezing, primary drying and secondary drying and the temperature-pressure combination are critical for the success of freeze-drying. The outcome of lyophilisation not only depends on the temperature at a particular phase, but also on the rate and manner in which temperature is changed (Abdelwahed et al. 2006b; Abdelwahed et al. 2006a). Thus the freeze-drying conditions have to be optimized according to the desired product characteristics. The driving force for the freeze-drying comes not from the vacuum, but from the difference in temperature between the sample and the condenser. Typically, the temperature of the condenser is approximately kept around -85°C in laboratory scale freeze-driers. Thus lower the temperature during primary drying, slower is the rate of sublimation of ice. However, there is a certain maximum temperature at which primary drying can be carried out to preserve the product characteristics (Franks 1998).

Due to the stress due to the low temperature and vacumm, freeze-drying is often carried out using excipients. Sugars especially mono and disaccharides are the most widely used cryoprotectants (Abdelwahed et al. 2006c). A series of excipients are screened to choose the most suitable one that can maximum preserve the properties of the formulation.

2.2 *Specific aims*

In this background, the following specific aims were defined for *in vitro* experiments

- Determination of the quantitative effect of formulation parameters on preparation of polymeric nanoparticles.

- Preparation of drug loaded nanoparticles of low polydispersity and average diameter around 100nm and their characterization.

- Optimization of a method for washing of particles for removal of unbound stabiliser.

- Development of freeze-drying method to allow dry storage of the nanoparticulate formulation.

2.3   Methods

2.3.1   Material

PLGA 50:50 block copolymer (RH 50-50, Molecular weight 35-40 kDa) was purchased from Boehringer Ingelheim KG (Ingelheim, Germany). Paclitaxel (Genexol®) was bought from Samyang Genex Co. (Seoul, Korea). Didodecyldimethylammonium bromide (DMAB) was purchased from Fluka Buchs SG, Switzerland). Glucose, Glycine, Lactose, Mannitol, PEG8000, Sorbitol, Sucrose, Trehalose, Xylitol, were purchased from Sigma-Aldrich (St. Louis, MO) and used as obtained.

2.3.2   Analytical method for estimation of paclitaxel

Paclitaxel absorbs in the UV region with a maxima at 227 nm. It does not fluoresce and being a lipophilic molecule (logP = 3.5), its chromatographic separation is best carried out using reverse phase octadecyl (C-18) or octyl (C-8) stationary phase. The compound is available in high purity from many sources and the solutions in methanol or ethyl acetate are claimed to be stable at -20°C (Supplier information).

The drug is extensively bound to plasma and tissue proteins (89-98%). Thus *in vivo* analysis requires a protein precipitation step and typical detection levels reported with plasma and tissue analysis have a limit of detection of 10ng in every ml or mg of analyte (sample size 500 µl or mg). The drug is stable in solution between pH 3-5, with rapid degradation in alkaline media. The internal standards used are docetaxel or a derivative or structural analogue. Metabolites of paclitaxel being more polar elute earlier than the parent drug. For its estimation in biological samples, liquid scintillation counting of radiolabeled drug was carried out (discussed in chapter 4).

2.3.2.1 *HPLC conditions*

The concentration of paclitaxel in samples was analyzed using HPLC on a C18 column (Lichrocart, Lichrospher®, 25cm x 4.6mm, 5μm, Merck, Germany or C_{18} Symmetry®, (25cm x 4.6mm, 5μm, Waters, USA) using mobile phase consisting of methanol, acetonitrile and 5 mM phosphate buffer of pH 2.5 (70.0 : 2.5 : 27.5).

The HPLC system consisted of a Waters, USA configuration with 996 Photodiode Array Detector or 2487 dual wavelength absorbance detector, 717plus auto sampler, and configured to Millennium[32] software version 3.05.01 or Surveyor, Thermo Scientific, UK configuration with Surveyor LC Pump, Quaternary Low pressure Gradient pump with built in Degasser, Surveyor AS, Variable Fill Autosampler, Surveyor PDA, ChromQuest 4.2 Software for Surveyor Control + Spectral Analysis. Detection of the compound was done by measuring absorbance at 227 nm. Flow rate was 0.7 ml per minute in isocratic mode.

2.3.2.2 *Preparation of calibration curve*

Primary stock solution (1mg/ml) of paclitaxel was prepared in methanol and diluted to 20μg/ml (using mobile phase), which served as the secondary stock. This was further diluted in mobile phase to obtain working standards in the concentration range of 0.1-10 μg/ml.

2.3.3   Characterization of nanoparticles

2.3.3.1 *Measurement of particle size and distribution*

The particle size was measured using dynamic light scattering (DLS) on Malvern Zetasizer (Nano ZS, Malvern, UK). The sizes reported are the z-average sizes; its explanation and the measurement settings of zetasizer are explained in Appendix D.

2.3.3.2 *Atomic force microscopy for size estimation*

A drop of the nanoparticle suspension was placed on a silicon wafer, air dried and the particles were imaged using an atomic force microscope (AFM) (Bioscope II, Veeco Instruments, USA) to check the surface texture and shape and to cross verify the size determined by zetasizer. Measurements were done with a scanning probe of force constant k ~ 40 N/m in Tapping Mode™.

2.3.4 Optimization of the particle preparation with DMAB

PLGA nanoparticles were prepared by employing the process of emulsification-solvent diffusion-evaporation under constant stirring (Kumar et al. 2004). Briefly, 50 mg of PLGA was dissolved in 2.5 ml ethyl acetate and the polymer solution in organic solvent was poured in 5 ml of aqueous phase containing the stabiliser and stirred on a magnetic stirrer (Polymix® PX-MS 15-1, Kinematica, Switzerland) to get a primary emulsion. This primary emulsion was then subject to high shear using a rotor shaft-casing type tissue homogeniser (Ultra-Turrax T-18 basic, IKA®-Werke GmbH & CO. KG, Germany). The size-reduced emulsion was then diluted with water and stirred for 4 hours to remove the organic solvent. The scheme is depicted in Figure 2.4. Blank nanoparticle preparation was optimized by varying the formulation parameters and concentration of stabilisers to understand their role in preparation of nanoparticles. The effect of variables like organic to aqueous phase ratio, stabiliser concentration, and process parameters like speed of the high shear homogeniser on the particle characteristics were studied.

2.3.4.1 *Removal of organic solvent*

To remove ethyl acetate from the emulsion, the external phase is diluted with water. The reason lies in the partial solubility of ethyl acetate in water and its

relative vapour pressure. Most organic solvents used for preparation of nanoparticles are either completely miscible (acetone, acetonitrile, alcohols) or immiscible (chloroform, dichloromethane) with water. To calculate the required quantity of water, ethyl acetate was added to water in steps, stirred and left to settle. The ratio at which the two phases could be distinctly seen was noted.
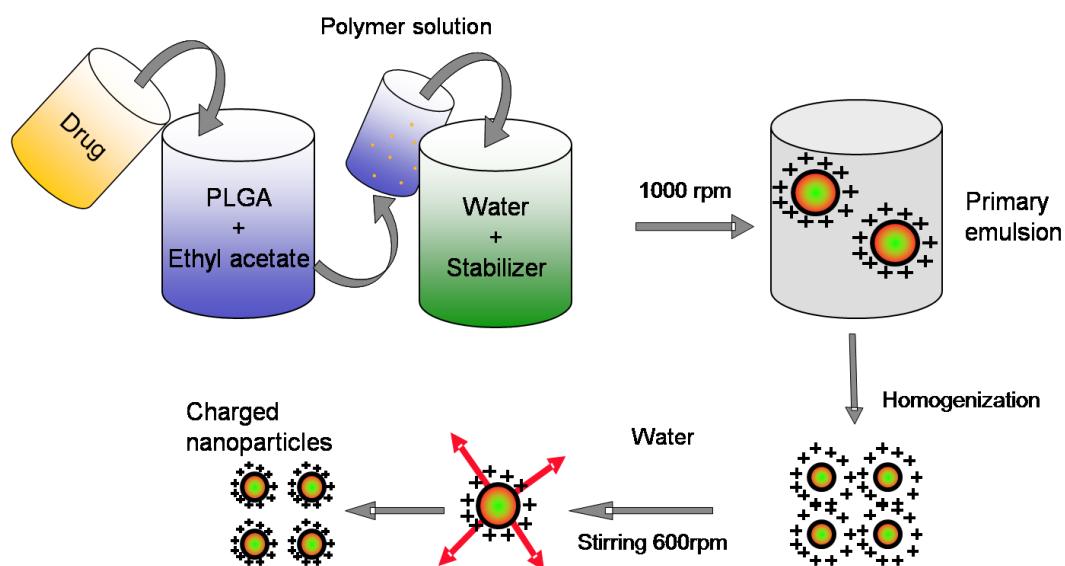
Figure 2.4: Particle preparation scheme

Additionally, after calculating the volume of water required that could take all the ethyl acetate, particles were prepared using half the required amount of water to see if the nanoprecipitation was instant or a gradual process. The hypothesis is that each individual globule precipitates as a nanoparticle when the ethyl acetate is removed from the system.

In one of the control experiments, stirring was withdrawn after addition of calculated volume of diluting water to determine if the system is thermodynamically stable enough to sustain till the ethyl acetate was evaporated.

In yet another experiment, vacuum distillation (Rotavapor, Buchi, USA)was

attempted to remove the organic solvent.

2.3.4.2 Effect of stabiliser concentration

Stabiliser can affect the emulsification process by influencing the viscosity and reducing the surface energy associated with the globules. Three different concentrations: 0.1, 0.33 and 1.0% w/v of DMAB in water were used to make nanoparticles by the method described earlier.

2.3.4.3 Effect of homogenisation speed

The surface free energy of droplets of internal phase in an emulsion is inversely proportional to the diameter. The stabiliser molecules align themselves at the interface to decrease the surface energy. In principle, this allows the globule size to be decreased still further. This energy can be provided through shear mills, high pressure homogenisers, sonication and mechanical shear homogenisers. For this project, the shear homogeniser was used. To see the effect of homogenisation on particle characteristics, speeds of 15000, 20000, 22000 and 24000 (maximum speed for the model employed) rpm of the Ultra turrax homogeniser (model T-18 basic) were investigated. The diameter of the rotor was 7.5 mm and the external diameter of static shaft was 10.0 mm in the tool employed (S 18 – N 10 G).

2.3.4.4 Effect of phase ratio

The ratio of the immiscible phases defines the arrangement of the stabiliser on the surface and globule size. It can also influence the viscosity of the emulsion. To see the effect of ratio of organic and aqueous phase, particles were prepared using ratios of 3:10, 5:10 and 10:10.

2.3.4.5 Effect of solvent

Acetone (completely miscible with water) and dichloromethane (1 part

soluble in 50 parts of water at 25°C) were also tried in place of ethyl acetate for preparation of nanoparticles.

2.3.5 Preparation of paclitaxel incorporated nanoparticles

In brief, paclitaxel was dissolved in 5 ml ethyl acetate and 50 mg PLGA was added to this solution and stirred for 2 hours. This solution was poured with stirring in 5 ml of aqueous 1.0% w/v DMAB solution. The primary emulsion so obtained was homogenized for 5 minutes by a shaft type tissue homogeniser at 15000 rpm (Polytron PT 4000, Kinematica, Switzerland).

The diameter of the rotor was 9mm and the external diameter of static shaft was 11.8 mm in the tool employed (PT-DA 4012/EC for Polytron 4000, Kinematica). Finally, this emulsion was diluted with 35 ml water and stirred at 800 rpm with a magnetic bar for 4-6 hours to remove the ethyl acetate. Nanoparticle suspension obtained was washed twice followed by centrifugation to remove the unbound drug and surfactant.

2.3.5.1 Effect of drug loading

A preliminary study to predict the drug loading by polymer was carried out by making solutions of paclitaxel and PLGA in ethyl acetate corresponding to drug to polymer ratio of 1, 2.5, 5, 10, 20 and 40% w/w. A drop of these solutions was placed on a clear glass slide and ethyl acetate was allowed to evaporate. A clear film was considered indicative of drug dissolved in polymer while whitish appearance was considered indicative of precipitation.

For preparation of drug loaded particles, 2, 5, and 10% w/w of paclitaxel relative to the polymer was first dissolved in ethyl acetate and then the polymer was dissolved. The rest of the procedure was same as for blank particles. Drug loaded nanoparticles were finally prepared incorporating 5%

(w/w of PLGA) paclitaxel.

2.3.5.2 *Estimation of drug entrapment*

Drug entrapment was calculated by dissolving an aliquot of the suspension of washed particles in acetonitrile and analyzing the paclitaxel by the validated HPLC method.

2.3.6 **Removal of unbound stabiliser**

The major proportion of DMAB used for preparing the emulsion is left in the solution while only a fraction is associated with the particle surface. Thus it is important to remove this unbound stabiliser from the suspension. The following two methods were explored.

2.3.6.1 *Dialysis*

Membrane for dialysis (molecular weight cut off 12,000 Da, Sigma, USA) was activated as per the supplier's protocol. Nanoparticle suspension as prepared was filled in the tubing, clamped at both ends using a polyester thread and left for dialysis for 72 hours with running tap water.

2.3.6.2 *Centrifugation*

The suspension was filled in 35 ml plastic centrifuge tubes and spun at various speeds (corresponding to predetermined equivalent relative centrifugal force) for fixed intervals of time (3K30, Sigma, USA or Avanti® J-E centrifuge, Beckman Coulter Inc., Fullerton, CA, USA). The supernatant was either spun again at a higher rcf (relative centrifugal force) or discarded. The pellet resuspended in distilled water. If the pellet was difficult to resuspend, the time of centrifugation was reduced.

2.3.6.3 *Estimation of bound stabiliser*

The amount of DMAB remaining bound with the particles was estimated by

mass balance. A calibration series was generated using concentrations of 1 to 100 µg/ml. Following centrifugation, the amount of DMAB was estimated in the supernatant after dilution. The amount of DMAB was calculated using double derivative UV spectroscopy at 212nm.

2.3.7 Freeze drying of nanoparticles

Drug loaded nanoparticles were centrifuged to remove the extra stabiliser and the following excipients were added as cryoprotectants before freeze drying the particles: Glucose, Glycine, Lactose, Mannitol, PEG8000, Sorbitol, Sucrose, Trehalose, and Xylitol. For the first experiment, the particles were frozen at -80°C for two hours and then dried under a vacuum drier for 25 hours at ambient temperature.

In subsequent experiments, temperature of the samples was regulated in a benchtop freeze-drier (EPSILON 2- 4, Martin Christ, Germany). Experimet 2 was carried out on a gradually increasing temperature scale (Figure 2.5).
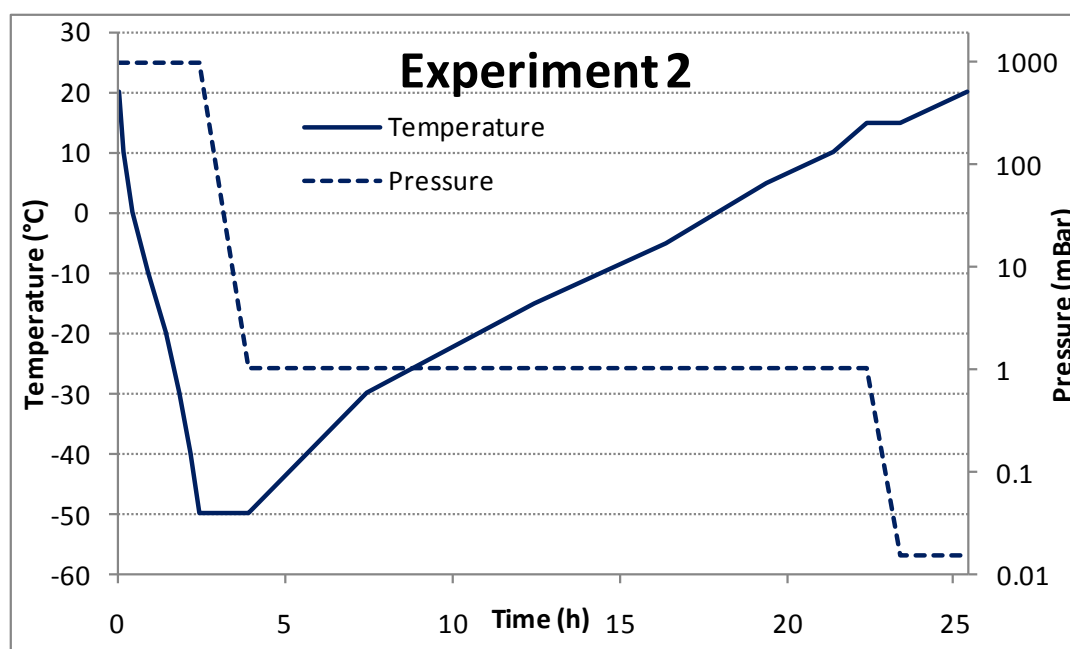
Figure 2.5: Conditions for freeze-drying experiment 2. (h):hours

In experiment 3, temperature was maintained at -45°C for 30 hours during main drying and the final stages of drying was carried out with cascading increase in temperature (Figure 2.6).
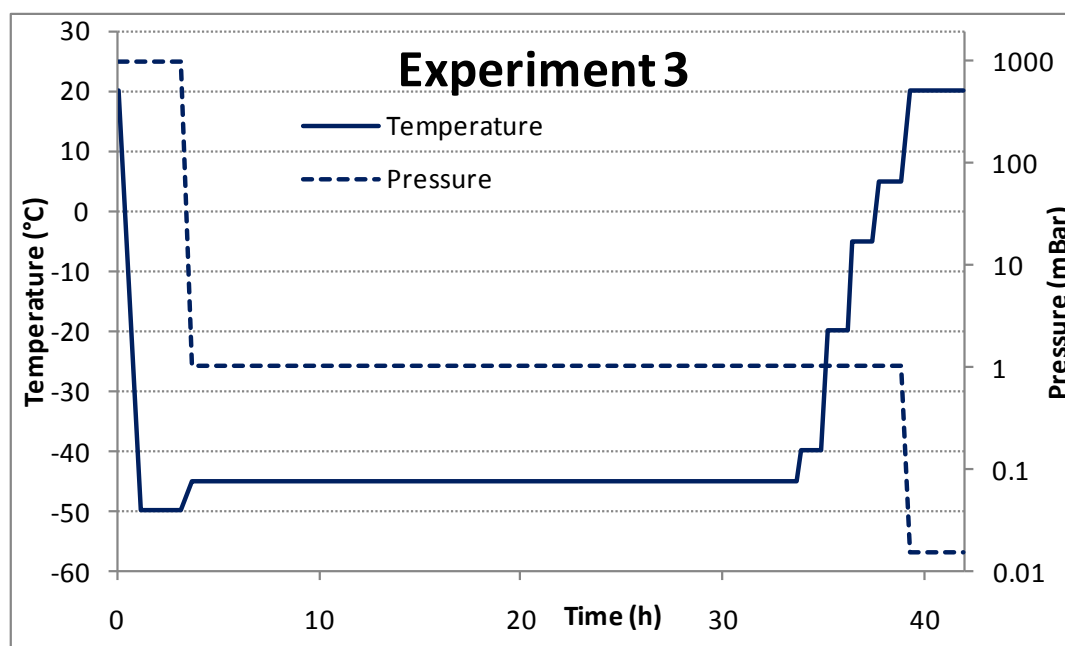
Figure 2.6: Conditions for freeze-drying experiment 3. (h):hours

Experiment 4 involved longer main drying and the temperature was maintained at -50°C for 48 hours (Figure 2.7). The vacuum applied during the primary and secondary drying phases was equivalent to a pressure of 1 and 0.015 mBar, respectively. For experiments 2, 3 and 4, the condenser temperature was kept at -85°C throughout the primary and secondary drying phases. The process was regularly monitored to check the appearance of the cake.

Following the end of freeze-drying, the sample vials were sealed. For analysis, the freeze-dried particles were reconstituted in 1 ml of distilled water with gentle shaking (no vortexing). Particle size and PDI were measured on zetasizer on automatic mode.
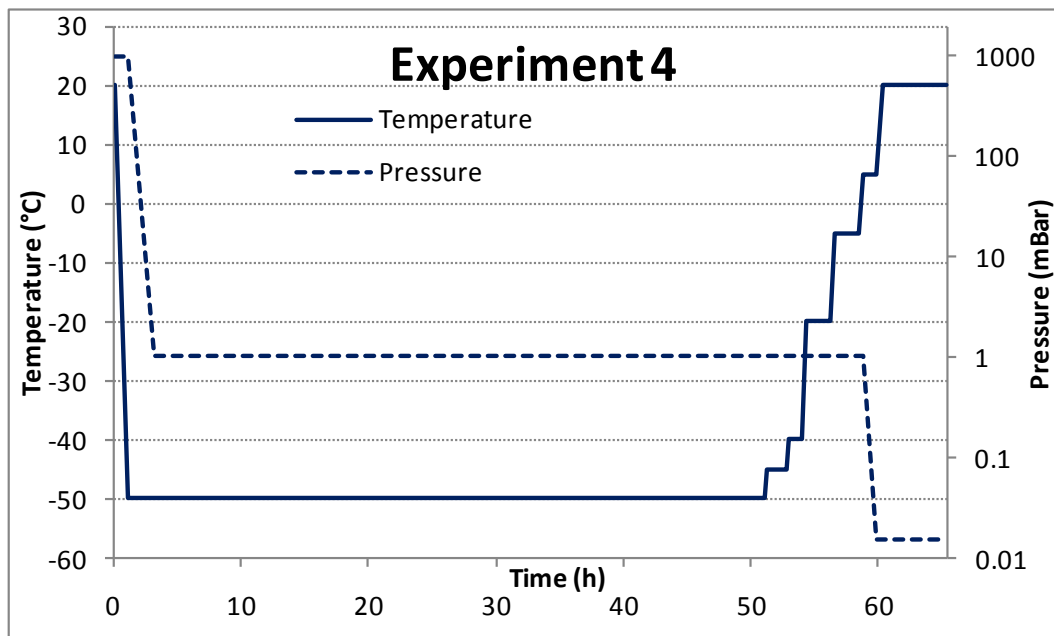
Figure 2.7: Conditions for freeze-drying experiment 4. (h):hours

2.4 Results

2.4.1 Analytical method for estimation of paclitaxel

The drug eluted in approximately 7-8 minutes in an 11 minute run. The regression correlation coefficient denoted by R^2 (sum of least squares method) was above 0.999. A representative calibration result is depicted in Figure 2.8. The limit of quantification was 10ng/ml.
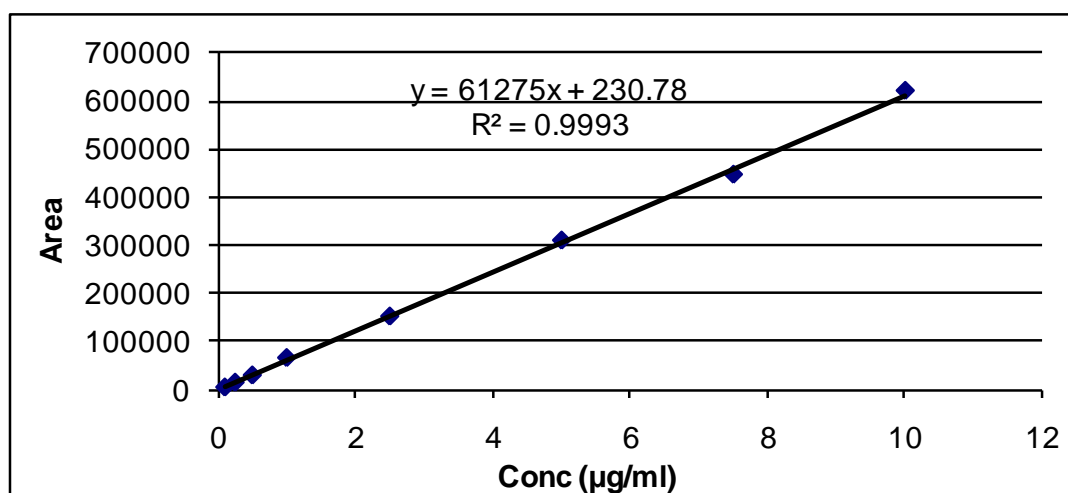
Figure 2.8: Calibration results of paclitaxel *in vitro* analysis by HPLC

2.4.2 Optimization of the particle preparation with DMAB

The particle size characteristics were measured for blank particles (no drug incorporated) prepared by varying the method of preparation.

2.4.2.1 Removal of organic solvent

Serial addition of ethyl acetate to water was able to generate a separate layer of ethyl acetate at top after 6.7 (±0.3) % of volume of water used. This implied that 2.5 ml of ethyl acetate would take 37.3 ml of water. Based on this, the protocol was set to addition of 35 ml of water to the 7.5 ml of emulsion in dilution phase.

Figure 2.9 shows the effect of this volume of water used for dilution on the

final particle size. FS (Full saturation) denotes addition of 35 ml of water, and SS (sub-saturation) denotes 17.5 ml. It can be seen that the volume of dilution did not make a significant difference in either particle size or PDI.
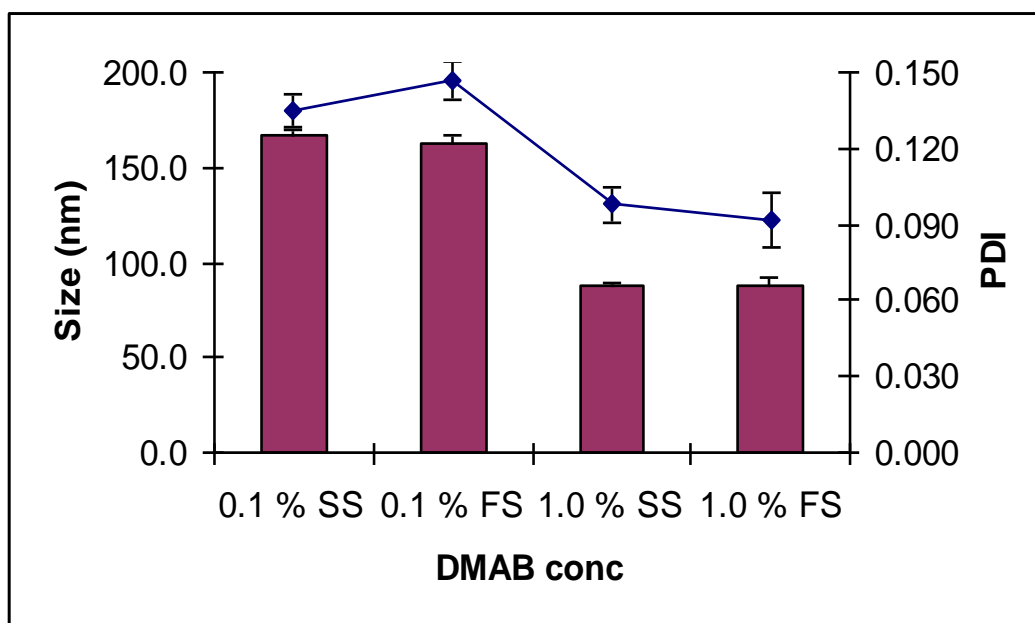
Figure 2.9: Effect of dilution of external phase of blank particles; % refers to the w/v concentration of DMAB used in the primary emulsion. FS: Full saturation; SS sub-saturation. (n=3) Error bars denote sd

The polymer precipitated when stirring was not continued after addition of water in the dilution step. Also, ethyl acetate could not be removed from the system by using vacuum distillation due to intense frothing.

2.4.2.2 *Effect of stabiliser concentration*

As seen in Table 2.2, by increasing the stabiliser concentration, a decrease in both particle size as well as PDI was observed.

2.4.2.3 *Effect of homogenisation speed*

An increase in the speed (rpm) of the shaft tissue homogeniser used to reduce the globule size of the emulsions resulted in decrease of particle size with a simultaneous increase in PDI (Table 2.3). This could be due to high shear forces disrupting the polymer chains of PLGA.

Table 2.2: Effect of DMAB concentration on blank particle characteristics; homogenisation speed 24000 rpm (maximum for the instrument), organic to aqueous phase ratio 1:2 (n=3).

DMAB concentration (%w/v in aq. phase)	Size (nm) ± s.d.		PDI ± s.d.	
0.1	163.2 ± 3.6		0.15 ± 0.01	
0.33	122.7 ± 3.1		0.13 ± 0.01	
1.0	87.1 ± 5.5		0.09 ± 0.01	
Kruskal-Wallis One Way Analysis of Variance on Ranks	there is a statistically significant difference (P = 0.004)		there is a statistically significant difference (P = 0.004)	
All pairwise multiple comparison procedures (Student-Newman-Keuls method)	Comparison	P value <0.5	Comparison	P value <0.5
	0.1 vs. 1.0	Yes	0.1 vs. 1.0	Yes
	0.1 vs. 0.33	Yes	0.1 vs. 0.33	Yes
	0.33 vs. 1.0	Yes	0.33 vs. 1.0	Yes

Table 2.3: Effect of shear speed of tissue homogeniser on blank particle characteristics; stabiliser concentration 1% w/v, organic to aqueous phase ratio 1:2 (n=3).

Speed (rpm)	Size (nm) ± s.d.		PDI ± s.d.	
15000	154.5 ± 6.1		0.06 ± 0.02	
20000	115.0 ± 2.3		0.07 ± 0.01	
22000	105.1 ± 1.9		0.08 ± 0.01	
24000	87.1 ± 5.5		0.09 ± 0.01	
Kruskal-Wallis One Way Analysis of Variance on Ranks	there is a statistically significant difference (P = 0.016)		there is a statistically significant difference (P = 0.039)	
All pairwise multiple comparison procedures (Student-Newman-Keuls method)	comparison	P value <0.5	comparison	P value <0.5
	15000 vs. 24000	Yes	15000 vs. 24000	No
	15000 vs. 22000	Yes	15000 vs. 22000	No
	15000 vs. 20000	Yes	15000 vs. 20000	No
	20000 vs. 24000	Yes	20000 vs. 24000	No
	20000 vs. 22000	Yes	20000 vs. 22000	No
	22000 vs. 24000	Yes	22000 vs. 24000	No

Table 2.4: Effect of organic to aqueous phase ratio on blank nanoparticle characteristics; homogenisation speed 24000 rpm, stabiliser concentration 1% w/v (n=3).

Organic to Aqueous Phase ratio	Size (nm) ± s.d.		PDI ± s.d.
10:10	95.1 ± 4.1		0.11 ± 0.01
5:10	87.1 ± 5.5		0.09 ± 0.01
3:10	72.0 ± 1.5		0.12 ± 0.01
Kruskal-Wallis One Way Analysis of Variance on Ranks	statistically significant difference (P = 0.011)		The differences in the median values among the treatment groups are not great enough to exclude the possibility that the difference is due to random sampling variability; there is no statistically significant difference (P = 0.086)
All pairwise multiple comparison procedures (Student-Newman-Keuls method)	Comparison	P value <0.5	
	10:10 vs. 3:10	Yes	
	10:10 vs. 5:10	No	
	5:10 vs. 3:10	Yes	

2.4.2.4 Effect of phase ratio

Table 2.4 shows that a higher ratio of aqueous to organic phase yields smaller particles probably by influencing the viscosity and distribution of stabiliser at the phase interface. The particles so prepared had a zeta potential of 75-85 mV at pH 4.5.

2.4.2.5 Effect of solvent

Using the method of emulsification-solvent diffusion-evaporation, nanoparticles could not be prepared with either acetone or dichloromethane. The polymer precipitated as lumps in the suspension and on the sides of the beaker. The precipitates did not allow estimation of particle size on the zetasizer (due to the range of the instrument).

2.4.3 Preparation of paclitaxel incorporated nanoparticles

2.4.3.1 Effect of drug loading

The film solubility test showed that the films were transparent up to a paclitaxel:PLGA ratio of 5% w/w.

Drug loaded particles prepared with 0.1% DMAB had a particle size around 170nm (Table 2.5). Paclitaxel concentrations higher than 5% resulted in precipitation. Attempts to load 10% drug led to precipitation along the walls of the beaker.

Table 2.5: Characteristics of particles made with 0.1% DMAB (n=3)

Stabiliser	Drug loading (%w/w of PLGA)	Size (nm)	PDI	Zeta potential (mV)
DMAB (0.1%)	2	167 ±7	0.09 ±0.02	76.0
DMAB (0.1%)	5	174 ±9	0.13 ±0.02	74.3

Particles prepared with 1% DMAB with an initial load of 5% w/w of paclitaxel relative to the polymer weight had an average particle size of about 121 (± 6) nm, with PDI of 0.09 (± 0.02), and a zeta potential of +75 mV (at pH 4.5).

2.4.3.2 Estimation of drug entrapment

The encapsulation efficiency was approximately 47 (±6) % with 0.1% DMAB. With 1% DMAB, this value was average of 44 (±3) % (in nanosuspension before centrifugation). The sample preparation method and analysis was found to be free of interference from the stabiliser(s) and/or polymer.

2.4.3.3 Atomic force microscopy for size estimation

The particles prepared were spherical and had a smooth surface (Figure 2.10)

when imaged with AFM and were not monodisperse. This interpretation was corroborated using zetasizer data (Figure 2.11).
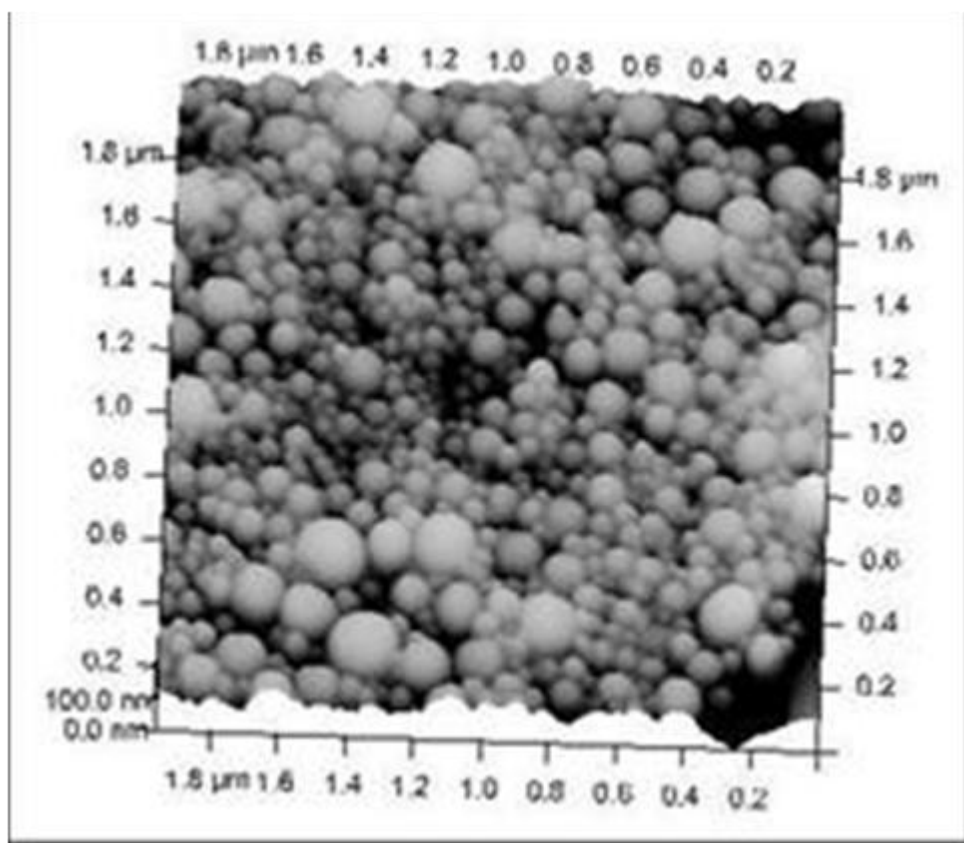
Figure 2.10: AFM image of drug loaded nanoparticles
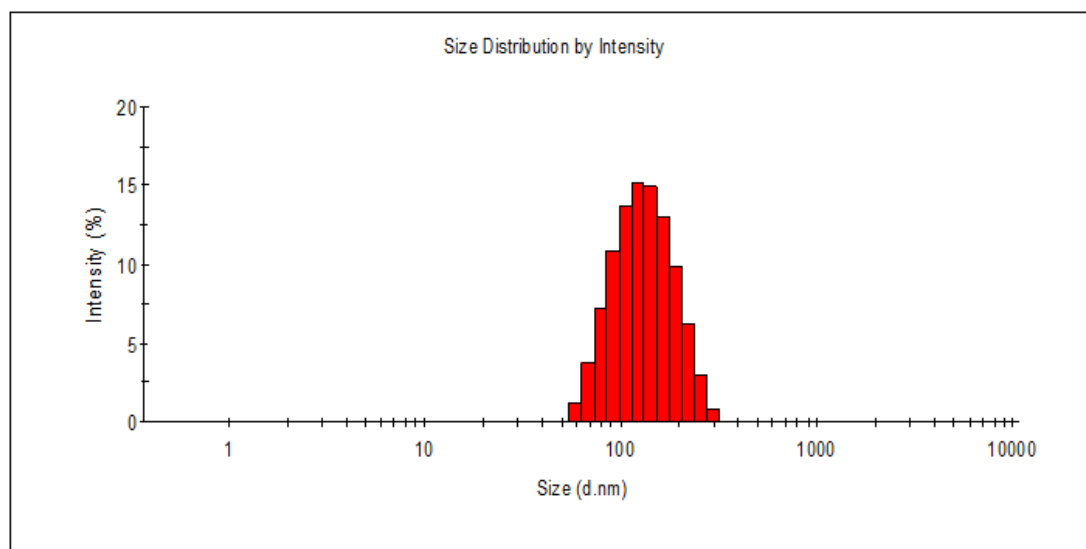
Figure 2.11: Representative size distribution by intensity for paclitaxel loaded nanoparticles

2.4.4 Removal of unbound stabiliser

2.4.4.1 Dialysis

Even after 72 hours of circulation of water around the dialysis membrane, DMAB did not leach out. The suspension was of a milky white appearance before the start of experiment and no change was observed after 72 hours.

2.4.4.2 Centrifugation

A single run of 15,000 rcf for 20 minutes was employed. This gave difficulties with redispersion of the particles. A step process of centrifugation was then used, each run lasting 5 minutes, using the following rcf settings: 8000, 12000, 16000, 20000, 30000, and 40000. After recovery and pooling of the pellets from all the runs, the redispersed particles were again collected as per the following rcf settings: 8000, 12000, 16000, 20000, 25000, 30000, 35000 and 40000. This protocol was followed to process up to 6 batches. For higher numbers, the time duration was reduced to 3 minutes for the two runs and a third centrifugation cycle was introduced using the following rcf values: 8000, 12000, 16000, 20000, 24000, 28000, 32000, 36000 and 40000.

In order to verify the efficiency of the process, the amount of drug was determined in the supernatant. As seen in Figure 2.12, the amount of drug in supernatant decreased gradually with the steps of the centrifugation.

Figure 2.13 depicts the decrease in drug content in supernatant as a function of centrifugal force for the 1st washing cycle. It may be noted that full recovery of nanoparticles is not attained in the wash cycle. The drug content in the final formulation after the 3rd centrifugation cycle is around 25% of the original amount loaded as compared to 33% after 2nd cycle.
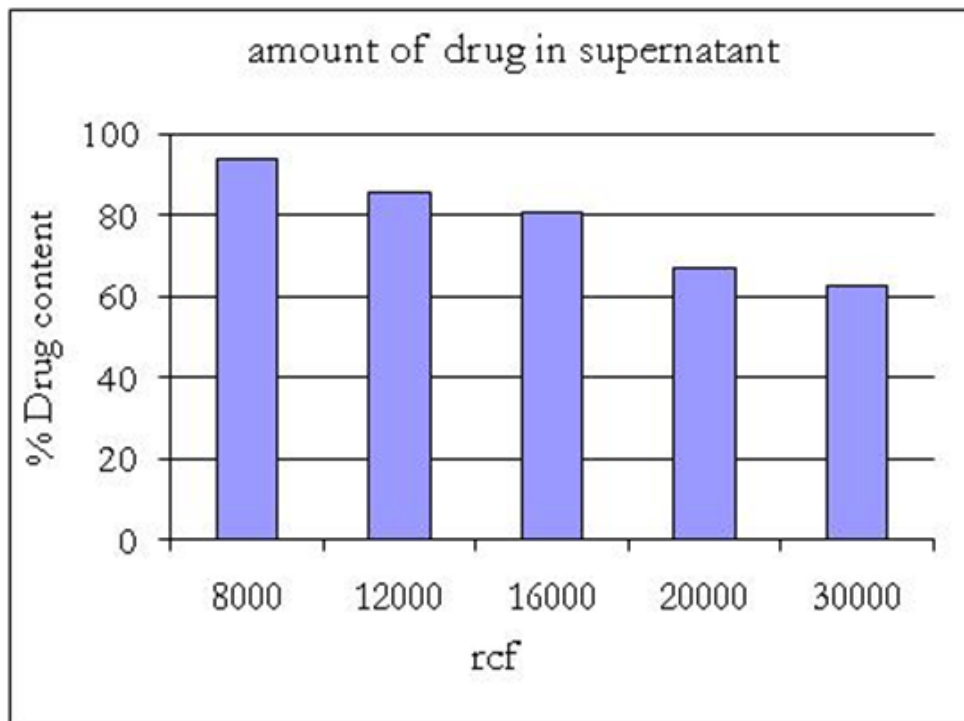
Figure 2.12: Decrease in drug content of supernatant of original suspension as a function of centrifugal force (n=1)
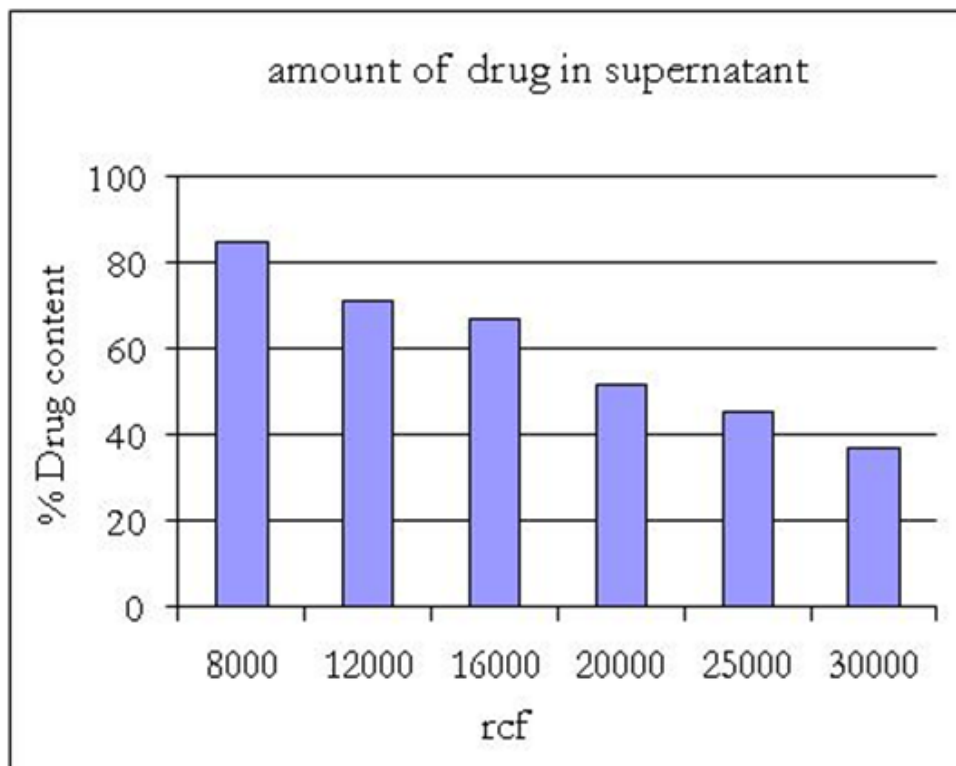
Figure 2.13: Decrease of drug content in supernatant of 1st washing as a function of centrifugal force (n=1).

2.4.4.3 Estimation of bound stabiliser

The calibration curve with double derivative spectroscopy analysis resulted in good correlation for quantitative analysis of DMAB in the range of 1-100 µg/ml (Figure 2.14).
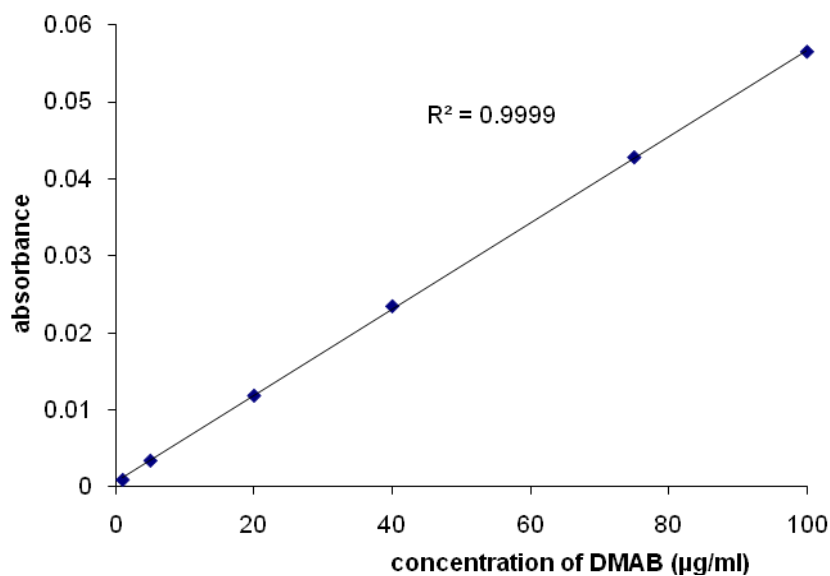
Figure 2.14: Calibration curve of analysis of DMAB

Table 2.6: Stabiliser bound and unbound

	Final suspension	in supernatant	in 1st washing	in 2nd washing
%DMAB detected	100	96.93	1.37	0.14
%DMAB remaining with particles by mass balance	100	3.06	1.69	1.55

The amount of DMAB bound to particles was estimated by determining the amounts in supernatant after centrifugation cycles. As shown in Table 2.6, only about 1.5% of the original amount of stabiliser was not recovered in the supernatant. Considering losses, the actual amount of stabiliser associated with the particles is expected to be even lower than this value.

2.4.5 Freeze drying of nanoparticles

The particle size and PDI of freeze dried particles are summarized in Table 2.7 and Table 2.8.

Table 2.7: Freeze drying of nanoparticles: sizing results experiment 1 & 2. Exc: Excipient, NP: nanoparticles

Excipient	NP conc (%w/v)	Exc Conc (%w/v)	Ratio Exc to NP	Experiment 1 Size (nm)	Experiment 1 PDI	Experiment 2 Size (nm)	Experiment 2 PDI
Initial Parameters				112.6	0.106	112.6	0.106
None	0.6	0	0	3972.0	1.000	3990.0	1.000
Glucose	0.6	5	8.333333	177.4	0.260	225.0	0.266
Glycine	0.6	5	8.333333	1923.0	0.961	2372.0	0.851
Lactose	0.6	5	8.333333	1012.0	0.805	371.7	0.496
Mannitol	0.6	5	8.333333	287.9	0.489	3623.0	0.660
PEG8000	0.6	5	8.333333	2199.0	1.000	308.9	0.624
Sorbitol	0.6	5	8.333333	319.7	0.695	2654.0	1.000
Sucrose	0.6	5	8.333333	183.2	0.268	318.4	0.350
Trehalose	0.6	5	8.333333	135.4	0.227	138.8	0.260
Xylitol	0.6	5	8.333333	137.3	0.263	130.2	0.263
Shading							
Size (nm)	≤ 150		$150 < \text{Size} < 200$		≥ 200		
PDI	≤ 0.150		$0.150 < \text{PDI} < 0.200$		≥ 0.200		

Experiment 1 was performed on a vacuum drier and without monitoring the sample temperature, and the PDI was increased with and without the excipients. The PDI and particle size increased for experiment 2 also. When the freeze drying was then carried out at -45°C, the particle size and PDI were maintained for some samples. Typically, a solid content higher than or equal to 6% w/v of the original suspension and an excipient to nanoparticle ratio of 3.75 or more were found better for preserving the size characteristics of nanoparticles (Table 2.7 and Figure Apx E.1). Increasing the duration of freeze-drying and reducing shelf (product) temperature to -50°C further improved the product profile in terms of size and PDI (Table 2.8 and Figure Apx E.2).

Table 2.8: Freeze drying of nanoparticles: sizing results experiment 3 & 4. Exc: Excipient, NP: nanoparticles

Excipient	NP conc % w/v	Exc Conc %w/v	Ratio Exc to NP	Total solid	Experiment 3		Experiment 4		Excipient % w/w total solids
					Size (nm)	PDI	Size (nm)	PDI	
Initial Parameters					123.4	0.036	123.4	0.036	
None	1	0	0	1	3859.0	1.000	4907.0	1.000	0
None	2	0	0	2	4766.0	1.000	4284.0	0.489	0
Glucose	2	2.5	1.25	4.5	184.8	0.382	377.8	0.416	56
Glucose	2	5	2.5	7	150.3	0.247	135.1	0.223	71
Glucose	2	7.5	3.75	9.5	138.5	0.230	132.7	0.161	79
Glucose	1	2.5	2.5	3.5	276.0	0.398	132.2	0.181	71
Glucose	1	5	5	6	128.2	0.079	141.2	0.187	83
Glucose	1	7.5	7.5	8.5	135.7	0.241	129.5	0.122	88
Glycine	2	2.5	1.25	4.5	2045.0	1.000	1108.0	0.987	56
Glycine	2	5	2.5	7	1511.0	0.946	2868.0	0.454	71
Glycine	2	7.5	3.75	9.5	7942.0	1.000	5291.0	0.419	79
Glycine	1	2.5	2.5	3.5	2624.0	1.000	632.0	0.553	71
Glycine	1	5	5	6	897.1	0.746	24600	0.693	83
Glycine	1	7.5	7.5	8.5	28980.0	0.590	7357.0	1.000	88
Lactose	2	2.5	1.25	4.5	667.8	0.606	1513.0	1.000	56
Lactose	2	5	2.5	7	329.3	0.427	148.2	0.288	71
Lactose	2	7.5	3.75	9.5	129.4	0.146	134.2	0.164	79
Lactose	1	2.5	2.5	3.5	0.0	0.000	176.6	0.317	71
Lactose	1	5	5	6	136.6	0.278	145.5	0.233	83
Lactose	1	7.5	7.5	8.5	137.2	0.195	148.2	0.240	88
Mannitol	2	2.5	1.25	4.5	1605.0	1.000	2199.0	0.745	56
Mannitol	2	5	2.5	7	287.3	0.323	199.1	0.210	71
Mannitol	2	7.5	3.75	9.5	242.7	0.275	703.2	0.684	79
Mannitol	1	2.5	2.5	3.5	148.4	0.161	187.0	0.196	71
Mannitol	1	5	5	6	137.9	0.200	215.3	0.253	83
Mannitol	1	7.5	7.5	8.5	673.3	0.675	477.6	0.424	88
PEG8000	2	2.5	1.25	4.5	1637.0	1.000	468.8	0.685	56
PEG8000	2	5	2.5	7	363.9	0.389	199.4	0.280	71
PEG8000	2	7.5	3.75	9.5	240.4	0.361	209.6	0.347	79
PEG8000	1	2.5	2.5	3.5	392.6	0.427	301.1	0.385	71
PEG8000	1	5	5	6	198.2	0.312	218.0	0.298	83
PEG8000	1	7.5	7.5	8.5	188.0	0.280	199.9	0.323	88
Sorbitol	2	2.5	1.25	4.5	2239.0	1.000	2217.0	0.942	56
Sorbitol	2	5	2.5	7	929.2	0.780	1090.0	0.753	71
Sorbitol	2	7.5	3.75	9.5	412.6	0.446	568.1	0.542	79
Sorbitol	1	2.5	2.5	3.5	691.0	0.688	924.2	0.747	71
Sorbitol	1	5	5	6	172.6	0.331	352.0	0.366	83
Sorbitol	1	7.5	7.5	8.5	154.9	0.235	243.1	0.431	88
Sucrose	2	2.5	1.25	4.5	128.9	0.114	128.9	0.113	56
Sucrose	2	5	2.5	7	128.6	0.193	165.6	0.369	71

Excipient	NP conc % w/v	Exc Conc % w/v	Ratio Exc to NP	Total solid	Experiment 3		Experiment 4		Excipient % w/w total solids
					Size (nm)	PDI	Size (nm)	PDI	
Sucrose	2	7.5	3.75	9.5	128.7	0.120	135.6	0.109	79
Sucrose	1	2.5	2.5	3.5	138.1	0.188	132.0	0.123	71
Sucrose	1	5	5	6	214.1	0.345	138.8	0.230	83
Sucrose	1	7.5	7.5	8.5	140.9	0.179	194.2	0.351	88
Trehalose	2	2.5	1.25	4.5	587.9	0.624	124.2	0.211	56
Trehalose	2	5	2.5	7	137.6	0.251	126.0	0.156	71
Trehalose	2	7.5	3.75	9.5	132.8	0.138	131.3	0.104	79
Trehalose	1	2.5	2.5	3.5	128.6	0.103	143.7	0.248	71
Trehalose	1	5	5	6	127.3	0.082	129.9	0.218	83
Trehalose	1	7.5	7.5	8.5	121.4	0.032	128.5	0.094	88
Xylitol	2	2.5	1.25	4.5	139.3	0.249	125.9	0.076	56
Xylitol	2	5	2.5	7	132.1	0.220	125.5	0.078	71
Xylitol	2	7.5	3.75	9.5	125.0	0.156	124.7	0.030	79
Xylitol	1	2.5	2.5	3.5	128.1	0.210	125.8	0.174	71
Xylitol	1	5	5	6	124.1	0.135	126.7	0.124	83
Xylitol	1	7.5	7.5	8.5	124.9	0.070	124.1	0.064	88

2.5 Discussion

HPLC is a highly efficient method of separation of analyte from a mixture and provides a reliable method of quantitative estimation of substance of interest. The high linearity over a broad range provided a means to accurately determine the amount of paclitaxel for drug loading studies.

It is now widely accepted that the performance of nanoparticulate formulation heavily depends on the particle size. Especially, particles smaller than 100 nm are considered desirable for drug delivery. However, most reported studies are in the range of 150-400 nm. On the other hand, specific objectives like tapping the EPR effect would require the particles to be bigger than a particular cut-off. This value can vary depending on the type of tumour being targeted. Thus the formulation developer should be able to either produce particles of a controlled size range or harvest the desired fraction from an encompassing pool. To be able to control the average particle size and the size range, the effect of different specifications of preparation conditions was studied. The method of preparation for this project was based on emulsification solvent evaporation. Though this method is one of the most widely used, it is not completely understood. Broadly, the thermodynamically stable emulsification of the two phases would require two critical inputs- (a) energy and (b) stabiliser.

Assuming spherical geometry, the volume of n_1 globules of average radius r_1 can be represented as

$$V_1 = n_1 \frac{4}{3} \pi r_1^3$$

If the globule size is changed to r_2, the number of globules will also change to n_2, so that

$$V_2 = n_2 \frac{4}{3} \pi r_2^3$$

But since the total volume of the internal phase is not changed, $V_1 = V_2$

Hence

$$n_1 \frac{4}{3}\pi r_1^3 = n_2 \frac{4}{3}\pi r_2^3$$

or

$$\frac{n_2}{n_1} = \frac{r_1^3}{r_2^3}$$

Similarly, using the formula for spheres, the ratio of surface areas shall be

$$\frac{S_2}{S_1} = \frac{n_2 4\pi r_2^2}{n_1 4\pi r_1^2}$$

Solving the above two equations, we get

$$\frac{S_2}{S_1} = \frac{r_1}{r_2}$$

Thus, the ratio of total surface areas of two different globule sizes is inversely proportional to the ratio of the diameters of the globules. A 40% decrease in average globule size of the internal phase will reflect as a 40% increase in total surface area of the globules. The increase in surface area brought about by decreasing the globule size requires the inclusion of the stabiliser or surfactant. These molecules align themselves at the interface between the two phases and reduce the surface tension, thereby reducing the thermodynamic instability. On dilution of this emulsion with water, ethyl acetate diffuses into water and with time evaporates away as a function of vapour pressure. It is postulated that each globule containing the polymer (and drug) dissolved in ethyl acetate precipitates to one particle. Thus the final particle characteristics depend heavily on the initial emulsion.

The study with variation of final volume of water added after homogenisation establishes that the migration of ethyl acetate in the water phase is not instantaneously complete. It is a slow process wherein equilibrium exists between the organic solvent dissolved in water and that

associated with the PLGA. The fact that stirring is required even after addition of water in the final dilution step proves that the homogenised system is not thermodynamically stable. Possibly, in absence of stirring, the diffusion layer of leaching ethyl acetate becomes sufficiently saturated so as to create bridges through which globules can fuse together. Another possibility is the formation of lamellar vesicles by DMAB that would aid such fusion. The precipitating polymer units then could fuse to further diffuse the interfacial energy by decreasing the surface area. A certain degree of agitation is thus necessary to prevent the boundary layer thickness from decreasing to these critical thresholds. A change in the design or dimensions or apparatus would warrant that a sufficient degree of spatial kinetics are maintained by agitation or mixing till any traces of ethyl acetate being associated with polymer units remain.

It was not possible to use vacuum distillation for a speedy removal of the organic solvent from the system because DMAB is a surfactant and rapidly formed foam with the escaping ethyl acetate.

Expectedly, the smallest particle size was obtained with 1% stabiliser. This is explained by better stabilization of the nanoglobules by a more comprehensive presence of the stabiliser at the interface of the two phases.

As previously mentioned, the energy required to decrease the particle size can be supplied by mechanical or pressure devices or sonication. For the purpose of this project, a conservative approach was taken considering the unknowns associated with sonication. Specifically, although migration of process between different apparatus for mechanical devices also has this caveat, it can still be overcome due to the wide variety of instrumentation and tools available. The sonication apparatus on the other hand provides a limited degree of control on operating parameters. A high speed tissue

homogeniser with a rotor within a shaft type of mixing tool was employed to introduce this energy into the system. Although the exact mechanism by which the energy is relayed to the system is not well explained, impact and shear are the two physical processes known to be involved. The higher speed imparts more energy that is trapped as the interfacial energy via the lowering of globule size and sustained till the nanoprecipitation by the DMAB. Since the rotor dimensions can vary, portability of rpm values between different types of homogenisers can be provided by using tip speed.

$$v = \omega r$$

Here v = tip speed in metre per second (m/s)

ω = angular velocity in radians per second (rad/s)

r = radius of rotor (m)

The angular velocity in rad/s can be calculated from rpm

$$\omega = \frac{2\pi}{60} \times rpm$$

As shown in Figure 2.15, there is a good correlation between the tip for the 7.5 mm rotor and the average particle size obtained.
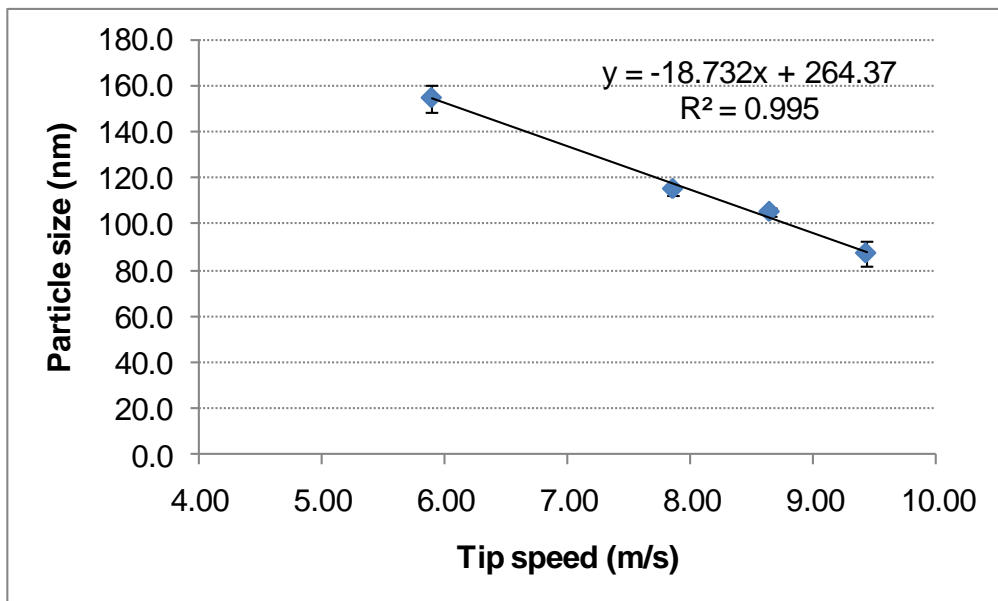
Figure 2.15: Correlation between tip speed (m/s) of homogeniser and particle size

A direct correlation was seen with ratio of organic to aqueous phases and particle size, with 3:10 ratio producing particles of average size ~70 nm. This can be explained by the ability of the stabiliser to effectively line the interface between the globules and the aqueous phase when the internal phase volume is lower.

In none of the parameters, a saturation effect was seen for the limits studied implying that it is possible to increase or decrease the particle size beyond the obtained values, but the effect might not be linear and would plateau outside a range. The foremost criteria to be set is the desired particle size and the particle preparation exercise should be carried out to then satisfy other product characteristics like drug loading and residual surfactant concentration. Additional factors like the practical limits of available instruments/techniques sometimes limit the extent to which the desirables can be achieved. For example, if centrifugation is the only method feasible for washing the particles, then the speeds of centrifuge creates a bottleneck for the lowest particle size that can be recovered as sediment.

The organic solvent used in the preparation of nanoparticles affects particle characteristics (Sahana et al. 2008). Ethyl acetate was the suitable organic solvent to formulate nanoparticles. The other two solvents viz. acetone and dichloromethane resulted in precipitation of the polymer with the method employed. Since acetone is miscible with water in all proportions, the gradual addition of water was not able to prevent clumping of the polymer. The high vapour pressure of dichloromethane also posed similar problems resulting in rapid precipitation of the polymer. With both these solvents, the particles prepared were bigger and of a higher PDI than ethyl acetate. In addition, there was always some precipitation of the polymer deeming the sample unsuitable for size measurement (PDI was 1.0). An interesting

observation was that introduction of the drug into organic solvent after polymer dissolution resulted in precipitation of paclitaxel along the sides of the mixing vessel. This suggests that the polymer chains still maintain some degree of inaccessibility for the solvent and drug and hence can affect drug release also. The limited loading capacity of the drug in the particles might be due to limited drug holding capacity of the PLGA used in this study.

Increasing the stabiliser concentration decreased the encapsulation of paclitaxel in the nanoparticles. This can be explained on the basis of the solubilising capabilities of surfactants like DMAB. It readily forms micelles in the aqueous environment, which incidentally is the form in which paclitaxel is administered in the marketed formulation Taxol®. A fraction of the drug can get solubilised in these micelles outside the ethyl acetate globules containing the polymer and thus is lost in the supernatant when the particles are harvested by centrifugation.

The estimation of drug in the supernatants of different centrifugation steps gave credible proof establishing that the drug is indeed entrapped within the nanoparticles and is not just distributed in the DMAB micelles or vesicles. Average recovery of drug (with respect to initial loading) after centrifugation was calculated to be 44, 33 and 25% after the end of 1st, 2nd and 3rd cycle. This reflects that after approximately 75% of particles are recovered in 2nd and 3rd centrifugation cycle. Extrapolating it to the 1st cycle, the actual amount of entrapment in particles can be considered to be 58% w/w of the original amount. Typically, two cycles of centrifugation were employed: first one to harvest the nanoparticles from the large volume of suspension and the second one to wash the unbound stabiliser. When more than 6 batches were to be centrifuged, only then a 3rd cycle was used to get rid of the extra stabiliser. This extra amount accumulates due to the residual supernatant left

following decanting.

DMAB could not be removed by dialysis. A possible explanation is provided by the fact that DMAB forms micelles as well as vesicles. These structures if sufficiently stable, can not pass through the 12,000 Da cut off membrane. An additional concern was that tap water was used for dialysis. It was observed during the project that chloride ions turn a solution of DMAB cloudy. Probably the chloride ions which could easily diffuse into the dialysis bag precipitated DMAB which then failed to leach out.

The final amount of DMAB still associated with the particles after washing once with water was less than 2% of the original amount. This shows that majority of the DMAB is only important in deciding the globule size of the initial emulsion which then decides the particle size. A rather small fraction either co-precipitates with the particles or is adsorbed at the surface to impart the positive zeta potential and hydrophilicity.

The particles were imaged using AFM. The size ranges imaged corresponded well with the data obtained from DLS. The smooth architecture of particles and monolayer of particles obtained from an aqueous dispersion signifies the excellent mobility of particles with respect of each other. Also, it can be seen from the DLS data (Figure 2.11) that although the particle size is reported to be of an average value around 115 nm, the size distribution ranges from 50 to 300 nm. According to the zetasizer instrument, this corresponds to a PDI of 0.1.

In freeze drying study, trehalose and xylitol were found to best preserve the particle size characteristics. More interestingly, the w/w excipient to nanoparticle ratio should be higher than or equal to 3.75 even with these cryoprotectants. Ratio of 2.5 was not able to preserve particle size and PDI. Also, a higher solid content (6%w/v or above) resulted in recovery of

nanoparticles with original size and PDI Appendix E. In terms of the process, it emerged that the primary drying of the formulation should be carried out below -45° C. This temperature is lower than the reported T_g' (frozen solution glass transition temperature) of the eutectic mixtures of most commonly used sugars in freeze-drying as well as the T_g' of PLGA. It represents the collapse temperature for the formulation (Saez et al. 2000). If the primary drying is carried out above this temperature, there is a tendency for the water to suddenly liquefy and the cake collapses (Franks 1998; Holzer et al. 2009). ,

2.6 Conclusions

- Stabilizer concentration and speed of homogenization were found to have an inverse correlation on the size of nanoparticles with the employed process of solvent emulsification-diffusion method. Low organic to aqueous phase ratio produced smaller particles with PLGA 50:50 copolymer composition. The formulation requires constant stirring until organic solvent is removed by evaporation.

- Using 1% DMAB, paclitaxel loaded particles of average hydrodynamic diameter of 125nm and PDI around 0.1 were prepared. With an initial drug loading of maximum 5% w/w of polymer weight, 44% entrapment was achieved. AFM images depicted smooth spherical surface.

- The particles can be collected from the suspension using stepwise centrifugation. The procedure also provides a method to remove the unbound stabiliser by repeating the procedure after washing with fresh water.

- Xylitol and trehalose can be used as cryoprotectants for lyophilization of the nanoparticles. Total solid content in the freeze-drying mixture should be equal to or more than 6%w/v and ratio of excipient to nanoparticles should be equal to or more than 3.75.

The developed formulation was then subjected to in vitro assays to establish the safety and efficacy of the particles towards cells grown in culture media. These tests are rapid and provide a primary screen before testing pharmaceutical products in animals. The next chapter focuses on experimentation carried out to evaluate the nanoparticles in cell culture assays.

3 Evaluation of formulation in cell culture

3.1 Introduction

With the cost of bringing new molecules to the market becoming more expensive, longer and increasingly challenging, we are witnessing a parallel climbing interest in novel drug delivery systems (Pillai et al. 2001). However the novelty that introduces functionality is also seen as potency that could go either way and hence the regulators demand that all innovations be proved safe prior to use. The primary concerns about these base carriers are biocompatibility and biodegradability. Proving safety of the nanoparticles is not just meant to satisfy the regulators but is an integral part of product development.

While new excipients are to be individually assessed, the USFDA maintains a list of material approved for use in humans and terms them **G**enerally **R**ecognized **A**s **S**afe (GRAS). The use of a GRAS substance is not subject to premarket review and approval by FDA.

Development of new pharmaceutical products often involves new material with no prior safety data. Such substances need to be screened for possible toxicity. Due to the caustic nature of quaternary ammonium compounds, such substances need to be screened for possible cytotoxicity. Above all, the concerns expressed over nanoparticles warrant a strong need that these particles and surfactants should be screened for their safety before they get to clinic.

Cell culture models provide rapid and simple methods to predict toxicity thereby reducing the need for animal testing that involve ethical considerations and significant costs. Primary culture of cells can be defined as a culture started from cells, tissues or organs taken directly from

organisms. A cell line is formed when a primary culture is subcultured. A cell line may be finite (survives for a fixed number of population doublings, usually around 40–60, before senescing and ceasing proliferation) or continuous (immortal, over 200 population doublings) (Source: UKCCCR guidelines for the use of cell lines in cancer research; (Schaffer and Terminology Committee Chair Tissue Culture 1990)).

3.1.1 Cytotoxicity assays

In vitro cytotoxicity or cell death assays are an important tool in the primary screening of efficacy of anticancer compounds. The cytotoxicity can be measured as

(a) damage to the cell membrane

(b) disruption of normal cell metabolism or cell viability

(c) generation of free radicals or reactive oxygen species.

(d) apoptosis

(e) release of inflammatory markers.

Most frequently used tests rely on the damage to the cellular integrity whereby certain dyes (e.g. trypan blue) that otherwise can not penetrate the plasma membrane enter the cell by diffusing freely through the compromised barriers. Some rely on leaching out of intracellular chemicals or enzymes like lactate dehydrogenase (LDH).

3.1.1.1 MTT assay

In this assay, cellular metabolic activity is evaluated. The yellow tetrazolium salt 2-(4,5-dimethylthiazol-2-yl)-3,5-diphenyl-2H-tetrazol-3-ium bromide (MTT) is converted by mitochondrial dehydrogenases of metabolically active cells to an insoluble purple formazan product (Figure 3.1) (Mosmann 1983). The insoluble salt is dissolved using either of the following: (a)

dimethylsulphoxide, (b) a solution of sodium dodecyl sulphate in dilute hydrochloric acid or (c) mixture of ethanol and an acid. The conversion by mitochondrial reductase can only occur in living cells and thus the amount of formazan dye which is spectrophotometrically detected between 500-600 nm is directly proportional to the cell viability.

2-(4,5-dimethylthiazol-2-yl)-3,5-diphenyl-2H-tetrazol-3-ium bromide

(E,Z)-1-(4,5-dimethylthiazol-2-yl)-3,5-diphenylformazan
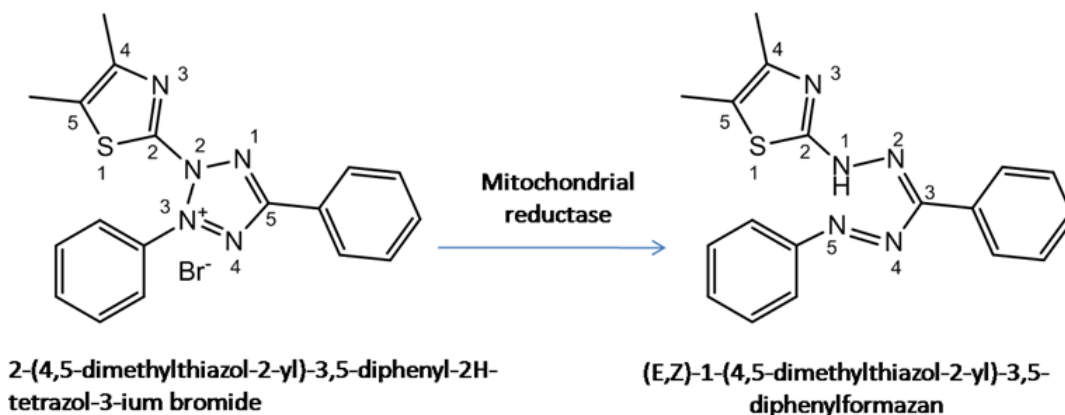
Figure 3.1: Conversion of MTT to formazan dye

3.1.1.2 LDH assay

LDH is a cytosolic enzyme that is readily released upon cell membrane damage; and is hence used as a tool to monitor cellular toxicity of test substances. LDH released into the assay medium can be measured via a coupled enzymatic assay. The LDH oxidizes lactic acid to pyruvic acid generating NADH and protons from NAD^+. A second enzyme called diaphorase then catalyzes the reduction of a yellow tetrazolium salt (3-(4-iodophenyl)-2-(4-nitrophenyl)-5-phenyl-2H-tetrazol-3-ium chloride) into a red formazan salt (Figure 3.2) which is colourimetrically detected at 490 nm. The advantage of this assay over MTT assay is that the formazan salt produced is water soluble and there is no need to dissolve any crystals (which can be hard to dissolve in MTT assay).
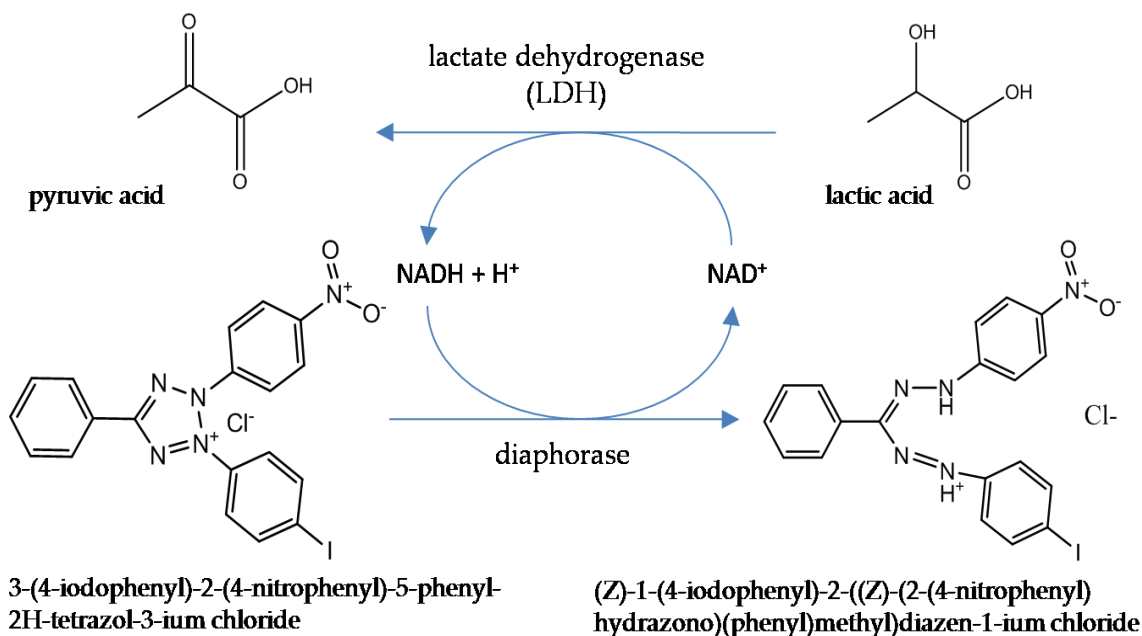
Figure 3.2: Chemistry of LDH cytotoxicity assay

3.1.1.3 AlamarBlue® assay

This assay is based on the conversion of resazurin (RZR) to resorufin (RRF) by the mitochondrial enzymes. It is a redox reaction where the blue/purple oxidized form RZR is converted to the pink reduced product RRF as depicted in Figure 3.3. The calculations suggested by the manufacturer were modified and are derived in Appendix F.

7-hydroxy-3-oxo-3H-phenoxazine 10-oxide   7-hydroxy-3H-phenoxazin-3-one
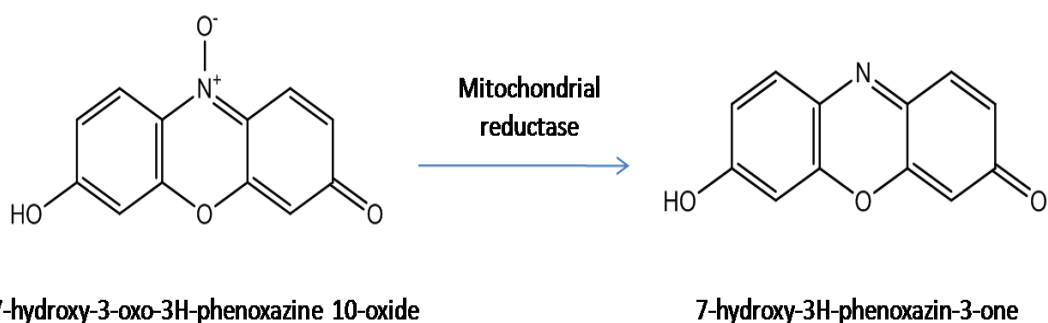
Figure 3.3: Chemistry of AlamarBlue® assay

3.1.2 Pgp efflux studies

Drug resistance is a common cause of treatment failure in anticancer therapy.

Frequently, the drug resistance is expressed through higher concentration of drug transporters that pump the drug out of the cells. Today a lot of research is focused on the drug transporters especially the Pgp (Chan et al. 2004). Pgp efflux systems and drug transport across cell monolayers such as those of Caco-2 provide important insights into the drug permeability and efflux. However, these systems are only average predictors of the transport and might not exactly mimic the *in vivo* outcome evaluated in animals or humans. A wide range of cell monolayer models have been developed that mimic the *in vivo* intestinal epithelium. Most of these consist of cancer cells that rapidly grow into monolayers maintaining if not all, majority of the characteristics of differentiated tissue types. Some cell models that are routinely used for permeability screening are Caco-2, MDCK, LLC-PK1, HT-29, and IEC-18 (Braun et al. 2000; Balimane and Chong 2005). HT-29 cells have the advantage of presence of mucus producing goblet cells, but the most popular in this category is the Caco-2 cell model (Bailey et al. 1996).

Caco-2 cells are derived from a human colon adenocarcinoma, and undergo spontaneous differentiation into enterocytes and are polarized with well established tight junctions. The *in vitro* permeability studies through these cells correlate well with the *in vivo* permeability results and thus they are considered as the gold standard for *in vivo* permeability surrogates (Artursson et al. 1996). The transport of particles can be studied by analyzing the concentrations on the two sides of membrane while ensuring membrane integrity by measuring the trans-epithelial electrical resistance (TEER). An interesting aspect to be explored is the role of Pgp on the transport of nanoparticles- whether they can efflux-out the particles the same way as substrate drugs.

3.1.2.1 Rhodamine 123 transport assay in Transswell® membrane plates

Rhodamine 123 is a lipophilic cationic compound (molecular mass 380.82) and is a substrate for Pgp (Jacques 2000). Transswell® membrane plates (Corning Life Sciences, Germany) consist of a 'well within a well' arrangement with a 10μm thick transparent polyester membrane at the bottom of the inner well that acts like a filter support on which cells can be attached. Culture medium is added in both the cells and the inner well represents the apical side of cells exhibiting uniformly polarized growth. The outer compartment represents basolateral side. Aliquots of media can be collected from both sides to determine transport across a monolayer of cells. Being a substrate of Pgp, rhodamine 123 is expected to concentrate on the apical side. The relative change of concentration and transport ratios can be calculated after challenge by an inhibitor or chemosensitizer.

3.1.2.2 Calcein-AM assay

Calcein acetoxy methyl ester (Calcein-AM) is a hydrophobic non-fluorescent compound that is readily transported both ways across the cell membrane. It is converted by esterases inside the cell to the polar and fluorescent Calcein which can not cross the cell membrane and thus gets entrapped inside the cell and can be detected quantitatively (Figure 3.4).

Additionally, Calcein is a substrate for the Pgp efflux pumps and is pumped out by cells that express this efflux transporter. In these cells, the concentration of Calcein is higher outside the cells compared to inside. Hence its entrapment inside the cell compared against a control that inhibits the Pgp activity can provide quantitative estimate of the degree of inhibition. Normally cyclosporin A or verapamil are used as the positive controls and the Pgp efflux inhibition is represented relative to that obtained with them.
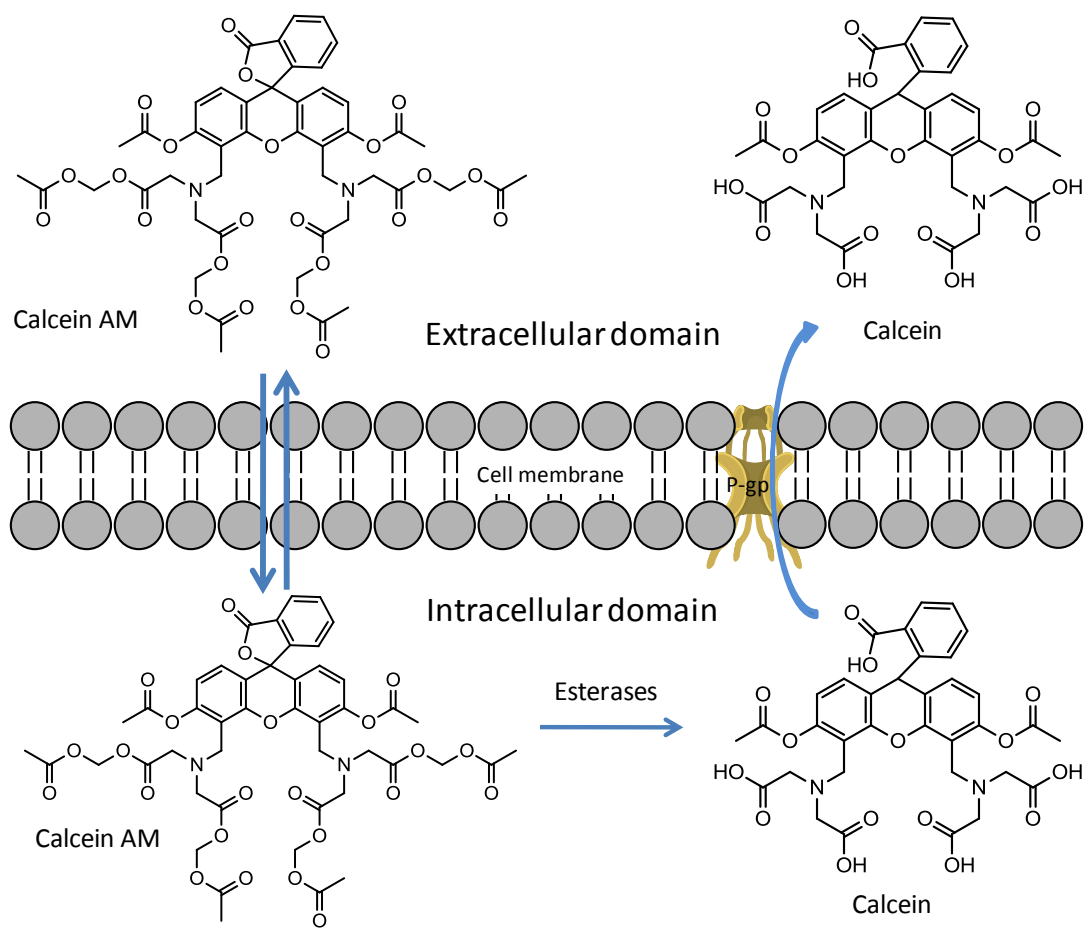
Figure 3.4: Calcein-AM transport and bioconversion to Pgp substrate Calcein

3.2 Specific aims

In this background, the following specific aims were defined for the cell culture experiments

- Assessment of the developed formulation by routinely used cytotoxicity assays

- Estimation of Pgp efflux inhibition by nanoparticles

- Determination of efficacy of developed nanoparticles in cytotoxicity towards cancer cells in culture.

- Determination of efficacy of developed nanoparticles in cytotoxicity towards drug resistant cells in culture.

3.3 Methods

3.3.1 Cell culture

Caco-2 cells, clone C2BBe1, were purchased at passage 60 from American Type Culture Collection (ATCC, Manassas, VA). MDCK II -mdr1 cells, which were a kind gift by Dr Piet Borst (Netherlands Cancer Institute, Division of Molecular Biology, Amsterdam) were used from passage 11 to 32. B16F0 cells were gifted by Dr Katherine Carter (SIPBS, University of Strathclyde, Glasgow). Cells were grown to ~90% confluence in 75 cm^2 T-flasks with appropriate cell culture medium supplemented with 10% foetal bovine serum (FBS) and where applicable, 1% non-essential amino acids (NEAA) or antibiotics . MDCK cells were grown in presence of 200µg/ml of geneticin (G418). Culture medium was changed every second day and cells were grown at a temperature of ~37 °C in an atmosphere of ~85% relative humidity and ~5% CO_2. On reaching confluency, the cells were split using Trypsin-EDTA and seeded at the required density. For toxicity studies, cells were seeded at a density of 10-20,000 cells/well (30-60,000 cells/cm^2). Experiments were done after the cells reached 50-90% confluency.

3.3.2 Cytotoxicity studies on DMAB

3.3.2.1 MTT assay

After incubating the cells with the surfactant or particles for 6 hours, 15 µl of MTT solution (5 mg/ml) was added to each well, followed by incubation at 37 °C for 3 hours. The cell culture medium including complex solution was carefully removed and 150 µl of MTT solvent was added to dissolve the formed formazan crystal. After shaking the plate for 30 min, absorbance was immediately measured at 570 nm using a microplate reader. Background

absorbance at 690 nm was subtracted. Cells incubated with buffer were used as a control. The cell viability was expressed as a percentage using the following equation:

$$cell\ viability\ (\%) = \frac{OD_{570-690}^{sample}}{OD_{570-690}^{control}} \times 100\%$$

3.3.2.2 LDH assay

Caco-2 cells were grown on 96-well tissue culture plates with a flat bottom (Greiner Bio-One GmbH, Frickenhausen, Germany) in medium supplemented with 1% NEAA for 8 days as previously described. In fresh Hank's balanced salt solution (HBSS pH 7.4) (~37 °C), monolayers were incubated (4 hours) with the analyte. After the incubation, LDH release into the supernatant was determined using the cytotoxicity LDH kit as described by Roche Diagnostics. Fresh HBSS and Triton X-100 (0.1%) in HBSS were used as negative and positive controls, respectively. LDH release has been expressed relative to control values. Experiments were performed with $n = 4$ for each concentration.

Cytotoxicity studies of paclitaxel nanoparticles were performed using the LDH release assay in cultured Caco-2, MDCK II mdr 1, Calu-3 and A549 cell lines, in an 8 hours incubation study in HBSS. The cells were grown using standard protocol using the prescribed medium.

Composition of HBSS: 0.137 M NaCl, 5.4 mM KCl, 0.25 mM Na_2HPO_4, 0.44 mM KH_2PO_4, 1.3 mM $CaCl_2$, 1.0 mM $MgSO_4$, 4.2 mM $NaHCO_3$.

3.3.3 Cytotoxicity studies of blank PLGA nanoparticles

Cytotoxicity of blank (containing no drug) PLGA nanoparticles made with DMAB was studied by using LDH and MTT assays.

Three different types of nanoparticles prepared with 1.0, 0.33 and 0.1% w/v

DMAB corresponding to average sizes of 100, 135 and 180 nm were tested at concentrations corresponding to 10, 100 and 1000 µg/ml in HBSS pH 7.4 buffer.

3.3.4 Pgp efflux study

3.3.4.1 Rhodamine 123 transport assay

Pgp inhibition assay was carried out with DMAB to assess if this compound has potential to inhibit Pgp and hence increase the bioavailability of drugs. Caco-2 cells were seeded on top of Transwell® inserts (type 3460, pore size 0.4 µm, area 1.13 cm^2) at a density of ~60,000 cells/cm^2. TEER was measured and only monolayers with a TEER > 350 Ω/cm^2, with background subtracted, were used for transport studies. Cells were grown for 21 days in DMEM supplemented with 10% foetal bovine serum (FBS) and 1% non-essential amino acids (NEAA). Culture medium was changed every second day and cells were grown at a temperature of ~37 °C in an atmosphere of ~85% relative humidity and ~5% CO_2.

Caco-2 monolayers were used 21–25 days after seeding. Rhodamine transport was assessed in absorptive (apical to basolateral, A → B) and secretory (B → A) directions. Prior to Rhodamine transport experiments, the monolayers were pre-incubated (1 hour) with DMAB solutions (3.3. 33, and 330 µM) on both sides. Subsequently, at $t = 0$ min, a solution of Rhodamine (13 µM in HBSS pH 7.4) was added to the donor compartment and pure HBSS to the receiver compartment, both sides contained DMAB solutions. Throughout the experiments, the plates were agitated using an orbital shaker (IKA®-Werke GmbH and CO KG, Staufen, Germany) at 100 ± 20 rpm. Samples were taken after 30, 60, 120, 180, and 240 min from the receiver compartment. After each sampling, an equal volume of fresh transport buffer

(~37 °C) was added to the receiver compartment. Experiments were performed for $n = 3$. To ensure integrity of the monolayers, TEER values were measured on the day of the experiment, after 1 hour of pre-incubation, and at the end of the experiment.

Flux was determined using receiver compartment Rhodamine steady-state appearance rates ($\frac{dQ}{dt}$; µg/s). Rhodamine was quantified using a CytoFluor-2 fluorescence plate reader (Perkin Elmer Biosystems, Weiterstadt, Germany) operating at excitation wavelength of 485 nm and emission wavelength of 530 nm. Apparent permeability (P_{app}) was calculated according to:

$$P_{app} = \frac{dQ}{dt}\frac{1}{C_0 A}$$

where A (cm²) is the nominal surface area of the monolayer and C_0 (µg/ml) is the RHO concentration in the donor compartment at $t = 0$. Relative change of P_{app} (cm/s) was calculated according to the equation:

$$Relative\ increase\ or\ decrease = (1 - \frac{P_{app}^{sample}}{P_{app}^{Rhodamine}}) \times 100$$

3.3.4.2 Calcein-AM assay

Pgp inhibition assay using Calcein-AM was performed in MDCK II mdr1 cell lines grown at a seeding density of 80,000 cells/well in a 96 well plate and performing the assay after 4-6 days. After removing the medium , the cells were washed with HBSS pH 7.4 buffer and pre-incubated with nanoparticles for 4 hours. HBSS pH 7.4 buffer was used as negative control and 10 µM Cyclosporine A as positive control (representing 100% Pgp inhibition). The pre-incubation solution was replaced with fresh sample containing 1 µM Calcein-AM and cells further incubated for 30 min following which the cells were washed with ice cold HBSS buffer. The cells were then lysed using 1% w/v Triton-X in HBSS over 10 min and the entrapped Calcein was

quantitatively estimated using fluorescence plate reader (excitation at 485 nm, emission at 520 nm).

The percentage inhibition was calculated using the following formula.

$$\% \, Relative \, inhibition = \frac{F_{test \, compound} - F_{negative \, control}}{F_{positive \, control} - F_{negative \, control}} \times 100$$

(here F denotes the fluorescence readings of the respective samples)

Three different types of nanoparticles prepared with 1.0, 0.33 and 0.1% w/v DMAB corresponding to average sizes of 100, 135 and 180 nm were tested at concentrations corresponding to 10, 100 and 1000 µg/ml in HBSS pH 7.4 buffer.

3.3.5 Cytotoxicity studies of drug loaded PLGA nanoparticles

Caco-2, MDCKII-mdr1, Calu-3 and A549 cells were exposed to nanoparticles prepared with 5% initial drug loading and the cytotoxicity was measured by LDH assay. Three different concentrations of particles corresponding to 10, 100, and 1000 µg/ml were used in the assay. The objective of this study was to determine the cytotoxicity of nanoparticles per se. The equivalent concentration of paclitaxel in the particles was 0.2, 2 and 20 µg/ml.

3.3.6 Efficacy studies in cells used for melanoma model in mice

AlamarBlue assay was used to determine the efficacy of the developed nanoparticulate formulation. B16F0 cells (a type of mouse melanoma) were used up to passage 10.

3.3.6.1 Cell proliferation studies

The murine melanoma cell line, B16F0 was cultured in RPMI 1640 supplemented with 2 mM L-glutamine, 100 U/ml penicillin, 100 μg/ml streptomycin, and 10% heat-inactivated foetal bovine serum. Cells were seeded at concentrations ranging from 25 to 6400 cells/well (100 µl of cell

suspension at concentrations varying from 250 to 64000 cells/ml). The cells were then incubated at standard conditions for 48, 72 and 96 hours following which the culture medium was replaced with AlamarBlue® solution at 10 times dilution of supplied stock in culture medium. The cells were further incubated for 24 hours and the absorbance was recorded in a plate reader at 570 and 600nm. The cell proliferation was calculated as discussed in Appendix F.

3.3.6.2 Cytotoxicity studies

Cells were seeded at a density of 800 cells/well (100 µl of cell suspension at concentration of 8000 cells/ml. After letting the cells attach and grow for 24 hours, they were incubated for a further 60 hours with the test substance suitably diluted in 50 µl of culture medium. At the end of 60 hours of incubation, 50 µl of 20% v/v AlamarBlue® in culture medium was added and the cells incubated for a further 12 hours, following which the absorbance was recorded in a plate reader at 570 and 600nm. The percent reduction of AlamarBlue® as compared to the positive control was calculated as discussed in Appendix F.

Paclitaxel in dimethylsulphoxide (DMSO) was compared with paclitaxel as Taxol® (micellar dispersion in mixture of cremophor EL and ethanol which was then diluted in normal saline), and that encapsulated in PLGA nanoparticles. Blank nanoparticles at PLGA weight equivalent doses were used as control.

3.3.7 Efficacy studies in cells used for carcinoma model in mice

Carcinoma is defined as a cancer that arises from epithelial cells. A2780 is a human ovarian carcinoma cell line that is sensitive to doxorubicin and a few other cytotoxic drugs. Resistance to drugs has been induced in this cell line;

2780AD being a variant that is resistant towards doxorubicin. The mechanism of resistance is over expression of the Pgp and this resistance is shared towards other anticancer drugs that are substrates (Dantzig et al. 1996). This cell line was used to induce tumours in nude mice and the study is discussed in Chapter 4.

3.3.7.1 Cell culture

The human ovarian carcinoma cells, A2780 and its resistant variant 2780AD was provided by Dr. T. C. Hamilton (Fox Chase Center, Philadelphia, PA). The 2780AD cells are about 65- and 540-fold resistant to doxorubicin and paclitaxel, respectively (Mistry et al. 2001). They were maintained in Roswell Park Memorial Institute 1640 (RPMI 1640) medium containing glutamine (2 mM) and foetal calf serum (10%).

Cells were grown to ~90% confluence in 75 cm^2 T-flasks Culture medium was changed on alternate days and cells were cultured at a temperature of ~37 °C in an atmosphere of ~5% CO_2 and ~85% relative humidity.

3.3.7.2 Cytotoxicity assay

Drug sensitivity was determined by a tetrazolium dye based assay. Cells were seeded at a density of 2 x 10^3 (2780AD) or 1 x 10^3 (A2780) cells per well in 96 well flat bottomed plates (Linbro from ICN Biomedicals Ltd., High Wycombe, Bucks, UK) and allowed to attach and grow for 48 hours. The plated cells were exposed for times ranging from 24-72 hours to the different formulations. After the end of incubation period, the challenge was withdrawn and the cells grown in fresh medium for 72 hours, following which cells were fed with medium containing HEPES buffer (10 mM) and MTT (50 μl, 5 mg/ml) was added to each well to assess metabolically active cells. Plates were incubated in the dark at 37°C for 4 hours, medium and

MTT removed and MTT-formazan crystals dissolved in dimethyl sulphoxide (200 μl/well). Glycine buffer (25 μl/well, 0.1 M, pH 10.5) was added and the absorbance measured at 570 nm in a multi-well plate reader (Model 3550 EIA reader, Bio-Rad, Hemel Hempstead, Herts., UK). A typical dose response curve consisted of eight drug concentrations and four wells were used per drug concentration. Within an experiment triplicate determinations were made for each treatment (n=12) and three dose response curves were obtained from separate plates.

3.3.7.2.1 Biological assay for the drug

Due to the high cost of the drug available from standard chemical suppliers, paclitaxel was purchased from a bulk drug manufacturer. This paclitaxel (Genexol) was compared against the paclitaxel procured from Sigma Aldrich. Free paclitaxel from both sources was dissolved in DMSO and 2780AD cell line was challenged with different concentrations for 72 hours. The absorbance was corrected for background and vehicle and converted to percentage survival.

3.3.7.2.2 Efficacy study of paclitaxel loaded nanoparticles

Nanoparticles containing paclitaxel were either prepared under sterile conditions or filtered through a 0.22 μm filter. Paclitaxel in DMSO and polymeric nanoparticles containing paclitaxel and equivalent amount of blank nanoparticles were diluted in cell culture medium. A2780 and 2780AD cell lines were challenged with different amounts of the formulation (corresponding to predetermined paclitaxel concentrations) for 24 hours. Free paclitaxel dissolved in DMSO was used as control at same concentration of paclitaxel. Four wells/plate were used for each concentration and 3 plates per experiment (n=12). Challenge was withdrawn after 24 hours and cells

were allowed to grow for 72 hours in cell culture medium and the absorbance recorded. The absorbance was corrected for background and vehicle and converted to percentage survival.

In another set of experiments, blank nanoparticles were compared against the drug loaded nanoparticles. The amount of nanoparticles used was normalized for that given for the given amount of drug. In another variation, the particles were exposed to the cell lines for 72 hours instead of 24. Additionally, HCT116 which is colon cancer cell line was challenged with drug loaded nanoparticles for 72 hours.

The data analysis was done by using Sigma plot Version 10.0 (Systat Software Inc.). Results are expressed in terms of the drug concentration required to kill 50% of the cells (IC_{50}) estimated as the absorbance value equal to 50% of that of the cells in the control untreated wells. For calculation of IC_{50} values, a sigmoidal logistic curve fit using 4 parameters was applied. The equation used was

$$y = y_0 + \frac{a}{1 + \left(\dfrac{x}{x_0}\right)^b}$$

a = the maximum value of y or max(y)

y_0 = the minimum value of y or min(y)

x_0 = $x50(x,y,.5)$ or interpolated x value at 50% of the amplitude using a Lowess smoothing of 0.5

$b = if(-xwtr(x,y,0.5)/20<-2, -2, if(-xwtr(x,y,0.5)/20>2, 2, -xwtr(x,y,0.5)/20))$

Estimation of b is done automatically by the software by the difference between the x values at 75% and 25% of the amplitude. The $xwtr(x,y,f)$ function returns $x75$-$x25$ for sigmoidal shaped functions using Lowess smoothing of f where value of f is between 0 and 1 and is optional. The $x75$ and $x25$ returns the x values for the y value 75% and 25% (respectively) of the

distance from the minimum to the maximum of smoothed data (if f is specified).

IC$_{50}$ values were calculated solving for x by substituting 'y' by 50 in the above equation.

3.4 Results

3.4.1 Cytotoxicity studies on DMAB

Both MTT (Figure 3.5) as well as LDH (Figure 3.6) assays performed with aqueous solutions of DMAB showed concentration dependent toxicity. The stabiliser was found to be non-toxic after 6-8 hours incubation at and below concentrations of 33µM. This is below the amount of surfactant remaining bound to the unwashed particles (less than 20µM when suspended at concentration of 1mg/ml). Fresh HBSS pH 7.4 and Triton X-100 (1% w/v) in HBSS pH 7.4 were used as negative and positive controls, respectively. LDH release has been expressed relative to control values. Experiments were performed with n = 4 for each sample.
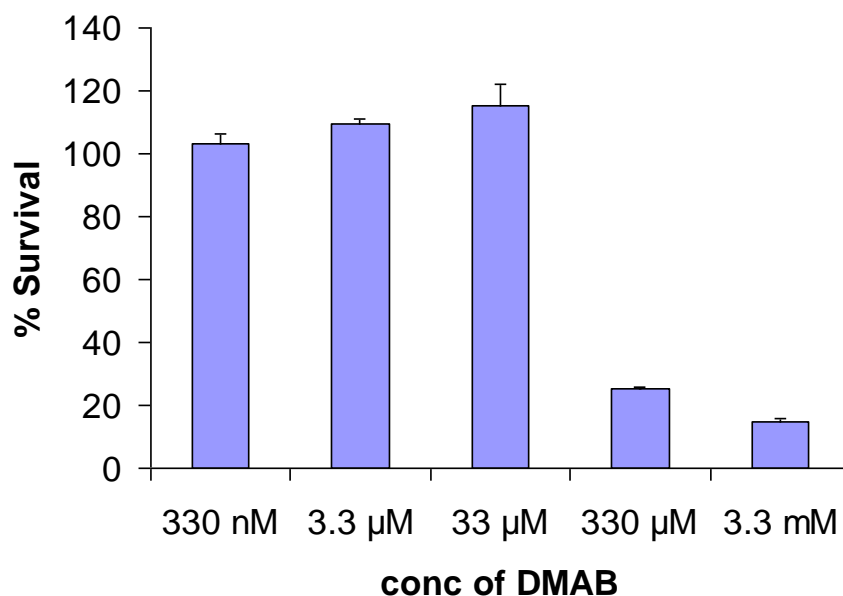
Figure 3.5: MTT assay for different concentrations of DMAB in MDCK II mdr1 cell line (n=4). Error bars denote sd.

3.4.2 Cytotoxicity studies of blank PLGA nanoparticles

Nanoparticles prepared with 1.0, 0.33 and 0.1%w/v DMAB (of sizes 100, 135

and 180 nm respectively after washing step) were also found to be non-toxic
to the cell lines in these two assays (Figure 3.7 and Figure 3.8).
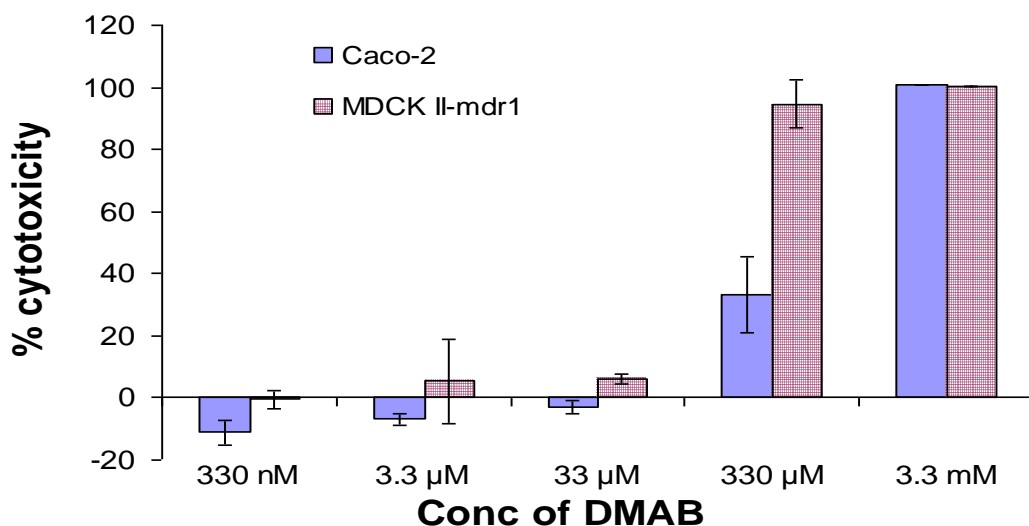
Figure 3.6: LDH assay for different concentrations of DMAB (n=4). Error bars denote
sd
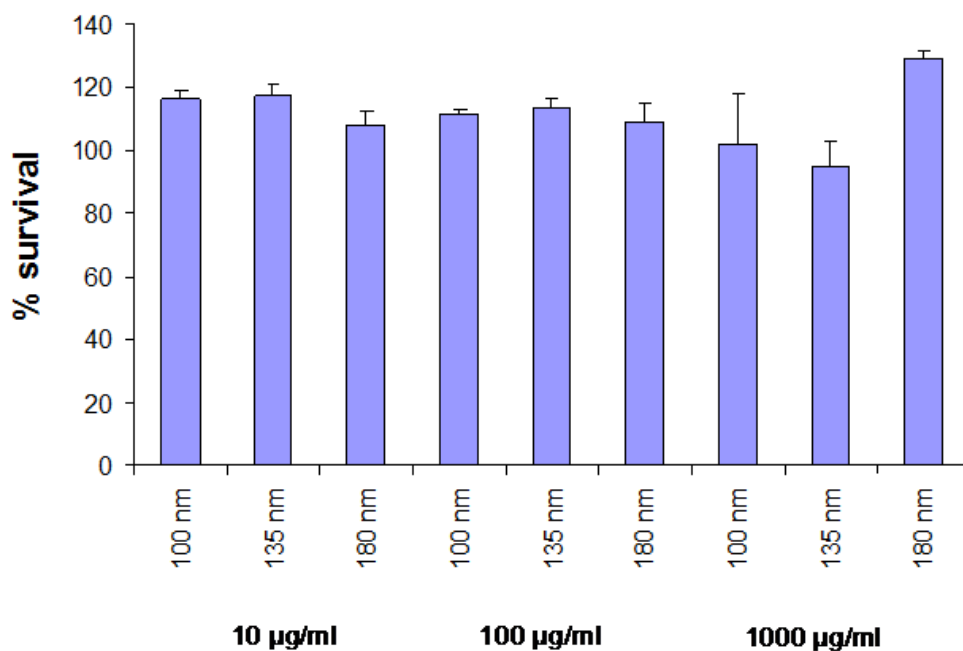
Figure 3.7: MTT assay with different nanoparticle concentrations of three sizes
stabilized with DMAB in MDCK II mdr1 cell line (n=4). Error bars denote sd.
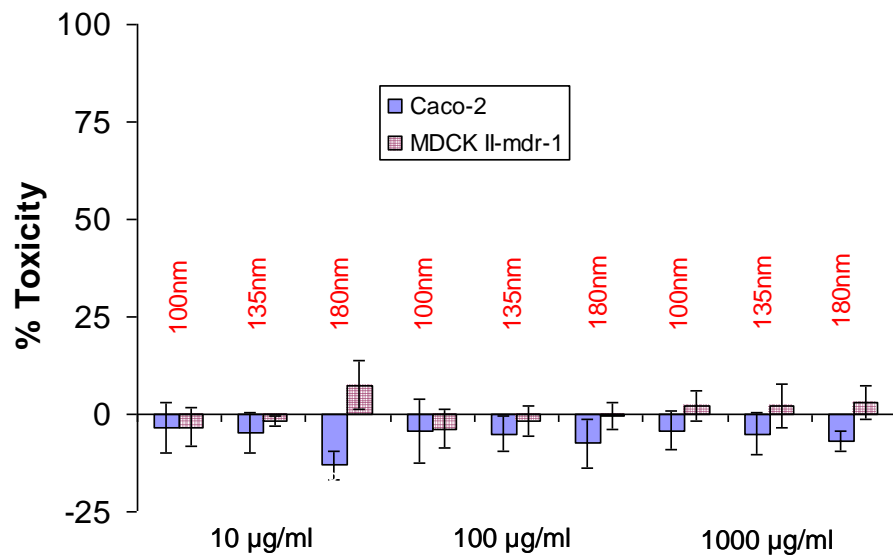
Figure 3.8: LDH assay with different nanoparticle concentrations of three sizes (n=4). Error bars denote sd.

3.4.3 Pgp efflux study

3.4.3.1 Rhodamine 123 transport assay

Figure 3.9 shows that DMAB does not inhibit Pgp efflux of Rhodamine. At higher concentrations, transport was increased on both sides of the monolayer. DMAB was found not to inhibit the efflux. There was an increase in transport on both sides (apical to basolateral and vice versa), presumably due to the interference with the integrity of the tight junctions as judged by a lowering of the TEER at the end of the 4 hour experiment.
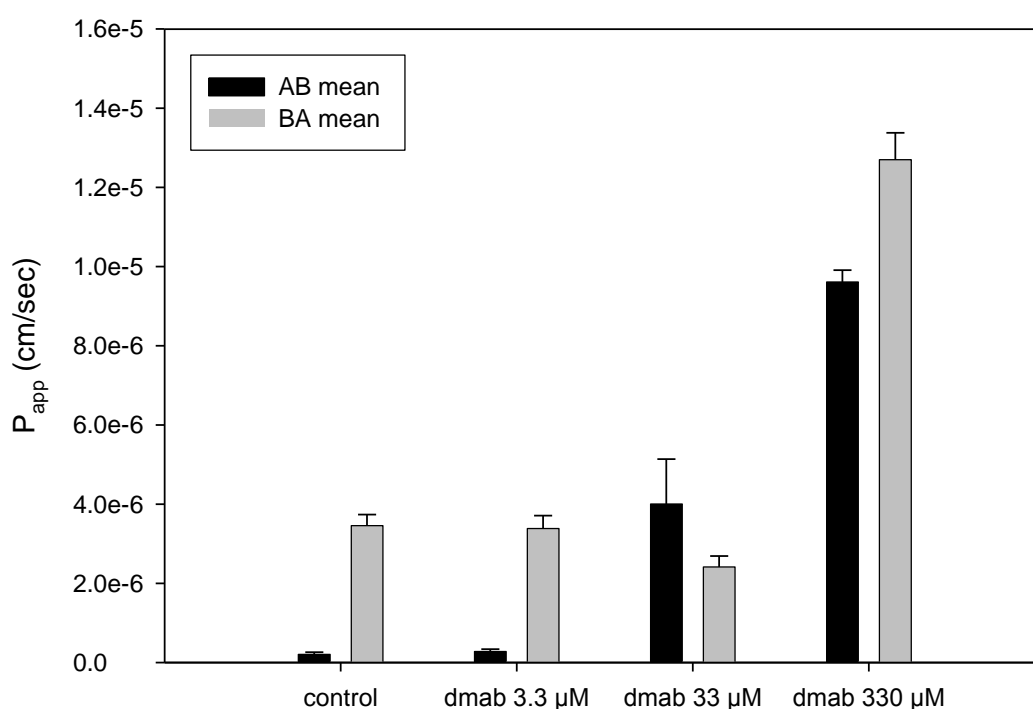
Figure 3.9: Effect of DMAB on the Pgp efflux of rhodamine across Caco-2 cell line in Transwell® plates (n=3). Error bars denote sd.

3.4.3.2 Calcein-AM assay

PLGA particles prepared with DMAB showed some inhibition of Pgp efflux of Calcein when compared to 10 μM Cyclosporin A in the MDCK cell lines as depicted in Figure 3.10.
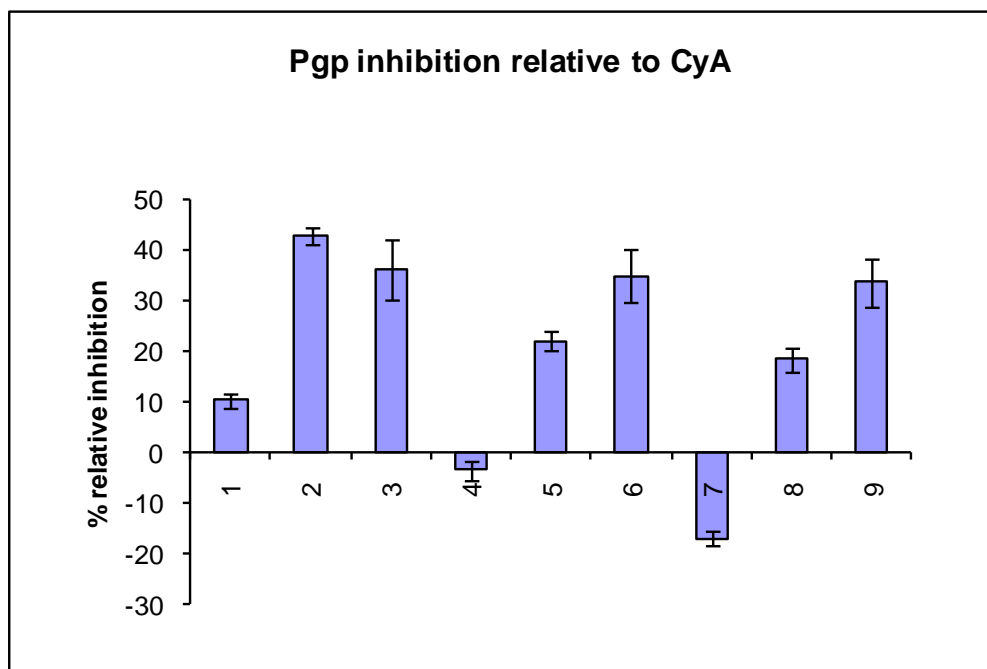
Figure 3.10: Calcein-AM Pgp inhibition assay in MDCK cell lines using DMAB stabilized nanoparticles. 1,2,3 had size of 100nm; 4,5,6 of 135 nm and 7,8,9 of 180 nm; 1,4,7 are at 1mg/ml concentration, 2,5,8 are at 100 μg/ml and 3,6,9 are at 10 μg/ml (n=4). Error bars

3.4.4 Cytotoxicity studies of drug loaded PLGA nanoparticles

The LDH release assay with paclitaxel loaded nanoparticles performed in cultured Caco-2, MDCK II mdr 1, Calu-3 and A549 cell lines show that slow dividing Calu-3 cells were found to survive even better in presence of nanoparticles when compared with buffer medium (Figure 3.11). On the other hand, Fast dividing A549 cells were found to die rapidly in presence of nanoparticles (to prove this, a control of blank DMAB nanoparticles was employed). Nevertheless, there was no significant toxicity of the drug loaded nanoparticles as compared to blank nanoparticles, but different cell types were affected to different degrees with the nanoparticles prepared.
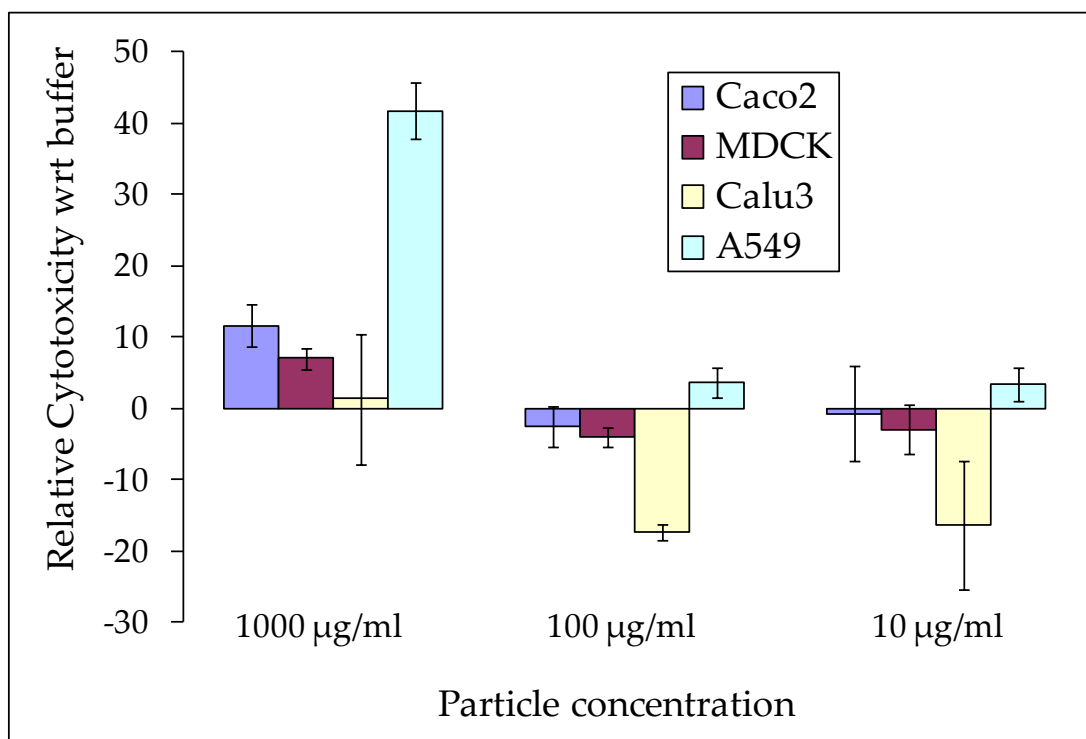
Figure 3.11: Concentration dependent cytotoxicity studies of paclitaxel loaded particles made with DMAB in LDH assay (n=4). Error bars denote sd.

3.4.5 Efficacy studies in cells used for melanoma model in mice

3.4.5.1 Cell proliferation studies

After incubation for 48, 72 and 96 hours, the cells yielded sigmoid proliferation profiles (Figure 3.12). However, the number of cells that corresponded to the mid-log phase differed significantly for the three time points studied. The cell density corresponding to mid log phase was calculated by dropping perpendiculars for the straightest part of the curve in log phase on the abscissa. The values obtained for 48, 72 and 96 hours corresponded to approximately 16000, 8000 and 3000 cells/ml.

The slope of the curves in log phase also increased as the time of incubation was increased. The number of cells in log growth phase were in very narrow range for the cells incubated for 96 hours. This corresponds to a total incubation time of 120 hours since the absorbance was recorded 24 hours
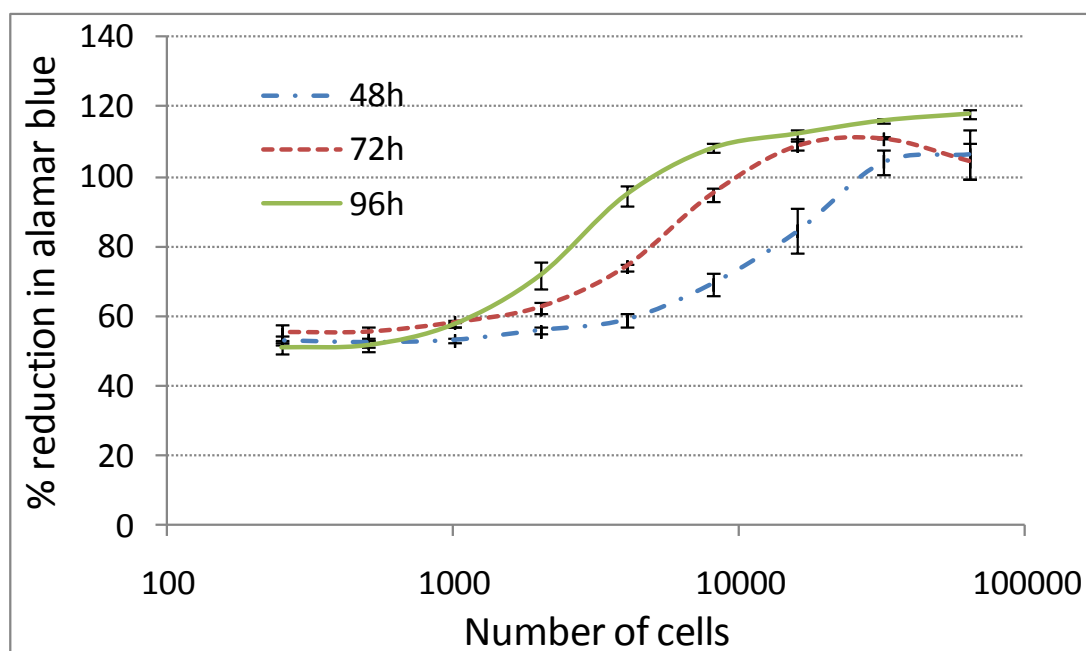
Figure 3.12: Cell proliferation study with B16F0 cells in AlamarBlue®
assay (n=4). Error bars denote sd.

after the addition of AlamarBlue®. The longest sustainable culture time
without changing cell culture medium was thus determined to be 96 hours
and the ideal cell density for the seeding in such study was decided to be
8000 cells/ml or 800 cells/well.

3.4.5.2 Cytotoxicity studies

Paclitaxel in DMSO as well as mixture of cremophor EL and ethanol showed
a maximum cell kill of 30% at any concentration (Figure 3.13). More
importantly, no concentration was able to kill all the cells. The maximum
reduction in cell survival brought about by the blank nanoparticles was 10%.
Nanoparticulate formulation exhibited a maximum reduction in cell survival
of 50% at concentration of 10 μM. The activity of blank nanoparticles and
drug loaded nanoparticles was similar up to paclitaxel equivalent of 1 μM.
No clear trend was visible with any of the profiles.

Paclitaxel apparently has limited activity against the B16F0 cells. A study to
rule out the effect of long incubation by exposing the formulations for lesser

time failed to show better activity of paclitaxel against these cells.
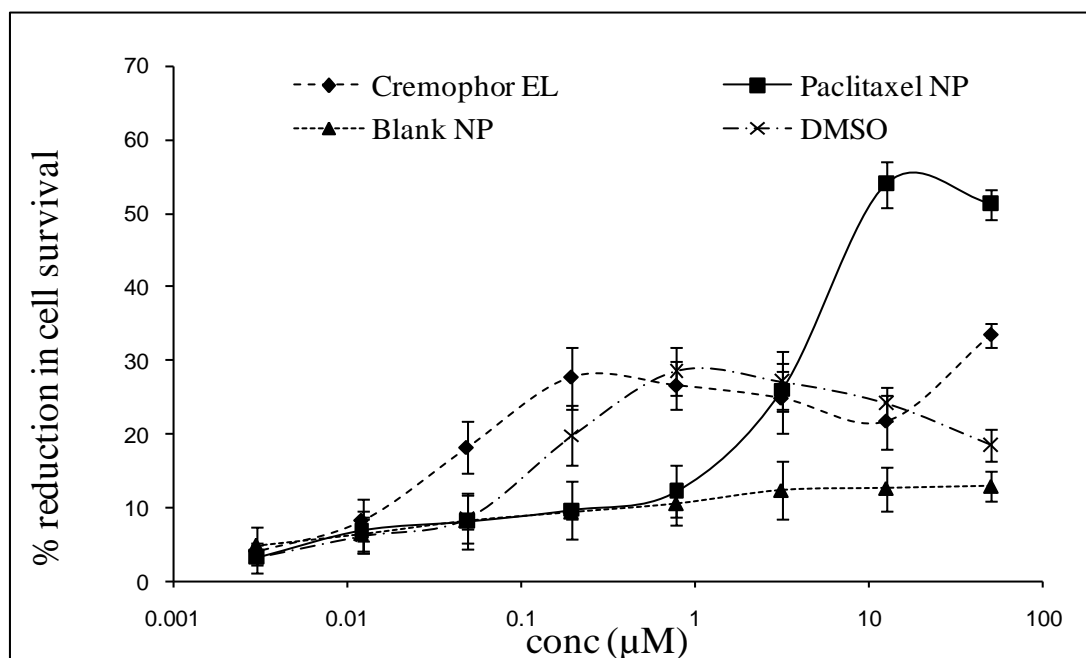
Figure 3.13: Cytotoxicity study with B16F0 cells in AlamarBlue® assay (n=4). Error bars denote sd.

3.4.6 Efficacy studies in cells used for carcinoma model in mice

MTT assay provided a simple and effective test for testing the cytotoxic activity of the developed formulation. Compared to the studies discussed previously which were to assess the cytotoxicity of the formulation to normal cells, the aim of the longer exposure studies was to determine the efficacy of paclitaxel in particulate formulation in improving the therapeutic activity against cancerous cells.

3.4.6.1 Biological assay for the drug

The cytotoxicity profile for the two sources of drugs almost overlapped. The IC_{50} value of drug from Sigma Aldrich was 2.24 (± 0.09) µM and that for Genexol was 2.01 (± 0.13) µM (Figure 3.14).
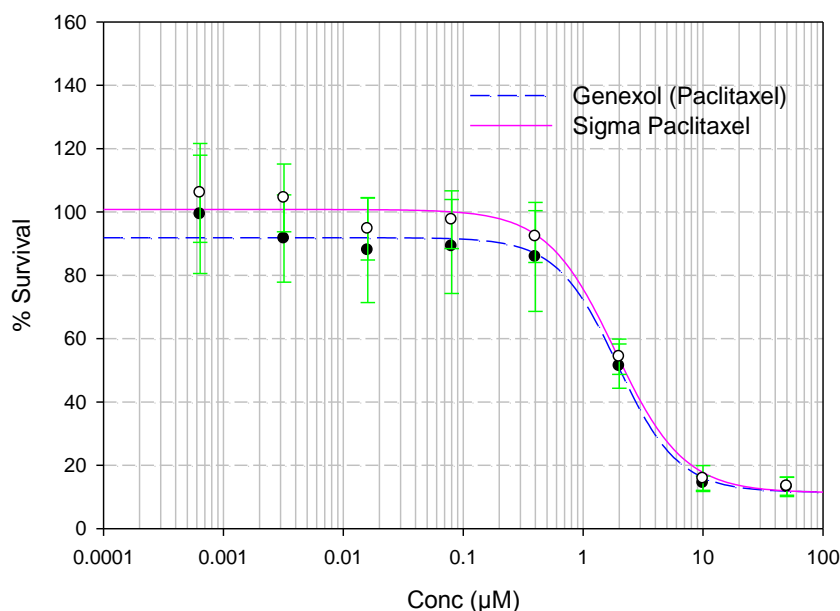
Figure 3.14: Comparison of cytotoxicity of Genexol® paclitaxel with commercial standard Sigma paclitaxel (n=12). Error bars denote sd

3.4.6.2 Efficacy study of paclitaxel loaded nanoparticles

The cytotoxicity of paclitaxel and the drug loaded nanoparticles is summarized in Table 3.1. A2780 is about 2000 fold more sensitive to paclitaxel than the drug resistant derivative (IC_{50} 2.26 ± 0.91 nM for A2780 cf 5240 ± 637 nM for 2780AD). In the drug sensitive cell line, the blank nanoparticles were relatively non-toxic to the cells with an IC_{50} based on the theoretical paclitaxel load of 1774 ± 129 nM. Formulation of paclitaxel with the nanoparticles increased the toxicity of the drug to the drug sensitive cell line A2780 by about 7 fold (free drug 2.26 ± 0.91 cf nanoparticle 0.30 ± 0.03 nM). The paclitaxel sensitivity of the drug resistant derivative was increased by prolonged exposure to the drug (Table 3.1). However, the nanoparticles themselves were toxic to the cells at the concentrations required to achieve paclitaxel IC_{50} concentration (3175 ± 79 nM for the blank particles cf the IC_{50} for paclitaxel of 2013 ± 73 nM). Interestingly, it was observed that with paclitaxel in DMSO, the cytotoxicity reached a plateau of about 30% survival

in the 24 hour exposure (Figure 3.15), while the value is closer to 10% in the 72 hour exposure (Figure 3.14).

When the 72 hour exposure was carried out in colon cancer cells, paclitaxel in nanoparticles killed all the cells at the concentrations studied while the blank nanoparticles gave IC_{50} value equivalent of paclitaxel concentration of 1540 ± 226 nM (Figure 3.16).

Table 3.1: Paclitaxel sensitivity of cell lines A2780 and the drug resistant derivative 2780AD to paclitaxel and paclitaxel nanoparticles. Sensitivity is expressed as the IC50 (mean ± sem of 3 estimations) defined as the concentration of drug required to reduce the absorbance of the wells to 50% of that of the control untreated cells.

	IC_{50} (nM)		
	A2780	2780AD	
	24 h	24 h	72 h
Blank Nanoparticles	1774 ± 129	-	3175 ± 79
Paclitaxel	2.26 ± 0.91	5240 ± 637	2013 ± 73
Paclitaxel nanoparticles	0.30 ± 0.03	1661 ± 89	903 ± 49
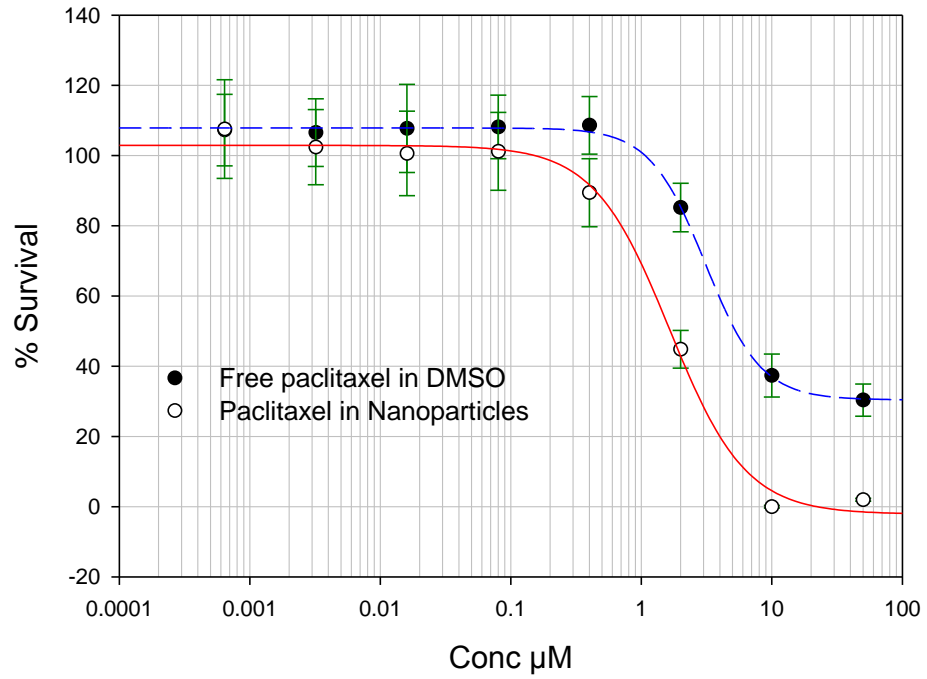
Figure 3.15: MTT assay of free and encapsulated paclitaxel in 2780AD cells (n=12). Error bars denote sd
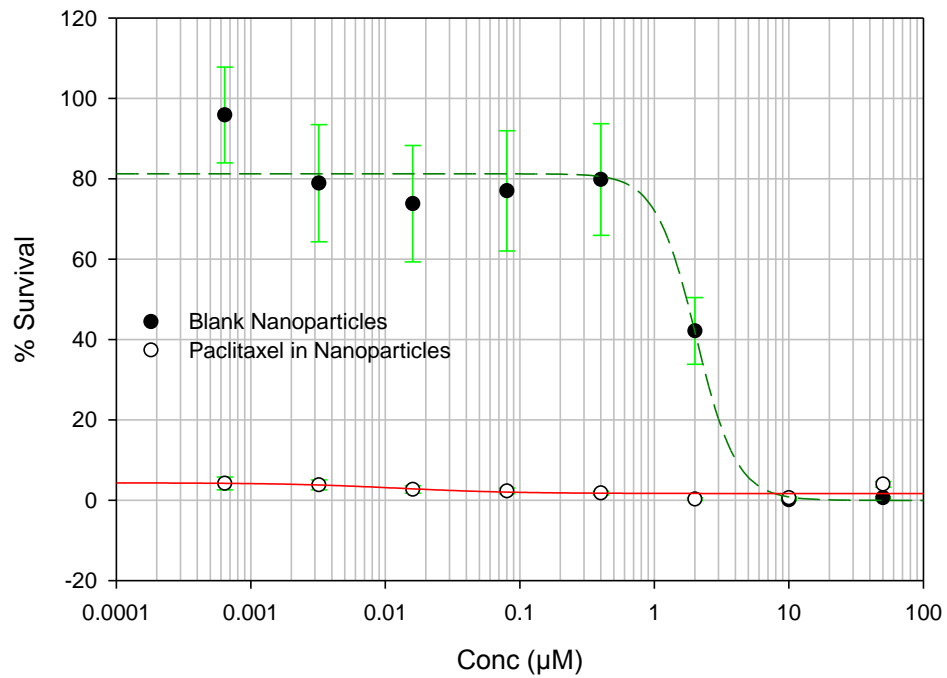
Figure 3.16: MTT assay of blank and drug loaded nanoparticles in HCT116 cells in 72 hour exposure study (n=12). Error bars denote sd

3.5 Discussion

It is a common practice to use the cytotoxicity assays as a tool to screen for toxicity as well as efficacy for anticancer formulations. Because of their very purpose, the cell kill can be portrayed as a mark of efficacy. However, the efficacy of anticancer drugs is in differential cytotoxicity wherein they kill only the cancerous cells and not the normal cells. A second important point to remember is that most of the cell culture is carried out on cell lines derived from cancers, exploiting their immortality. So for the definition of the assay, the cells are defined as any cells in some cases and cancer cells when the context is efficacy of drug in killing cells.

Both LDH and MTT assays performed with MDCK and Caco-2 cell lines proved that the DMAB solutions at and below the concentrations of 33 μM are not significantly toxic to the cells. This is the concentration in the final preparation that roughly corresponds to the bound surfactant on the nanoparticles with the highest concentration of surfactant (1%) used. However, it may be noted that there will always be a rapid dilution of the formulation in the body fluids. Although DMAB causes significant cell death in a 6-8 hours exposure study with cells above these concentrations, such local high concentrations are not expected unless the formulation is (actively or passively) being accumulated at a particular site. Thus at the level used, DMAB is a safe stabiliser despite its caustic chemistry. However, this makes the process of particle washing a very critical requirement, ensuring that the particles themselves, with low amounts of bound stabiliser are safe for transit exposure to various body tissues.

Similarly, a study performed with three different sized (100, 135, and 180 nm) particles made using DMAB proved that particles at or below a concentration of 100 μg /ml cause no significant toxicity to the cells. Smaller

size particles (100 nm) showed significant toxicity at 1mg/ml, but at a lower concentration of 100 µg/ml, they were equivalent to the control (buffer). In terms of percentage survival, 135 and 180 nm particles produced similar effects as control at all the three concentrations.

Although quaternary ammonium salts are caustic to tissues, DMAB stabilized nanoparticles were found to be safe in cytotoxicity assays in various cell lines. This study establishes the utility of DMAB in producing very small particles with preformed polymers and should encourage more exhaustive use of this surfactant. The aforementioned particles are safe to cells in a short term exposure toxicity study establishing safety to different kinds of cells during transit to target site.

A significant challenge in this kind of study is maintaining the cell line over a long period of time without replacing the culture medium. Removal of culture medium would also remove the formulation that has not been taken up, thus necessitating repeated exposure to fresh formulation and in that, one of the significant purposes of dose reduction is defeated.

Studies were conducted to understand the Pgp efflux inhibition of Rhodamine 123 in the Transwell® membrane filter Caco-2 monolayer transport assay. DMAB was found not to inhibit the efflux. There was an increase in transport on both sides (apical to basolateral and vice versa), presumably due to the interference with the integrity of the tight junctions as judged by a lowering of the TEER at the end of the 4 hour experiment. The aim of this exercise was to assess if the surfactant as such possesses Pgp inhibiting activity and if at all there is a possibility of preventing the efflux of substrate drugs.

The Calcein-AM assay shows that the particles interfere with the efflux, the mechanism of which is not clear. Pgp acts by a selective way of chemical

recognition of substrates. However, Figure 3.10 depicts relative inhibition as compared to cyclosporine and might not be significant per se.

In the LDH cytotoxicity assay performed with DMAB stabilized PLGA particles of encapsulated paclitaxel at 2 % (w/w of particles), no significant toxicity was seen in Caco-2, MDCK II mdr 1, Calu-3, and A549 cell lines at concentrations at or below 100 μg/ml. Even for 1mg/ml concentration, only the A549 cell lines exhibited upto 40% cell disruption after 6 hour incubation, while the other cells survived well in the presence of the particles. The reason for cell death of the A549 cultures is not clear, though it is worth noting that they are very fast dividing cells and might take up any released paclitaxel faster than the other cells. However, in the other cell lines studied, the particles did not cause a significant toxicity in comparison to the control. Another point worth considering is that these tests in a short term study give an indication of toxicity while they can indicate efficacy of an anticancer formulation in a long term study when studied in cancer cell lines. Additionally, since the aim of this study was to establish the safety of the particles and not the efficacy of paclitaxel in the encapsulated formulation, the benchmark for concentration was the amount of nanoparticles rather than the paclitaxel as such.

The AlamarBlue® assay based on metabolic reduction of the dye resazurin was carried out to estimate the efficacy of the formulation. Since drugs are known to be released slowly from a hydrophobic matrix like PLGA, there should be sufficient time allowed for paclitaxel to be released from the particles and exhibit its effect. On the other hand, there is a limitation of how long can a culture be maintained without replacing the nutrient medium. Moreover, since a positive growth control is also used in the design of the assay, the number of cells might become so much that they start dying of

nutrient deprivation. The proliferation assay was thus carried out to estimate a suitable number of cells that would grow and multiply at a rate suitably accommodating the two opposing factors. It can be seen in growth curves in the proliferation study that the number fraction in log phase of metabolic activity is significantly smaller when the time of incubation is increased to 96 hours. This particular time point represents a total culture time of 120 hours since the dye was added after 96 hours and absorbance was read after a further 24 hours. In another experiment done, it was found out that the most consistent and dependable readings of absorbance are obtained 12 hours after the addition of AlamarBlue®. As a compromise, it was decided that the best seeding density is thus around 8000 cells/ml or 800 cells per well, with a total incubation time of around 100 hours.

For the efficacy study, cells were hence seeded at the density mentioned above. The cells were allowed to attach and grow for 24 hours following which they were incubated with the formulation for 60 hours. AlamarBlue® was then added and absorbance was measured after a further incubation of 12 hours, representing a total culture time of 96 hours. The % reduction in AlamarBlue® with respect to a positive growth control (containing no challenge substance, but only cells) showed that paclitaxel is not very active against the particular strain of B16F0 cell line. A possible explanation can be drug resistance by over-expression of the efflux pumps. However, such pumps are saturable and thus a high concentration of paclitaxel in DMSO or cremophor should have exhibited 100% cell kill. Thus the drug resistance seems to be due to some other reason. Another interesting aspect is that at a high concentration, the particles were able to achieve a higher cell kill. This suggests that at low concentrations, paclitaxel was either metabolized or degraded at a fast rate.

The formulation was then studied for efficacy in a cell line that exhibits over-expression of the Pgp efflux transporters. The aim was to explore the possibility of the developed nanoparticle formulation to impart benefit by protecting paclitaxel from being pumped out of the cancer cells. Liposomes have been shown to increase the accumulation of doxorubicin in multiple drug resistant (MDR) Chinese hamster LZ, human breast cancer MCF-7/ADR, and the ovarian carcinoma SKVLB cell line as a result of changes in the intracellular vesicular transport (Thierry et al. 1993). In a study with drug resistant cell lines, it has been shown that doxorubicin encapsulated in polymer-lipid nanoparticles was accumulated to a higher degree within the cell compared to free doxorubicin (Wong et al. 2006).

The mechanisms by which drug resistance is reversed depend majorly on the type of drug. The material used for manufacturing the carrier system itself may have inherent activity. Lipid partitioning of the substrate in the membrane structure has been postulated as essential for efflux and the lipid type can affect the interaction with the substrate (Romsicki and Sharom 1999). Liposomes increased vinblastine accumulation in resistant human lymphoblastic leukemic cell CEM/VLB$_{100}$ even when the drug was co-administered in free form rather than incorporated within the liposomes, probably due to amalgamation of lipidic components into cell membrane lipids and subsequent alteration in membrane fluidity (Warren et al. 1992). Pluronic block copolymers have been shown to sensitize MDR cell lines to cytotoxics (Kabanov et al. 2002). A micellar formulation of pluronic-doxorubicin conjugate SP1049C is presently undergoing Phase II clinical trials for Pgp targeted therapy (Valle et al.).

Polymeric nanoparticles have been documented to reverse drug resistance in cancer cell lines based on the hypothesis of transport through endocytic

pathways (Cuvier et al. 1992). However, local high concentrations of drug released from polymeric nanoparticles adsorbed on to resistant P388/ADR cell surface have also been proposed to reverse resistance (Verdière et al. 1997). A coculture of these cells with macrophages showed beneficial effects especially when combined with cyclosporin A, which is an inhibitor of the Pgp efflux transporters (Soma et al. 1999). The cytotoxic and the inhibitor have been encapsulated into a single nanoparticulate carrier system (Emilienne Soma et al. 2000).

Due the high cost of the drug from standard suppliers, it was purchased from a bulk manufacturer. Although the ultraviolet spectroscopy based assay of the procured drug was within acceptable limits, a biological assay was carried out in terms of the cell kill obtained against the standard chemical supplier. The results indicated that the two sources were chemically as well as biologically equivalent. The IC_{50} values were almost same for both the sources.

It can be seen in Figure 3.15 that in the case of paclitaxel dissolved in DMSO, at and above 1 μM concentration, the percentage survival started to decline denoting saturation of the energy dependent Pgp efflux. For the nanoparticulate formulation, this effect started from 0.2 μM onwards indicating improved potency. Even more striking is the observation where the cytotoxicity from dissolved paclitaxel exhibited a saturated plateau; survival was reduced to zero in the higher concentrations of the nanoparticulate formulation. Paclitaxel is a phase specific anticancer drug, acting on cells in mitotic (M) phase. Synchronous cultures in G1, S and G2 are not affected by it. A typical cell cycle is depicted in Figure 3.17. When an asynchronous cell culture is challenged with paclitaxel, a plateau is obtained in the maximum cell kill beyond a particular concentration. This value

corresponds to the concentrations needed to block cells in mitosis. The plateau survival value of the cells vary according to the durations of exposure times and are proportional to the percent of cells not expected to enter M (paclitaxel sensitive phase) during that period (Whatever cells enter M phase will die, those that will not enter M phase will survive.
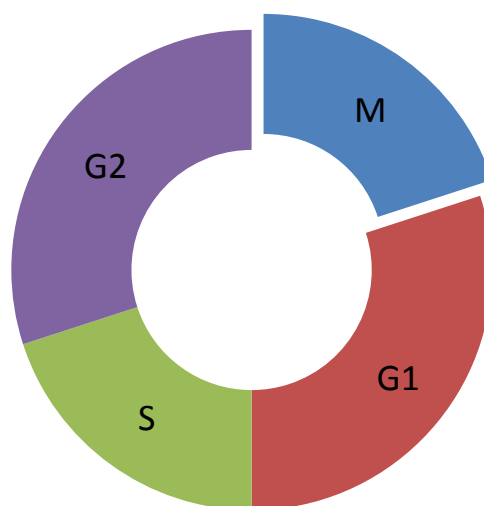
Figure 3.17: Phases of cell cycle (clockwise)

An important corollary is that if the duration of exposure is higher than the life cycle of all the cells, then all the cells will die (Lopes et al. 1993). This observation has important implications in anticancer drug delivery. It suggests that beyond a particular concentration, a phase-specific anticancer drug will not have any beneficial value and will only result in non-target toxicity. On the other hand, a certain minimum concentration maintained over longer duration will still ensure that all sensitive cells are killed. This approach is in stark contrast to the practiced highest tolerated dose approach after which the non-target cells are allowed time to recover and the chemotherapy cycle is repeated. It hints towards an opportunity for drug delivery strategies that not only target the cancer, but also maintain sustained drug levels.

The paclitaxel loaded nanoparticles retained activity in cell lines *in vitro*. Interestingly, the formulation was able to increase the sensitivity of the already relatively sensitive cell line A2780 by about 7 fold (Table 3.1). The nanoparticles were non-toxic to the cells at the concentrations required to deliver sufficient paclitaxel to the cells. For comparison the IC_{50} concentrations of the blank nanoparticles is expressed in paclitaxel equivalents i.e. the amount needed to give the required concentration of paclitaxel. Since the IC_{50} of the blank particles is about 500 fold greater than the concentration required to deliver the IC_{50} concentration of paclitaxel (Table 3.1) the increased toxicity of the drug loaded nanoparticles cannot be explained by toxicity of the nanoparticle itself. By contrast, the drug resistant variant 2780AD is about 2000 fold resistant to paclitaxel and in order to deliver this concentration of paclitaxel the nanoparticles are used at close to their toxic concentration. Thus we cannot exclude the possibility that the increased activity in this cell line is due to combined toxicity of the paclitaxel and the nanoparticles.

As shown in Figure 3.16, in an experiment carried out in a colon cancer cell line HCT116, it was found that the paclitaxel loaded nanoparticles killed all the cells at all concentrations studied while the blank nanoparticles exhibited an IC_{50} value of 1540 ± 226 nM. This cell line does not exhibit over-expression of the Pgp and responds to paclitaxel and this experiment established that there is a good gradient in the cytotoxicity of nanoparticles as a function of their paclitaxel content.

The observed IC_{50} values of the blank nanoparticles raise questions about the inherent cytotoxicity of the polymeric nanoparticles per se. One possible explanation is that the particles, merely with their physical presence beyond a particular threshold, are interfering with structural integrity dynamics or

metabolic process of the cells. An alternate hypothesis could be that they are making a physical barrier on the surface of cells that inhibits transport of nutrition across the cells and this effect is dependent on the concentration. Clearly, the washing of the well contents by aspiration of medium is ineffective in disturbing this association with the cells. The particles being positively charged are expected to interact with the negatively charged residues at the surface of the cell membrane. Although it is assumed that the particles are internalized, this process is saturable as indicated by the concentration dependent results.

3.6   Conclusions

- PLGA nanoparticles prepared with DMAB were found to be non-cytotoxic to the cells relative to buffer solution. DMAB itself was found to be safe to the cells in culture below its reported critical micellar concentration suggesting that if persisting in final formulation at a lower amount, it would make a safe stabiliser. Drug loaded nanoparticles were also found to be relatively non-toxic in the short term exposure to cells suggesting that paclitaxel is not immediately released from the nanoparticles. Thus these particles are not expected to cause cytotoxicity to those cells with which they come in contact during absorption and transport in body.

- DMAB was not found to be modulating the efflux. PLGA particles stabilized with DMAB mildly inhibit the Pgp efflux pump in comparison to cyclosporine A via an unknown mechanism.

- Paclitaxel is not active against B16F0 mouse melanoma; however the nanoparticulate formulation was able to marginally improve its cytotoxicity in cell culture.

- The nanoparticulate formulation was shown to be about sevenfold more potent than free paclitaxel against cell line A2780 and the poly(lactic-co-glycolic acid)(PLGA) nanoparticles alone were nontoxic to the cells at the concentrations required to deliver the drug. The mechanism of increase in potency is not understood, but is consistent with mild efflux inhibitory action in Calcein-AM assay.

The encouraging results paved the way for the efficacy studies in animals wherein the formulation was administered orally to animals and the efficacy was evaluated against the traditionally used formulation.

4 *In vivo* evaluation in cancer models

4.1 *Introduction*

Preclinical animal studies are an essential component of drug development process. Animal models are invaluable tools in the anticancer drug discovery programmes all around the world. Four major categories of cancer models are used:

a) naturally occurring mutants

b) transplants (xenografts)

c) genetically engineered animals

d) chemical carcinogenesis

Although many species are used, mice and rats provide the majority of models due primarily to (i) a gene-pool closely matching to humans, (ii) availability of many strains and (iii) being amenable to genetic engineering. Especially in the last two factors, the mice outperform the rat.

The naturally occurring mutants carry an inherent propensity to develop tumours. The strains are chosen by selective breeding of inbred generations or isolating responders to mutagenic agents like N-ethyl-N-nitrosourea. Extensive gene-mapped profiling has been carried out on a wide number of available strains.

Xenograft or transplants are the most widely used models. Although they do not provide much information on the initiation aspects, they are valuable in understanding the progression and metastasis. The transplants can be localized in a small area like the subcutaneous tissue or given intravenously and the cancer cells normally migrate to a preferred site. Localized tumours are especially useful due to the possibility of non-invasive measurement of size and ease of access. However, the rate of metastasis from the

subcutaneous injection sites is extremely low and cells need to be given intravenously. Additionally orthotopic xenografts are increasingly being used to best mimic the actual *in vivo* conditions. Both human and animal cancer cells can be transplanted into a recipient animal. Interspecies transplantation is carried out in genetically modified strains, especially those with down-regulated immunity like the nude mice to maximize acceptance into the host. While cells of same species are easily accepted in host especially if syngeneic, immunodeficient animals have to be used for transplanting cells of a different species to ensure histocompatibility. The development of nude mice was an important milestone in this direction wherein a gene knockout resulted in a strain that had a very low level of immunity and thus accepted a wide variety of cells as transplants.

The advances in understanding of genetics has opened another arena of modification of the germline of the laboratory animal, notably the mice for inducing new genes. The alteration is affected by either introduction of extra DNA into the normal coding sequence or through mutation. The resulting transgenic mice have provided new insights into the cell signalling and expression pathways that can be targeted for management or treatment of cancer. A significant advancement in this direction is the introduction of oncogenes and knocking out of the tumour suppressor genes (TSG).

The chemical carcinogenesis approach was initiated in 1915 by Katsusaburo Yamagiwa when he started a study in Japan involving application of coal tar on the skin of rabbits and a few animals developed tumours after about one year (Jonkers and Berns 2005). The chemical carcinogens provide a simple way to induce tumours in experimental animals. The most commonly used chemicals for inducing breast cancer are 7, 12 dimethylbenz-anthracene (DMBA) and alkylating agents like N-methylnitroso-urea (Matulka and

Wagner 2005).

No single animal model can provide a complete means to mimic the human cancers. It has been summarily witnessed since systematic studies in cancer research were initiated, that more than one screen is required to judge the therapeutic potential of new agents or treatment regimens. The developed nanoparticulate formulation of paclitaxel was screened in three different tumour models in rodents.

4.1.1 Chemical carcinogenesis model in rats

The DMBA model was originally reported long back in 1950s (Geyer et al. 1951) and modified later on (Huggins et al. 1961). DMBA is an experimental carcinogen routinely used for induction of breast cancer in animals (Constantinou et al. 2001; Davis and Kuttan 2001) and is implicated in DNA-adduct formation (El-Bayoumy et al. 2003; Kumar et al. 2005). The agent can cause cancers in a wide range of tissues depending on the route of administration. DMBA requires metabolic activation by mixed function oxidase systems to become carcinogenic (Thompson 2000). A single oral dose of the compound administered at the time of sexual development in female rats has shown high incidence of mammary tumours. Typically the dosing is carried out by oral gavage of this polycyclic aromatic hydrocarbon dissolved in edible oil. Interestingly low to moderate levels of estrogens stimulate and high levels inhibit the mammary carcinogenesis (Welsch 1985). Sprague Dawley (SD) and Wistar-Furth rats exhibit the greatest susceptibility to this mammary carcinogenesis model. Doses ranging between 5 and 20 mg per rat have been reported, and are often calculated based on body weight and 100mg/kg body weight is the most widely used dose. Optimal sensitivity is seen in animals between 50 and 65 days of age (Thompson 2000).

4.1.2   Lung cancer model in mice

Metastasis is one of the major reasons for treatment failure in cancer chemotherapy. Melanomas are very fast multiplying type of cancers derived from the melanocytes (melanin producing skin cells). B16F0 (ATCC CRL-6322) is a melanoma cell line derived from C57BL/6J mice and is widely studied along with its highly metastatic clone B16F10. The melanoma cells manifest as black coloured patches in the otherwise reddish organs. Lung is the principal site of metastasis, followed by the liver. Usually, the cells are transplanted when in log phase of growth into syngeneic mice. After systemic administration, the cells invade and inhabit the lungs and frequently also colonise the liver. One disadvantage of this model is that disease progression can not be followed without invasive procedures.

Lung cancers are some of the most difficult ones to treat or manage, often due to the problem of delivery of sufficient amount of drug to the target cells. To assess the utility of the developed formulation of paclitaxel, it was studied in the B16F0 cancer model in mice.

4.1.3   Pgp over-expressing ovarian carcinoma xenograft in mice

Curiously, it was believed that nanoparticles of 185 nm can not be of utility in solid tumours implanted subcutaneously in animals because they would not diffuse out of the vascular endothelium and migrate to the cancer cells (Verdière et al. 1997). The ovarian carcinoma cell line A2780 discussed earlier in cell culture experiments has been challenged with drugs to develop and select resistant strains like 2780AD. The Pgp over-expressing cell lines exhibit profound resistance and a study was carried out in nude mice by transplantation of these cells in the subcutaneous tissue in the flanks of the animals. The aim was to explore the possibility of the developed nanoparticle formulation to impart benefit by protecting paclitaxel from being pumped

out of the cancer cells and reverse the drug resistance.

4.2 *Specific aims*

In this background, the following specific aims were defined for the *in vivo* experiments

- Evaluation of efficacy of orally delivered nanoparticles in cancer models in experimental animals.

- Evaluation of therapeutic activity of nanoparticles in drug resistant cancer in experimental animals.

- Establishing that particles are taken up following oral administration by measuring the drug in the tissues.

4.3 Methods

4.3.1 Chemical carcinogenesis model in rats

4.3.1.1 Induction of mammary tumours

The animal studies were conducted after approval of the institutional animal ethics committee of NIPER, India. At 47 to 50 days of age, female SD rats were administered DMBA dissolved in vegetable oil at a dose of 100mg/kg body weight (Constantinou et al. 2001; Davis and Kuttan 2001). The animals were regularly examined and breasts palpitated to examine the incidence and progression of cancerous lumps.

4.3.1.2 Treatment of animals

The treatment was started on 4 groups of 5 animals each after 22nd week of DMBA administration as follows: Group 1 received no treatment; Group 2 received paclitaxel (7.5 mg/kg body weight) in cremophor EL (oral gavage), Group 3 received paclitaxel (7.5 mg/kg body weight) in cremophor EL (i.v.), Group 4 received paclitaxel (3.75 mg/kg body weight) in the form of nanoparticles (oral gavage), frequency of administration being once in three weeks for all the three treatment groups (3 doses). The dose was calculated based on conversion to weight basis from the human dose of 175 mg/m^2 given to breast cancer patients. The oral nanoparticles group was given half the dose. Two weeks after the administration of the third dose (30th week from administration of the carcinogen), animals were sacrificed and the tumours were removed and their weight was measured.

Where appropriate, the data are presented as mean ± sem calculated over at least three data points. The tumour masses were compared by one way analysis of variance (ANOVA) followed by Tukey test; P value less than 0.05

was considered to denote a statistically significant difference.

4.3.2 Lung cancer model in mice

4.3.2.1 Induction of lung cancers

Experiments on C57BL6 mice were carried out under a Project Licence issued under the U.K. Home Office Animals (Scientific Procedures) Act 1986. The murine melanoma cell line, B16F0 was cultured in RPMI 1640 supplemented with 2 mM L-glutamine, 100 U/ml penicillin, 100 μg/ml streptomycin, and 10% heat-inactivated foetal bovine serum. The cell line was used for the experiments while the cells were in the log phase of growth. A suspension corresponding to 10^6 cells in sterile cell culture medium were injected through the tail vein of the animals. Before the treatment study, one animal was sacrificed at the scheduled end point and the lung was isolated to confirm the viability of the transplant. For the treatment study, the cells were injected through the tail vein. The cells were administered into the peritoneal cavity to those animals in which the tail vein injection could not be made.

4.3.2.2 Treatment of animals

The animals were divided in three groups of six animals each. Group 1 received no treatment, Group 2 was given the nanoparticulate formulation of paclitaxel by oral gavage (15mg/kg body weight) and Group 3 received paclitaxel (15mg/kg body weight) in cremophor EL:ethanol mixture diluted in saline. A single dose was given on day 8 and the animals were sacrificed on day 16.

The data are presented as mean ± sem calculated over at least three data points. The tumour masses were compared by Kruskal-Wallis One Way ANOVA on ranks followed by Student-Newman-Keuls pairwise multiple comparison.

4.3.3 Pgp over-expressing ovarian carcinoma xenograft in mice

Experiments on nude mice were carried out under a Project Licence issued under the U.K. Home Office Animals (Scientific Procedures) Act 1986 and adhering to the United Kingdom CCCR guidelines. The drug resistant 2780AD cells grown in cell culture flasks were harvested by exposure to trypsin-EDTA, washed three times in PBS, and implanted subcutaenously in 24 female nude mice (2×10^6 cells in 0.1 ml). When the tumours reached a mean diameter of 0.5–1.0 cm, the animals were randomized into groups of 6 and treated on days 0 (start of treatment), 2, and 4. Group 1 received no treatment, Group 2 received paclitaxel (15mg/kg body weight, i.v.) in cremophor and ethanol mixture diluted in dextrose solution, Group 3 received blank nanoparticles (orally) and Group 4 received the nanoparticulate formulation of paclitaxel (orally) equivalent to 15mg/kg body weight of paclitaxel.

Further for comparison, the drug sensitive A2780 cells were implanted using the same protocol as above in 18 female nude mice which were divided in 3 groups of 6 animals each. The animals were treated on days 0, 2 and 4; Group 1 received no treatment, Group 2 received paclitaxel (15mg/kg body weight, i.v.) in cremophor and ethanol mixture (5%:5% v/v) diluted in dextrose solution (90% v/v), Group 3 received the nanoparticulate formulation of paclitaxel (orally) equivalent to 15mg/kg body weight of paclitaxel.

Mice were weighed daily and tumour volumes were estimated by caliper measurements assuming spherical geometry.

$$V = \pi \frac{d^3}{6}$$

The data are presented as mean ± sem calculated over at least three data points. Graphs were plotted using SigmaPlot 10.0.

4.3.4 Tissue distribution study in chemical carcinogenesis model

Experiments on SD rats for the tissue distribution studies were carried out under a Project Licence issued under the U.K. Home Office Animals (Scientific Procedures) Act 1986. Normal paclitaxel was spiked with C-14 labelled paclitaxel for a dose of 7.5 mg/kg body weight (containing 0.24μCi/mg of paclitaxel) for i.v. formulation and 3.75 mg/kg body weight (containing 0.67μCi/mg of total paclitaxel) in nanoparticles administered orally. For i.v. formulation 6 mg paclitaxel was dissolved in each ml of a mixture of 50:50 v/v cremophor EL and ethanol). The dose was administered to female SD rats (n=3) 13 weeks after administration of carcinogen. Animals were sacrificed 24 h after dosing and their tissues were collected and frozen at -20°C until analysis. The estimation of radioactivity from C-14 labelled paclitaxel was carried out by liquid scintillation counting (Tri-Carb 1500, Packard, USA). Tissues were homogenized in phosphate buffered saline at 20000 rpm for 1-2 min (Polytron 4000, Kinematica, Switzerland), mixed with two volumes of Soluene-350 tissue solubilizer and incubated for 4 hours at 50°C. Hydrogen peroxide (50-200 μl) was added with constant vortexing to bleach coloured samples, 3.5 ml of scintillation cocktail (Ultima Gold, Perkin Elmer, Amsterdam, Netherlands) was added and samples read for 10 minutes. Radioactive counts were normalized on a C-14 quench curve and background values were subtracted. Paclitaxel concentration was calculated from the known dilution of the labelled drug.

4.4 Results

4.4.1 Chemical carcinogenesis model in rats

After 22 weeks, the single oral dose of DMBA resulted in tumour induction in 100% of the rats taken up for the study. At the end of treatment schedule, tumour volumes were recorded for the treatment groups. As seen in Figure 4.1, the animals treated orally with nanoparticulate formulation of paclitaxel had lower tumour burden in comparison to untreated and paclitaxel in cremophor EL treated groups. Although the difference between groups 3 and 4 is not statistically significant, the dose of paclitaxel in nanoparticles by oral route was half that of i.v. paclitaxel in cremophor EL. More significantly, orally administered nanoparticles showed significantly lower tumour burden than the drug given orally in cremophor EL.
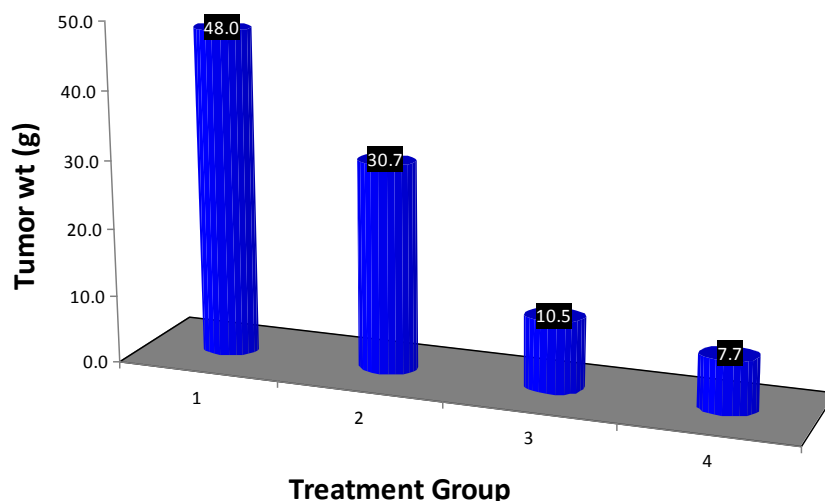
Figure 4.1: Tumour burden in female SD rats (5 animals per group). Groups: (1) no treatment; (2) Paclitaxel (7.5 mg/kg) in cremophor EL (oral), (3) Paclitaxel (7.5 mg/kg) in cremophor EL:ethanol mixture (i.v.), (4) Paclitaxel (3.75 mg/kg) in the form of nanoparticles (oral). P value for group1 vs. group4: 0.005; group1 vs. group3: 0.009; group1 vs. group2: 0.284; group2 vs. group4: 0.013; group2 vs. group3: 0.034; group3 vs. group4: 0.948. P value smaller than 0.05 signifies a statistically significant difference between the compared groups.
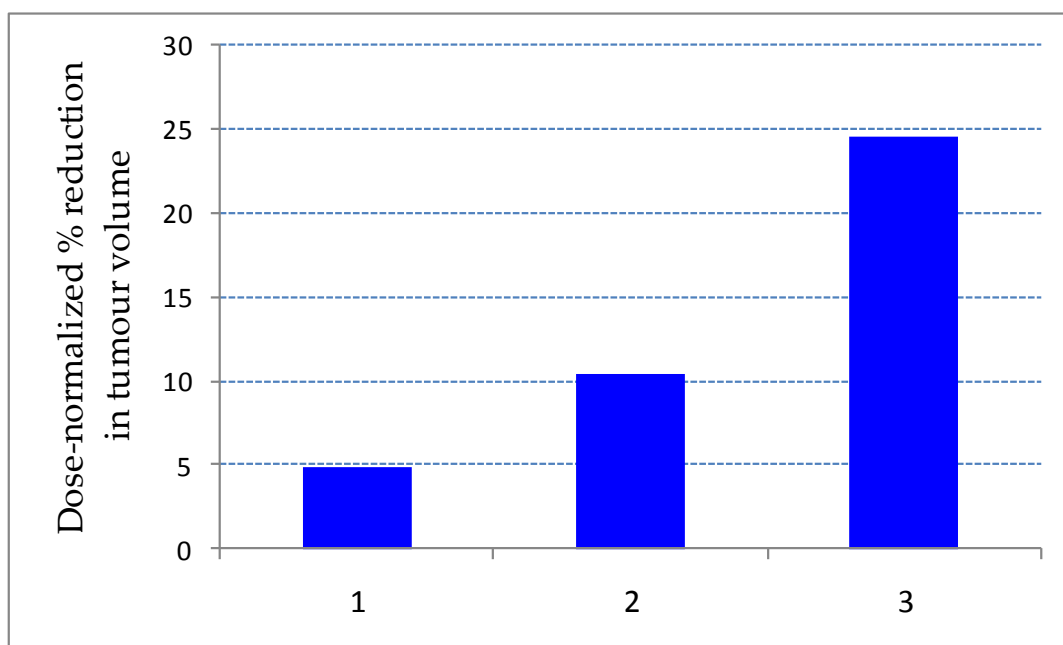
Figure 4.2: Dose normalized percent reduction in tumour volumes compared to untreated control. Groups: (1) Paclitaxel (7.5 mg/kg) in cremophor EL (oral), (2) Paclitaxel (7.5 mg/kg) in cremophor EL:ethanol mixture (i.v.), (3) Paclitaxel (3.75 mg/kg) in the form of nanoparticles (oral).

Figure 4.2 shows the dose normalized reduction in the tumour size where the percent reduction in tumour volume is divided by the mg dose of paclitaxel.

4.4.2 Lung cancer model in mice

In the pilot study, it was established that the transplanted cells ended up invading and colonizing the lungs, where black patches were seen. Two animals out of the 5 in the oral NP Paclitaxel group died before the planned termination of the study triggering premature end-point for the study. Incidentally, both these animals were injected with the B16F0 cells via the i.p. route since i.v. injection could not be administered. Figure 4.3 shows the average weight of lungs across the different treatment groups. The variation between the groups was not significantly greater than the variation within the groups indicating that neither the free paclitaxel nor the nanoparticulate formulation was effective in checking the growth of the melanoma.
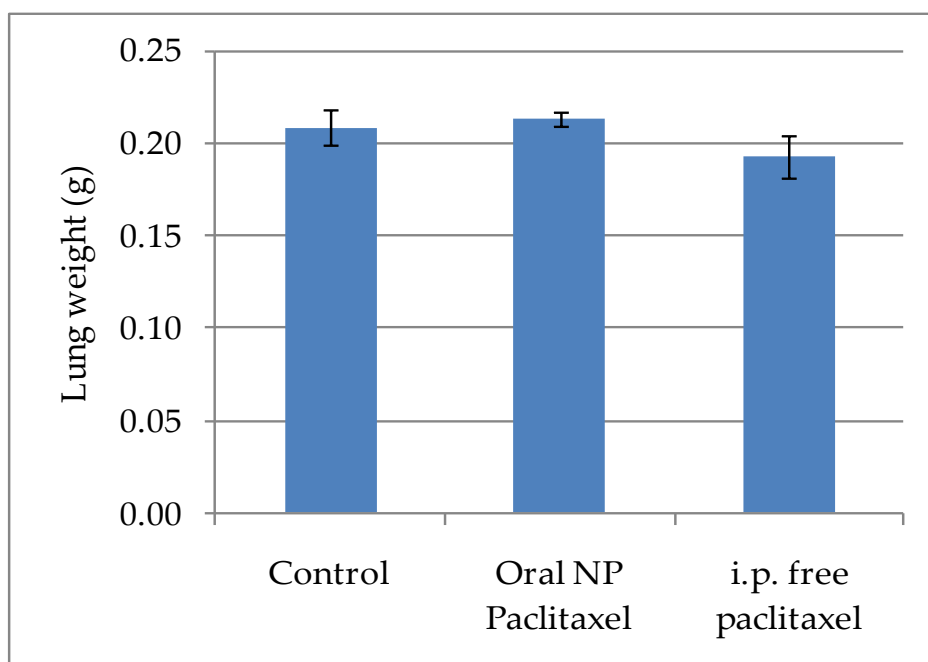
Figure 4.3: Lung weight in male C57BL6 mice (6 animals per group). Groups: (Control) no treatment; (Oral NP Paclitaxel) Paclitaxel (15 mg/kg) in nanoparticulate formulation (oral), (i.p. free paclitaxel) Paclitaxel (15 mg/kg) in cremophor EL (i.p.). (n=3-6). Error bars denote sem. Kruskal-Wallis One Way ANOVA on Ranks suggested that there is no statistically significant difference (P = 0.341).

Figure 4.4 shows that the variation between liver weights of the different groups was not significantly greater than the variation within the groups. This corroborates the results of the lung weight measurements. The animals treated with free paclitaxel had slightly lower body weight (Figure 4.5).

4.4.3 Pgp over-expressing ovarian carcinoma xenograft in mice

4.4.3.1 Efficacy studies in tumours induced with drug resistant cells

Tumours derived from the drug resistant variant of A2780 (2780AD) are resistant to the maximum tolerated dose (15mg/kg x 3) of the intravenous paclitaxel preparation Taxol® (Figure 4.6) However, the nanoparticulate formulation caused a significant decrease in the rate of growth of tumours. The effect of blank nanoparticles (not containing paclitaxel) was similar to the control group indicating neutral nature.
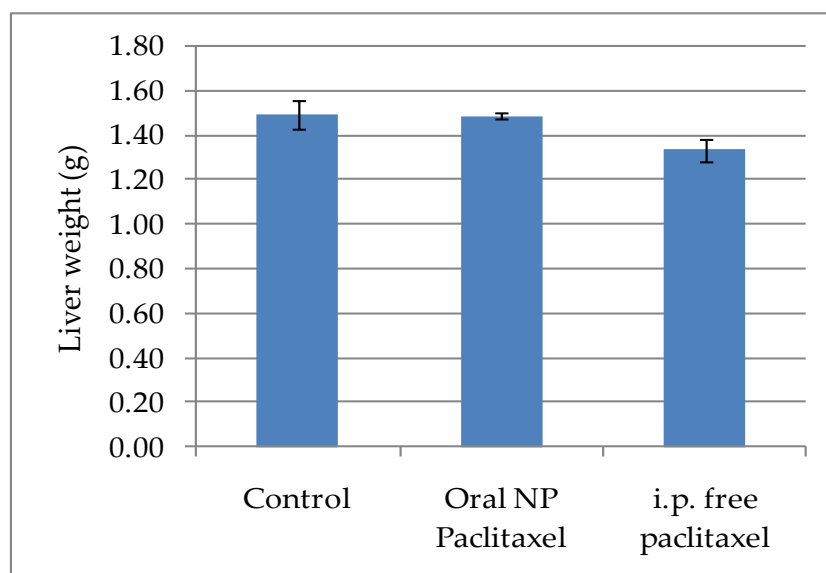
Figure 4.4: Liver weight in male C57BL6 mice (6 animals per group). Groups: (Control) no treatment; (Oral NP Paclitaxel) Paclitaxel (15 mg/kg) in nanoparticulate formulation (oral), (i.p. free paclitaxel) Paclitaxel (15 mg/kg) in cremophor EL (i.p.). (n=3-6). Error bars denote sem. Kruskal-Wallis One Way ANOVA on Ranks suggested that there is no statistically significant difference (P = 0.090).
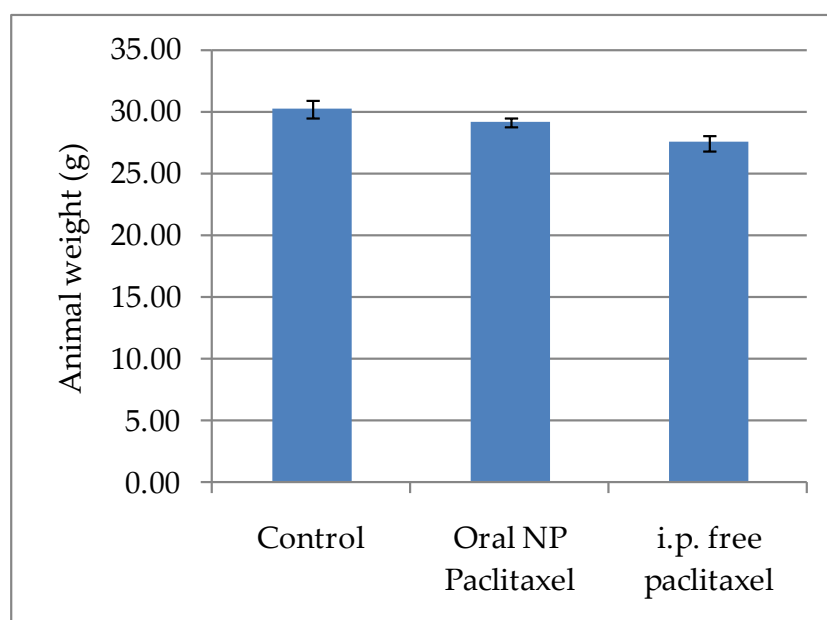
Figure 4.5: Weight of male C57BL6 mice (6 animals per group). Groups: (Control) no treatment; (Oral NP Paclitaxel) Paclitaxel (15 mg/kg) in nanoparticulate formulation (oral), (i.p. free paclitaxel) Paclitaxel (15 mg/kg) in cremophor EL (i.p.). (n=3-6). Error bars denote sem. Kruskal-Wallis One Way ANOVA on Ranks followed by Dunn's pairwise comparison suggested that there is a statistically significant difference between control group and i.p. free paclitaxel group (P = 0.038).

The comparison of average body weights indicated that Taxol® resulted in a mild decrease, but the other treatment groups did not cause any change in body weight (Figure 4.7). The animals in Taxol® group recovered after cessation of treatment.

4.4.3.2 Efficacy studies in tumours induced with drug sensitive cells

The tumours induced with drug sensitive cell line A2780 responded better to Taxol® treatment compared to the nanoparticles containing paclitaxel (Figure 4.8). Interestingly, Taxol® resulted in significant reduction in body weights of the animals in this case also (Figure 4.9). The average growth of increase in tumours treated with nanoparticulate formulation of paclitaxel was similar for both drug sensitive and the drug resistant cells.
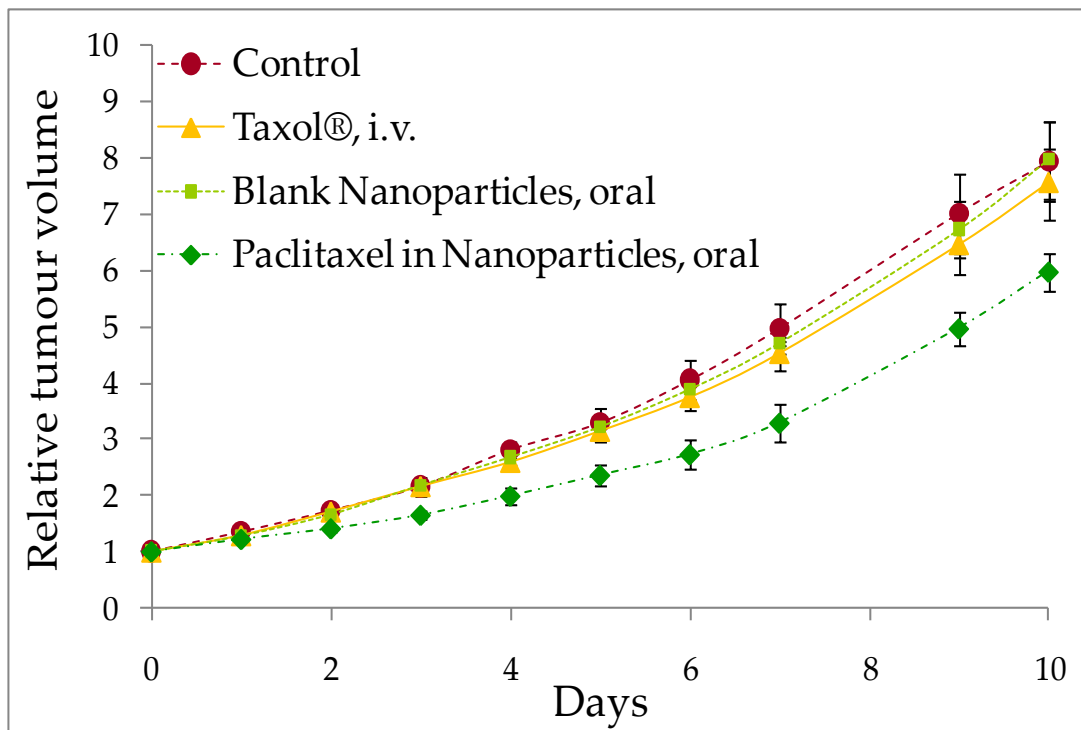
Figure 4.6: Relative tumour volumes in 2780AD cell-line induced xenograft study. Treatment was carried out on days 0, 2 and 4 (n=6). Error bars denote sd
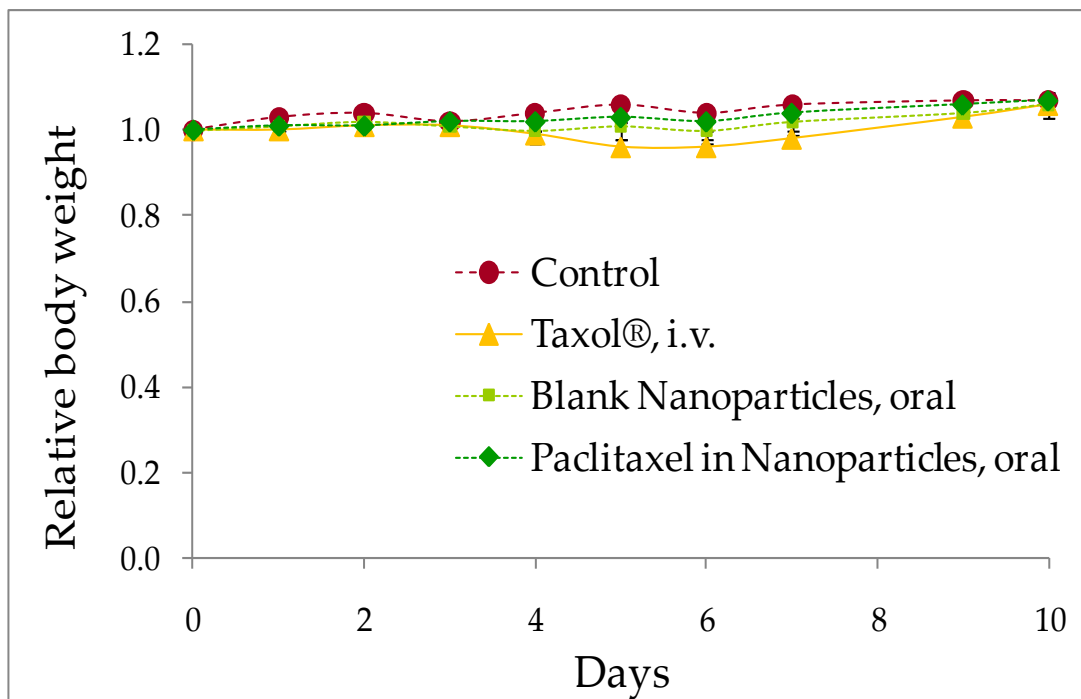
Figure 4.7: Relative body weight in resistant cell-line induced xenograft study. Treatment was carried out on days 0, 2 and 4 (n=6). Error bars denote sd
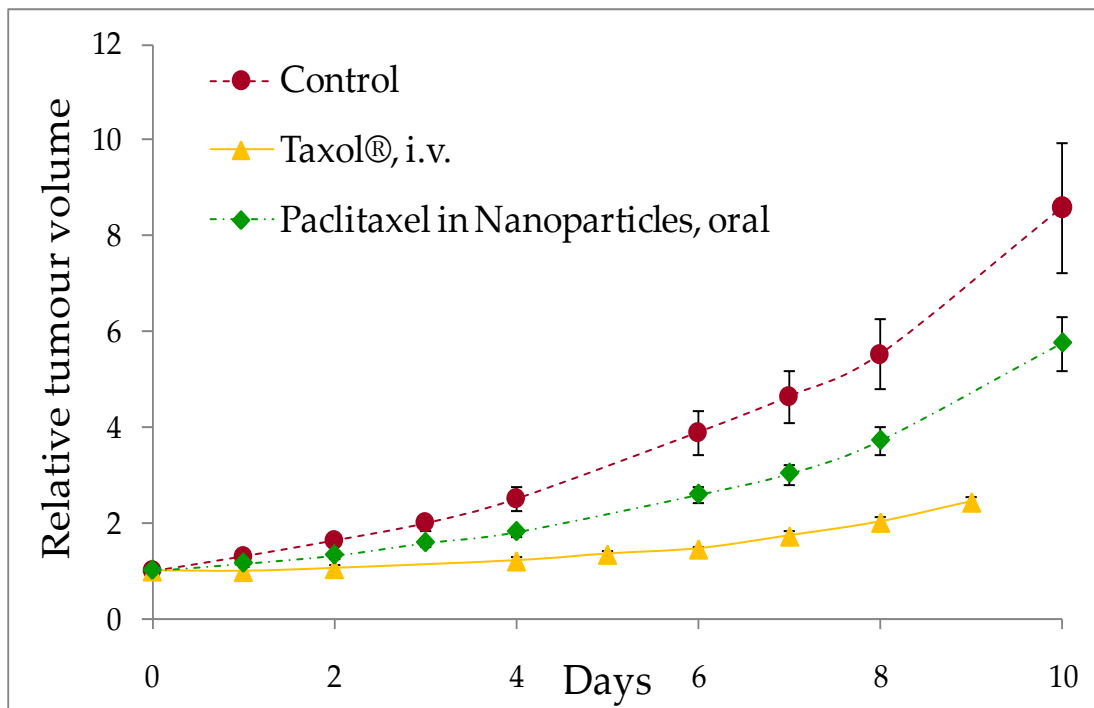
Figure 4.8: Relative tumour volumes in A2780 cell-line induced xenograft study. Treatment was carried out on days 0, 2 and 4 (n=6). Error bars denote sd
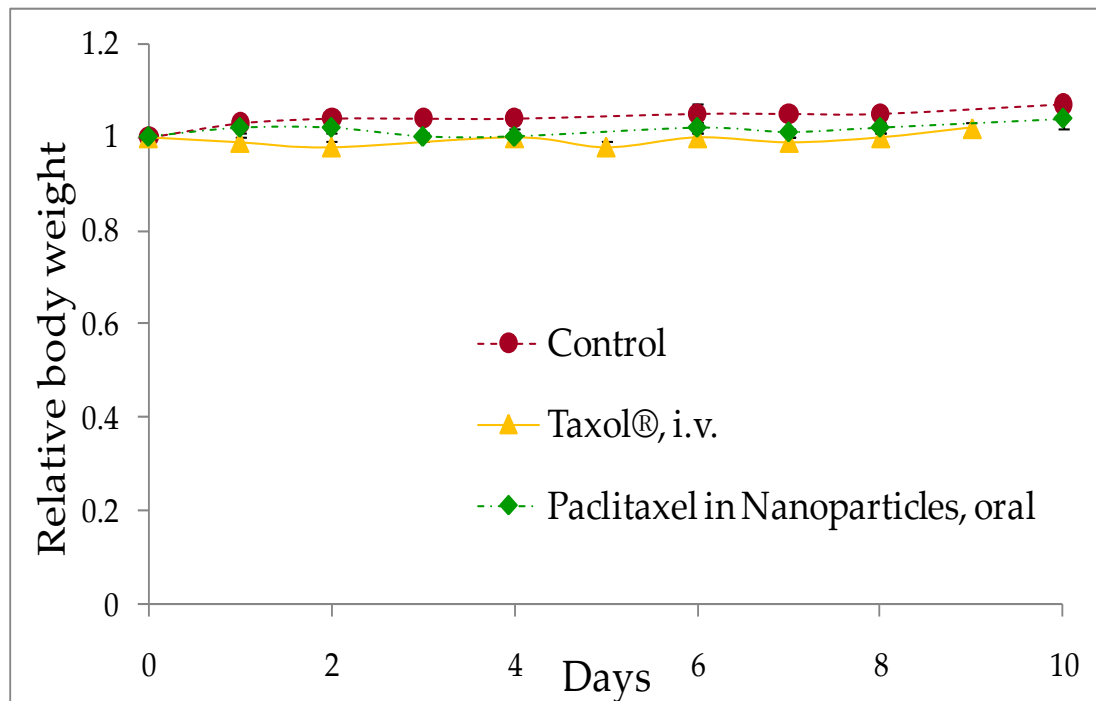
Figure 4.9: Relative body weights of mice in A2780 cell-line induced xenograft study. Treatment was carried out on days 0, 2 and 4 (n=6). Error bars denote sd

126

4.4.4 Tissue distribution study in chemical carcinogenesis model

Within 24 hours of oral administration of nanoparticles, paclitaxel was detected in tissues (Figure 4.10). The levels achieved in liver, tumour and kidney were almost 10% of those seen with the i.v. formulation, however the oral dose used was half of the i.v. dose. The proportion of drug in lungs and spleen after oral administration was comparatively higher than that attained after i.v. injection.
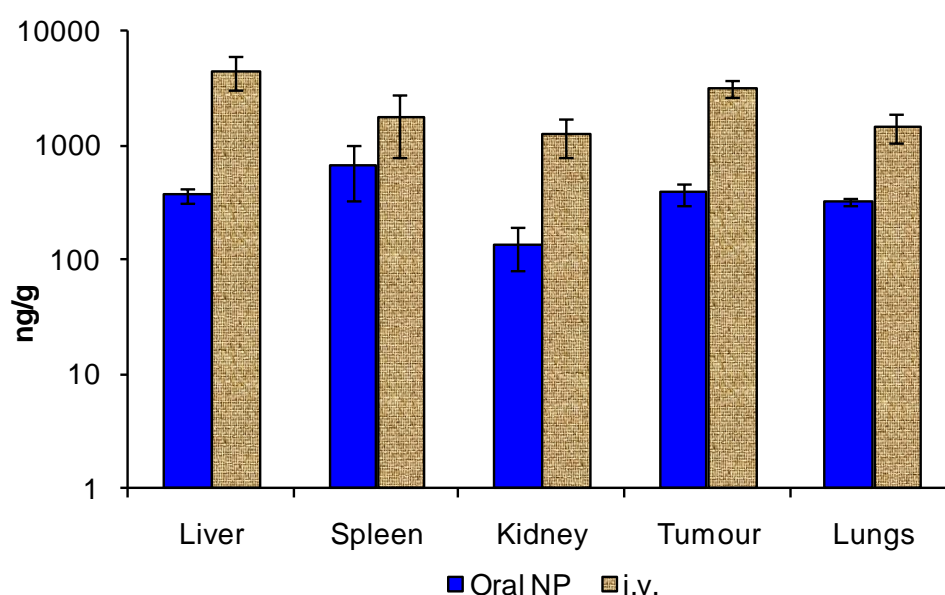
Figure 4.10: Tissue distribution of paclitaxel in rats (n=3) bearing mammary tumours 24 hours after dose. Oral NP group received 3.75 mg/kg and i.v. group received 7.5 mg/kg paclitaxel. Concentration of drug is denoted as nanogram of drug per gram of tissue. Error bars denote sem

4.5 Discussion

The *in vivo* study in the chemical carcinogenesis model in rats provides an encouraging proof of concept of utility of nanoparticulate anticancer formulations, highlighting the efficacy of paclitaxel incorporated in nanoparticles. It is worth noting that the human breast cancers bear many similarities to DMBA induced breast tumours in rats especially at the ultrastructural level (Rehm 1990). These models provide the most accurate determination of the metabolic pathways and aberrations responsible for initiation, development and spread of neoplasms. The nanoparticle formulation was found to be equally effective as the free drug treatment group but at half the dose. The average tumour weight measured after the orally administered paclitaxel in cremophor EL was roughly 3-fold higher than nanoparticulate formulation.

Although increase in oral bioavailability seems to be the most probable explanation of these findings, there nevertheless exists another prospective explanation for the improved comparison with the intravenous paclitaxel. The particles of mean size 125 nm used for the animal experiment have a potential to extravasate into the tumour from the vasculature and trapped by the EPR effect (Maeda 1992). Duncan and coworkers have reviewed studies using liposomes, nano- and microparticles and indicated that the capillary escape cut off size can be as large as 200 nm–1.2 μm in some animal tumour models (Duncan 1999). The EPR effect might be the key to the efficacy of the nanoparticle formulation because of their preferential accumulation in the tumours (Maeda 1992). It has been observed in other studies that size of the nanoparticles is the key for maintaining them in circulation and that smaller particles stay in systemic circulation for longer times compared with the larger particles (Mittal et al. 2007; Sahana et al. 2008). Therefore, longer

circulation times can result in cumulative accumulation of the particles in the tumours. Although not conclusively proved by this study, it is an exciting prospect that needs further mechanistic investigation.

Furthermore, by administering the drug intravenously, smaller average tumour weights were seen. Although the effect was comparable for the intravenous paclitaxel and orally administered particles, the dose of the drug in nanoparticulate formulation was only 50% of that administered intravenously with cremophor EL. This result indicates increased potency of the nanoparticulate formulation over the conventional treatment. The effect is highlighted in a more conspicuous manner in Figure 4.2 where the higher efficacy of nanoparticulate formulation compared to free drug is apparent. In addition, this result suggests increased oral bioavailability of paclitaxel when administered via the nanoparticles compared to the cremophor EL formulation.

The lung cancer induced by transplanted melanoma cells did not respond to paclitaxel treatment. As seen with the cell culture experiments, even micellar paclitaxel did not yield any reduction in lung or liver weight in the animals. The B16F0 cells are aggressively multiplying cells and are used to study metastasis. It might have been possible to see the therapeutic effect with a longer study, but the metastasis inflicted mortalities forced a premature termination. The affected animals had been injected with the cells intraperitoneally assuming that the cancer cells will migrate to the lungs. Small patches were indeed seen in the lungs, but the bulk of the metastasis was along the gastrointestinal system, which caused the unexpected mortality in the animals. Nevertheless, being an aggressive cancer, the melanoma was expected to respond to intravenously administered micellar paclitaxel, but it did not show any significant difference with respect to

control. Similar results were obtained in the cell culture experiments and it is evident that the particular strain under study was not sensitive towards paclitaxel.

In view of the promising activity seen in the cell lines *in vitro* we evaluated the particles in human tumour xenografts *in vivo*. Immunodeficient animals have the advantage that we can study the same human tumour cells that we use for the *in vitro* studies in an *in vivo* model.

Although transplantation models have been useful for cancer research, they have serious limitations, which significantly reduce their value as models for human cancer. They do not develop spontaneously in the natural organ, nor do they have growth rates and metastatic characteristics that resemble the natural history in humans. Further, an important limitation of the transplant model is the lack of metastasis from the subcutaneous site (Jonkers and Berns 2005).

The drug resistant derivative of A2780 (2780AD) has the MDR phenotype and is very resistant to the group of drugs involved (Plumb 1990). Although this is an *in vitro* derived drug resistant cell line it provides a useful model to evaluate strategies to circumvent drug resistance mechanisms. It has been shown that sensitivity to paclitaxel can be increased by treatment with an inhibitor of the drug efflux pump (Mistry et al. 2001).

Interestingly, a statistically significant reduction in the growth rate of tumours was seen in the drug-resistant cells in the group treated with the developed nanoparticulate formulation (Figure 4.6). Taxol®, which is a micellar formulation of paclitaxel in cremophor EL and ethanol, did not show any effect in the 2780AD cells. Clearly, there is an appreciable scope to further improve the efficacy of the nanoparticulate formulation. The mechanism of the drug sensitization is not clear. Possibly, the entrapment of

the drug inside the nanoparticles shields it from the efflux transporters. As and when the drug is released, the shares are split between sequestering the tubulin and efflux scavenging by Pgp. In comparison, when the free drug is absorbed by the cells, it is more actively pumped out from the cell. The difference in this gradient gives credence to particle trafficking mechanisms via structural engulfment rather than hypothesis of Fickian diffusion across the intracellular and paracellular routes. Also, since tubulin is one of the essential components of the structural architecture of cell, there is a higher chance of the bound paclitaxel to escape the efflux pump and contribute to tubulin depletion within the cell. Further, due to the enhanced permeation and retention (EPR) effect of the tumour environment, the particles are expected to accumulate and produce a constantly available supply of sheathed paclitaxel to the cancer cells (Maeda 1992). If loss in body weight is considered to be a rough reflection of the systemic side-effects, this also explains its relative lack when paclitaxel is given as the nanoparticulate formulation in comparison to the micellar Taxol® (Figure 4.7).

Tumours established from the drug sensitive A2780 cell line show a marked growth inhibition when treated with the maximum tolerated dose of paclitaxel (15/mg/kg i.v. x 3, Figure 4.8). Paclitaxel has very limited bioavailability when given by the oral route. However, although not as effective as the standard treatment regimen the orally delivered paclitaxel nanoparticles showed activity in this model. This result differs from that of an earlier study in chemically induced rat tumour model where nanoparticulate formulation at half the dose was equivalent to the micellar one (Bhardwaj et al. 2009). The positive aspect was that it once again demonstrated that oral delivery of paclitaxel is not only possible but also efficacious. The relative inferior efficacy against the micellar formulation can

be explained by a difference in the oral uptake or due to dose sensitivity. Rapidly multiplying cells generally exhibit higher sensitivity to a cytotoxic drug compared to those multiplying slowly (Lopes et al. 1993). The absolute cell kill in that case is proportional to the drug concentration presented which shall be higher for the i.v. formulation compared to the oral formulation. Slowly multiplying cells, on the contrary would require a sustained exposure of the drug, which will be provided by a formulation that can protect the drug from degradation. It is evident from Figure 4.6 and Figure 4.8 that the 2780 AD and A2780 cells grow aggressively in the subcutaneous implants, expanding to 8 times the volume from the starting date of the treatment. Using the L1210 Leukaemia transplantation model, it has been shown that a given dose of a drug will kill a fixed fraction, not a fixed number, of widely different-sized leukaemia cell populations (Skipper et al. 1964). This model, also known as the log-cell-kill model, is still the pre-eminent model of tumour growth and therapeutic regression (Jonkers and Berns 2005). Thus, in the aggressive tumour, the lower bioavailability of the oral nanoparticulate formulation provided smaller reduction in the growth rate of the tumours. Inclusion of a Pgp modulator along with the cytotoxic drug might further reduce the chances of treatment failure.

The mechanisms by which nanoparticles are taken up are under constant debate. To prove that nanoparticles enable the oral delivery of paclitaxel, the best way is to detect and quantify the drug in the plasma and body tissues after oral administration of the nanoparticles. Initial trials for development of a sensitive method of analysis of paclitaxel in biological tissues with HPLC met with limited success. Due to the sensitivity of detection, liquid scintigraphy estimation of radioactively labeled paclitaxel was carried out. The *in vivo* drug distribution study established that the drug appeared in the

body tissues within 24 hours of administration of the nanoparticles. The levels in kidney and liver were not appreciably higher with respect to other tissues signifying that the particles are not trapped by these clearance organs. Paclitaxel was not detected in the brain with either i.v. formulation or with the nanoparticles. This study corroborated the findings of the efficacy studies in the DMBA mammary tumour model and Pgp over expressing cancer model. It was established that nanoparticles make paclitaxel orally bioavailable. Though the levels seen with the oral formulation are much lower than the i.v. free drug, it is worth noting that the oral dose was half the i.v. dose. It has been shown by our group that drugs encapsulated in nanoparticulate formulations appear in the systemic circulation using the same polymer-stabiliser combination (Hariharan et al. 2006; Mittal and Kumar 2009). It is worth noting that the tumour levels do not show any significant accumulation with respect to other body tissues. The explanation is that the EPR effect allows a gradual build up of circulating macromolecules. A study with i.v. administration of nanoparticles or one that monitors the tissue levels for longer duration can provide more insight in this quest.

The presented study provides an exciting strategy to improve the sensitivity of drug resistant cancers especially of those for which resistance is mediated via over-expression of efflux transporters. The results in tumour model in nude mice demonstrate the possibility to deliver paclitaxel by oral route and the prospect of such formulations in increasing response to anticancer drug therapy.

4.6   Conclusions

- Orally administered nanoparticles containing paclitaxel significantly reduced the tumour burden in chemically induced breast cancer in female SD rats. Orally administered nanoparticles were equally efficacious as the intravenously administered micellar equivalent of the marketed formulation. Paclitaxel was not found to be effective against B16F0 melanoma cells induced tumours in mice

- Orally administered nanoparticles containing paclitaxel significantly reduced the tumour growth rate in Pgp over-expressing drug resistant cell line induced transplanted tumours in nude mice and were better than the micellar formulation. The particles also significantly reduced the tumour growth rate in Pgp normal-expressing drug sensitive cell line induced transplanted tumours in nude mice but the effect was greater with the micellar formulation. It can also be concluded that nanoparticle formulation is of more utility than the immediately available micellar formulation in slow growing tumours.

- Tissue distribution study establishes that oral delivery of paclitaxel is possible; drug encapsulated in nanoparticles appeared in body tissues within 24 hours.

Overall, the efficacy of the formulation in eliciting therapeutic response by reducing tumour burden in animals has established that nanoparticles allow oral delivery of paclitaxel and can improve its activity.

Summary

The aim of this study was to test the hypothesis that a nanoparticulate formulation can circumvent the hurdles of poor biopharmaceutical properties of paclitaxel and enable its oral delivery. The concluded studies establish that polymeric nanoparticles can enable the oral delivery of a BCS class IV compound and can impart significant benefit in therapy.

The study focussed on understanding the process of nanoparticle preparation from preformed biodegradable polymer using the process of emulsification solvent diffusion evaporation. It was shown that the design of homogeniser, the stabiliser concentration, solvent, speed of homogenisation and phase ratios of organic and aqueous components play a role in determining the size and PDI of nanoparticles. While homogenisers differ in design and speeds, a good correlation was established by comparing the tip speed of the homogeniser shaft with the size of particles produced. By understanding the role of formulation parameters, the degree of control on particle size was established.

Paclitaxel was then incorporated in the nanoparticles. The average diameter of the optimized particles using 1% w/v DMAB as stabiliser was 125 nm Even though both the drug and polymer are hydrophobic, a limited amount of paclitaxel could be entrapped within the PLGA nanoparticles (2-2.5% w/w). The process of recovery of particles from the suspension was optimized using stepwise centrifugation with gradually increasing rcf. Centrifugation was also utilised for washing the unbound stabiliser from these particles. A comprehensive screening of commonly used lyoprotectants showed that the particles can be lyophilised without causing changes in size or PDI using either trehalose or xylitol. The ratio of excipient to nanoparticles and the required concentrations were also optimised. AFM depicted

spherical geometry and smooth surface.

Cytotoxicity studies carried out on the stabiliser revealed that it is not cytotoxic to cells at concentrations lower than the CMC. The blank nanoparticles were also found to be non-cytotoxic to the cells in short term exposure study in MTT and LDH assays. P-gp inhibition studies carried out using a substrate rhodamine-123 show that DMAB does not have any intrinsic inhibitory activity against efflux in Caco-2 cells. The particles however showed some activity inhibiting the efflux of Calcein-AM in Pgp overexpressing MDCKII mdr1 cell line. Interestingly, nanoparticles decreased the IC_{50} of paclitaxel by 7 folds in drug resistant cancer cell line. This corroborates the results in the Calcein-AM assay.

Cytotoxicity studies carried out in B16F0 cell line showed that free paclitaxel in either DMSO or cremophor EL is not active against this cell line. However, at higher doses, paclitaxel exhibited 50% cytotoxicity in cell culture when it was incorporated in nanoparticles. Like the cell culture data, no effect was however seen in B16F0 cells induced cancers.

In DMBA induced breast cancer model in SD rats, orally administered particles were equally efficacious in reducing tumour burden at half the dose of i.v. micellar form. The drug loaded nanoparticles also showed significant reduction in growth of drug resistant tumours where free drug did not show any response. The drug distribution study carried out with radiolabeled drug proves that particles are taken up after oral administration. The collective conclusion of the above studies is that nanoparticles circumvented the biopharmaceutical hurdles of solubility, permeability and efflux to allow paclitaxel to elicit therapeutic benefit after oral administration.

The study provides a proof of concept of increase in oral bioavailability of poorly water soluble drugs using paclitaxel as a model drug.

Future Directions

The present study has on one hand revealed positive results, and run into intriguing challenges on the other. Both of these aspects need to be explored further. There is a scope of significant improvement in the developed formulation. The concerned areas pertain to not only the design of the formulation, but also the understanding of its performance in the cell culture and *in vivo* studies.

The drug loading with PLGA nanoparticles was low on a weight proportion basis. The particles could take up only 5% w/w of initial drug load and the final drug content in the particles was approximately 2.9% of the polymer weight. A typical chemotherapy cycle with paclitaxel uses dose of 135-175 mg/m^2 of the patient body surface area. This translates to roughly 4.6-6.0 grams of PLGA per cycle. Clearly, there is a need to increase drug content in the particles. A good primary screening for the polymers can be carried out using the semi-quantitative solid-state drug-polymer solubility study (Panyam et al. 2004).

Since paclitaxel is a hydrophobic drug, polymers with higher hydrophobicity than the 50:50 PLGA can be tried as the base material for nanoparticles. This can include other PLGA copolymer compositions containing higher content of lactic acid (higher proportion of lactic acid in PLGA results in higher hydrophobicity). A completely different polymer can also be tried that would allow higher drug solubility. A wide range of biodegradable polymers are available to choose from.

This study has used only the emulsification solvent evaporation method. Alternatively, other methods of particle preparation can be explored, like salting out, spray drying, dialysis etc. Instead of the nanospheres consisting of solid core, nanocapsules can be explored that will afford higher drug

loading in the core (Ishihara and Mizushima 2010).

The developed formulation involves a very labour and time intensive step of centrifugation to wash the unbound surfactant from the particles. It also causes decrease in particle yield with every cycle. Thus there is a need to explore particle washing without using centrifugation. This would allow easy scale-up of the process to be able to produce batches for clinical requirements. Dialysis in chlorine free water can be tried (chloride ions precipitate the DMAB). As an alternative, particles can be prepared without using a surfactant (nanoprecipitation is carried out by adding a solvent like alcohol to the ethyl acetate- water emulsion). The process has been reported in the literature from various groups, but needs to be optimized for obtaining particles with low polydispersity.

In freeze-drying study, it is possible that a ratio lower than 3.75 and higher than 2.5 might be the minimum ratio required. This aspect needs further mechanistic studies especially to understand the specific interaction of the sugars with the nanoparticles. A better understanding of the chemistry or physicochemical and especially thermal properties of the excipients explored in the freeze-drying study will provide insight into why some of them are better than others. Nanoparticles made from other polymers can be included in this study to ascertain if the process involves just the water-excipient interaction or if the material of the polymer can also influence the process and outcomes of freeze-drying. It might also be necessary to modulate the tonicity of the formulation with the added excipients. Although the product is intended for oral route, any additional studies in animals might include parenteral administration and then tonicity will become an important factor to prevent pain or inflammation at site of injection.

A drug release study needs to be carried out to establish the rate and phases

in which the drug is released from the medium. One challenge in carrying out this study is in establishing sink conditions in the medium owing to the very low aqueous solubility of paclitaxel. The introduction of plasma proteins can significantly improve sink conditions in the medium since paclitaxel binds extensively to them. Additionally, since the *in vitro* conditions are significantly simplistic in comparison to those found in the body, it is important to include the ingredients of the physiological fluids. Addition of isolated human or rodent plasma into the medium would make the release more bio-relevant. This would have to involve ways to prevent microbial growth in the medium over a long duration of study with periodic sampling. The HPLC method of analysis would have to be modified to ensure separation of the drug from the plasma components.

While the study has shown that drug encapsulated in nanoparticles was detected in various tissues after oral administration, the mechanism of particle uptake and transport has not been established. It is now generally accepted that the particles are taken up via both paracellular as well as transcellular routes across the intestinal barrier. Additionally, the drug was labelled with radioactive isotope and not the polymer. A study needs to be carried out using radiolabelled polymer to establish the permeation and transport of nanoparticles. Tissues can be collected and analyzed at various time points to track the particles and especially to establish if trapping occurs in tumour tissue.

The above discussion also points to the fact that the drug detected and estimated might be inside the nanoparticles or might have been released. Although it seems unlikely that such rapid release might have occurred, it needs to be proved that the drug was still inside the nanoparticles. Further work is required to establish an analytical method for the polymer itself. It

can be done by employing radiolabelling or a covalently bound tag with the polymer which is not easily cleaved in the body.

This would allow a pharmacokinetic study of the drug as well as the nanoparticles in the body. Since the nanoparticles act as mobile depots of drug in the body, the presently reported pharmacokinetic studies of drugs actually reflect combined pharmacokinetics of the drug and nanoparticles. It would be interesting to know the fate of the nanoparticles and how much time does the body take to complete excrete them.

The Pgp inhibitory potential of nanoparticles or improvement in efficacy of drugs that are substrates of efflux transporters is an exciting avenue that needs to be further explored. The study in animals has shown that the nanoparticles help in reducing the rate of growth tumours, but the mechanism is not clear. Mechanistic studies are warranted in this direction to better understand the reasons behind better therapeutic efficacy of encapsulated drugs.

Finally, an attempt can be made to attach functional moieties to the nanoparticles to allow active targeting to the tumours. This would significantly reduce the required dose of the drug and result in lower non-target organ toxicity.

References

Abdelwahed, W., Degobert, G. and Fessi, H. (2006a). "Freeze-drying of nanocapsules: Impact of annealing on the drying process." International Journal of Pharmaceutics **324**: 74-82.

Abdelwahed, W., Degobert, G. and Fessi, H. (2006b). "A pilot study of freeze drying of poly(epsilon-caprolactone) nanocapsules stabilized by poly(vinyl alcohol): Formulation and process optimization." International Journal of Pharmaceutics **309**: 178-188.

Abdelwahed, W., Degobert, G., Stainmesse, S. and Fessi, H. (2006c). "Freeze-drying of nanoparticles: Formulation, process and storage considerations." Advanced Drug Delivery Reviews **58**: 1688-1713.

Alcaro, S., Ventura, C. A., Paolino, D., Battaglia, D., Ortuso, F., Cattel, L., Puglisi, G. and Fresta, M. (2002). "Preparation, characterization, molecular modeling and in vitro activity of paclitaxel-cyclodextrin complexes." Bioorganic & Medicinal Chemistry Letters **12**: 1637-1641.

Allen, T. M. and Cullis, P. R. (2004). "Drug delivery systems: Entering the mainstream." Science **303**: 1818-1822.

Alonso, M. J. (2004). "Nanomedicines for overcoming biological barriers." Biomedical Pharmacotherapy **58**: 168-172.

Amidon, G. L., Lennernas, H., Shah, V. P. and Crison, J. R. (1995). "A theoretical basis for a biopharmaceutic drug classification: the correlation of in vitro drug product dissolution and in vivo bioavailability." Pharmaceutical Research **12**: 413-420.

Anderson, J. M. and Shive, M. S. (1997). "Biodegradation and biocompatibility of PLA and PLGA microspheres." Advanced Drug Delivery Reviews **28**: 5-24.

Ankola, D. D., Viswanad, B., Bhardwaj, V., Ramarao, P. and Kumar, M. N. V. R. (2007). "Development of potent oral nanoparticulate formulation of coenzyme Q10 for treatment of hypertension: Can the simple nutritional supplements be used as first line therapeutic agents for prophylaxis/therapy?" European Journal of Pharmaceutics & Biopharmaceutics **67**: 361-369.

Artursson, P., Palm, K. and Luthman, K. (1996). "Caco-2 monolayers in experimental and theoretical predictions of drug transport." Advanced Drug Delivery Reviews **22**: 67-84.

Bailey, C. A., Bryla, P. and Malick, A. W. (1996). "The use of the intestinal epithelial cell culture model, Caco-2, in pharmaceutical development." Advanced Drug Delivery Reviews **22**: 85-103.

Bala, I., Hariharan, S. and Kumar, M. N. V. R. (2004). "PLGA nanoparticles in drug delivery: The state of the art." Critical Reviews in Therapeutic Drug Carrier Systems **21**: 387-422.

Balimane, P. V. and Chong, S. (2005). "Cell culture-based models for intestinal permeability: A critique." Drug Discovery Today **10**: 335-343.

Bardelmeijer, H., Ouwehand, M., Malingré, M., Schellens, J., Beijnen, J. and van Tellingen, O. (2002). "Entrapment by Cremophor EL decreases the absorption of paclitaxel from the gut." Cancer Chemotherapy and Pharmacology **49**: 119-125.

Bardelmeijer, H. A., Beijnen, J. H., Brouwer, K. R., Rosing, H., Nooijen, W. J., Schellens, J. H. M. and van Tellingen, O. (2000). "Increased oral bioavailability of paclitaxel by GF120918 in mice through selective modulation of P-glycoprotein." Clinical Cancer Research **6**: 4416-4421.

Benacerraf, B., Bilbey, D., Biozzi, G., Halpern, B. N. and Stiffel, C. (1957). "The measurement of liver blood flow in partially hepatectomized rats." Journal of Physiology **136**: 287-293.

Bhardwaj, V., Ankola, D., Gupta, S., Schneider, M., Lehr, C. M. and Kumar, M. (2009). "PLGA nanoparticles stabilized with cationic surfactant: Safety studies and application in oral delivery of paclitaxel to treat chemical-induced breast cancer in rat." Pharmaceutical Research **26**: 2495-2503.

Bhardwaj, V., Hariharan, S., Bala, I., Lamprecht, A., Kumar, N., Panchagnula, R. and Kumar, M. N. V. R. (2005). "Pharmaceutical aspects of polymeric nanoparticles for oral delivery." Journal of Biomedical Nanotechnology **1**: 235-258.

Birrenbach, G. (1973). Über Mizellpolymerisate, mögliche Einschlussverbindungen (Nanokapseln) und deren Eignung als Adjuvantien. ETH. Zürich.

Birrenbach, G. and Speiser, P. P. (1976). "Polymerized micelles and their use as adjuvants in immunology." Journal of Pharmaceutical Sciences **65**: 1763-1766.

Brahn, E., Tang, C. and Banquerigo, M. L. (1994). "Regression of collagen-induced arthritis with taxol, a microtubule stabilizer." Arthritis & Rheumatism **37**: 839-845.

Braun, A., Hammerle, S., Suda, K., Rothen-Rutishauser, B., Gunthert, M., Kramer, S. D. and Wunderli-Allenspach, H. (2000). "Cell cultures as tools in biopharmacy." European Journal of Pharmaceutical Sciences **11**: S51-S60.

Bromberg, L. (2008). "Polymeric micelles in oral chemotherapy." Journal of Controlled Release **128**: 99-112.

Brown, J. M. and Giaccia, A. J. (1998). "The unique physiology of solid tumors: Opportunities (and problems) for cancer therapy." Cancer Research **58**: 1408-1416.

Buckton, G. (1995). Interfacial phenomena in drug delivery and targeting. A. T. Florence and G. Gregoriadis, Chur, Harwood Academic Publishers.

Cao, L., Sun, D., Cruz, T., Moscarello, M. A., Ludwin, S. K. and Whitaker, J. N. (2000). "Inhibition of experimental allergic encephalomyelitis in the Lewis rat by paclitaxel." Journal of Neuroimmunology **108**: 103-111.

Carney, D. N. (1991). "The pharmacology of intravenous and oral etoposide." Cancer **67**: 299-302.

Chan, L. M. S., Lowes, S. and Hirst, B. H. (2004). "The ABCs of drug transport in intestine and liver: Efflux proteins limiting drug absorption and bioavailability." European Journal of Pharmaceutical Sciences **21**: 25-51.

Choi, J.-S., Choi, H.-K. and Shin, S.-C. (2004a). "Enhanced bioavailability of paclitaxel after oral coadministration with flavone in rats." International Journal of Pharmaceutics **275**: 165-170.

Choi, J.-S. and Jo, B.-W. (2004). "Enhanced paclitaxel bioavailability after oral administration of pegylated paclitaxel prodrug for oral delivery in rats." International Journal of Pharmaceutics **280**: 221-227.

Choi, J.-S., Jo, B.-W. and Kim, Y.-C. (2004b). "Enhanced paclitaxel bioavailability after oral administration of paclitaxel or prodrug to rats pretreated with quercetin." European Journal of Pharmaceutics and Biopharmaceutics **57**: 313-318.

Choi, J.-S. and Shin, S.-C. (2005). "Enhanced paclitaxel bioavailability after oral coadministration of paclitaxel prodrug with naringin to rats." International Journal of Pharmaceutics **292**: 149-156.

Constantinou, A. I., Xu, H., Cunningham, E., Lantvit, D. D. and Pezzuto, J. M. (2001). "Consumption of soy products may enhance the breast cancer-preventive effects of tamoxifen." Proceedings of the American Association for Cancer Research **42**: Abstract #4440.

Couvreur, P., Tulkens, P. and Roland, M. (1977). "Nanocapsules: a new type of lysosomotropic carrier." FEBS Letters **84**: 323-326.

Crosasso, P., Ceruti, M., Brusa, P., Arpicco, S., Dosio, F. and Cattel, L. (2000). "Preparation, characterization and properties of sterically stabilized paclitaxel-containing liposomes." Journal of Controlled Release **63**: 19-30.

Cuvier, C., Roblot-Treupel, L., Millot, J. M., Lizard, G., Chevillard, S., Manfait, M., Couvreur, P. and Poupon, M. F. (1992). "Doxorubicin-loaded nanospheres bypass tumor cell multidrug resistance." Biochemical Pharmacology **44**: 509-517.

Daniel, M.-C. and Astruc, D. (2003). "Gold nanoparticles: Assembly, supramolecular chemistry, quantum-size-related properties, and applications toward biology, catalysis, and nanotechnology." Chemical Reviews **104**: 293-346.

Dantzig, A. H., Shepard, R. L., Cao, J., Law, K. L., Ehlhardt, W. J., Baughman, T. M., Bumol, T. F. and Starling, J. J. (1996). "Reversal of P-glycoprotein-mediated multidrug resistance by a potent cyclopropyldibenzosuberane modulator, LY335979." Cancer Research **56**: 4171-4179.

Davis, L. and Kuttan, G. (2001). "Effect of *Withania somnifera* on DMBA induced carcinogenesis." Journal of Ethnopharmacology **75**: 165-168.

Derjaguin, B. and Landau, L. (1941). "Theory of the stability of strongly charged lyophobic sols and of the adhesion of strongly charged particles in solutions of electrolytes." Acta Physicochimica **14**: 633-662.

Derjaguin, B. V. (1993). "Main factors affecting the stability of colloids." Progress in Surface Science **43**: 109-114.

Deryagin, B. V. (1992). "Summary of development of the theory of stability of colloids and thin films." Russian Chemical Bulletin **41**: 1321-1328.

Desai, N., Trieu, V., Yao, R., Labao, E., De, T. and Soon-Shiong, P. (2004). "Increased transport of nanoparticle albumin-bound paclitaxel (ABI-007) by endothelial gp60-mediated caveolar transcytosis: a pathway inhibited by Taxol." European Journal of Cancer Supplements **2**: 182-143.

Desai, N., Trieu, V., Yao, Z., Louie, L., Ci, S., Yang, A., Tao, C., De, T., Beals, B., Dykes, D., Noker, P., Yao, R., Labao, E., Hawkins, M. and Soon-Shiong, P. (2006). "Increased antitumor activity, intratumor paclitaxel concentrations, and endothelial cell transport of cremophor-free, albumin-bound paclitaxel, ABI-007, compared with cremophor-based paclitaxel." Clinical Cancer Research **12**: 1317-1324.

Dordunoo, S. K., Oktaba, A. M. C., Hunter, W., Min, W., Cruz, T. and Burt, H. M. (1997). "Release of taxol from poly(ε-caprolactone) pastes: Effect of water-soluble additives." Journal of Controlled Release **44**: 87-94.

Duncan, R. (1999). "Polymer conjugates for tumour targeting and intracytoplasmic delivery. The EPR effect as a common gateway?" Pharmaceutical Science & Technology Today **2**: 441-449.

Duncan, R. (2005). "Nanomedicine gets clinical." Materials Today **8**: 16-17.

Dye, D. and Watkins, J. (1980). "Suspected anaphylactic reaction to Cremophor EL." British Medical Journal **280**: 1353.

Edlund, U. and Albertsson, A. C. (2002). "Degradable polymer microspheres for controlled drug delivery." Advances in Polymer Science **157**: 67-112.

Ehrlich, A., Booher, S., Becerra, Y., Borris, D. L., Figg, W. D., Turner, M. L. and Blauvelt, A. (2004). "Micellar paclitaxel improves severe psoriasis in a prospective phase II pilot study." Journal of the American Academy of Dermatology **50**: 533-40.

Einstein, A. (1905). "Über die von der molekularkinetischen Theorie der Wärme geforderte Bewegung von in ruhenden Flüssigkeiten suspendierten Teilchen." Annalen der Physik **322**: 549-560.

El-Bayoumy, K., Das, A., Boyiri, T., Desai, D., Sinha, R., Pittman, B. and Amin, S. (2003). "Comparative action of 1,4-phenylenebis(methylene)selenocyanate and its metabolites against 7,12-dimethylbenz[a]anthracene-DNA adduct formation in the rat and cell proliferation in rat mammary tumor cells." Chemico-Biological Interactions **146**: 179-190.

Eldridge, J. H., Hammond, C. J., Meulbroek, J. A., Staas, J. K., Gilley, R. M. and Tice, T. R. (1990). "Controlled vaccine release in the gut-associated lymphoid tissues. I. Orally administrated biodegradable microspheres target the Peyer's patches." J Control Rel **11**: 205-214.

Emilienne Soma, C., Dubernet, C., Bentolila, D., Benita, S. and Couvreur, P. (2000). "Reversion of multidrug resistance by co-encapsulation of doxorubicin and cyclosporin A in polyalkylcyanoacrylate nanoparticles." Biomaterials **21**: 1-7.

Feng, Z., Zhao, G., Yu, L., Gough, D. and Howell, S. (2010). "Preclinical efficacy studies of a novel nanoparticle-based formulation of paclitaxel that out-performs Abraxane." Cancer Chemotherapy and Pharmacology **65**: 923-930.

Florence, A. T. (1997). "The oral absorption of micro- and nanoparticulates: Neither exceptional nor unusual." Pharmaceutical Research **14**: 259-266.

Foss, M., Wilcox, B. W. L., Alsop, G. B. and Zhang, D. (2008). "Taxol crystals can masquerade as stabilized microtubules." PLoS One **3**: e1476.

Franks, F. (1998). "Freeze-drying of bioproducts: putting principles into practice." European Journal of Pharmaceutics and Biopharmaceutics **45**: 221-229.

Frey, E. and Kroy, K. (2005). "Brownian motion: a paradigm of soft matter and biological physics." Annalen der Physik **14**: 20-50.

Gad, S. E. and Philip, W. (2005). Biocompatibility. Encyclopedia of Toxicology. New York, Elsevier**:** 280-285.

Gao, P., Rush, B. D., Pfund, W. P., Huang, T., Bauer, J. M., Morozowich, W., Kuo, M. S. and Hageman, M. J. (2003). "Development of a supersaturable SEDDS (S-SEDDS) formulation of paclitaxel with improved oral bioavailability." Journal of Pharmaceutical Sciences **92**: 2386-2398.

Gelderblom, H., Baker, S. D., Zhao, M., Verweij, J. and Sparreboom, A. (2003). "Distribution of paclitaxel in plasma and cerebrospinal fluid." Anti-Cancer Drugs **14**: 365-8.

Gelderblom, H., Verweij, J., Nooter, K. and Sparreboom, A. (2001). "Cremophor EL: the drawbacks and advantages of vehicle selection for drug formulation." European Journal of Cancer **37**: 1590-1598.

Geyer, R. P., Bleisch, V. R., Bryant, J. E., Robbins, A. N., Saslaw, I. M. and Stare, F. J. (1951). "Tumor production in rats injected intravenously with oil emulsions containing 9,10-dimethyl-1,2-benzanthracene." Cancer Research **11**: 474-478.

Goodman, J. and Walsh, V. (2001). The story of taxol : nature and politics in the pursuit of an anti-cancer drug, Cambridge ; New York, Cambridge University Press.

Gradishar, W. J., Tjulandin, S., Davidson, N., Shaw, H., Desai, N., Bhar, P., Hawkins, M. and O'Shaughnessy, J. (2005). "Phase III trial of nanoparticle albumin-bound paclitaxel compared with polyethylated castor oil-based paclitaxel in women with breast cancer." Journal of Clinical Oncology **23**: 7794-7803.

Haldar, S., Chintapalli, J. and Croce, C. M. (1996). "Taxol induces bcl-2 phosphorylation and death of prostate cancer cells." Cancer Research **56**: 1253-1255.

Haldar, S., Jena, N. and Croce, C. M. (1995). "Inactivation of bcl-2 by phosphorylation." Proceedings of the National Academy of Sciences of the United States of America **92**: 4507-4511.

Hamada, H., Ishihara, K., Masuoka, N., Mikuni, K. and Nakajima, N. (2006). "Enhancement of water-solubility and bioactivity of paclitaxel using modified cyclodextrins." Journal of Bioscience and Bioengineering **102**: 369-371.

Hanes, J. (2006). "New polymeric nanomedicines for targeted and controlled drug delivery." Nanomedicine: Nanotechnology, Biology and Medicine **2**: 273-273.

Hariharan, S., Bhardwaj, V., Bala, I., Sitterberg, J., Bakowsky, U. and Kumar, M. N. V. R. (2006). "Design of estradiol loaded PLGA nanoparticulate formulations: A Potential oral delivery system for hormone therapy." Pharmaceutical Research **23**: 184-196.

Hobbs, S. K., Monsky, W. L., Yuan, F., Roberts, W. G., Griffith, L., Torchilin, V. P. and Jain, R. K. (1998). "Regulation of transport pathways in tumor vessels: Role of tumor type and microenvironment." Proceedings of the National Academy of Sciences of the United States of America **95**: 4607-4612.

Holzer, M., Vogel, V., Mäntele, W., Schwartz, D., Haase, W. and Langer, K. (2009). "Physico-chemical characterisation of PLGA nanoparticles after freeze-drying and storage." European Journal of Pharmaceutics and Biopharmaceutics **72**: 428-437.

Holzgrabe, U. (2005). "Paclitaxel zur Alzheimer-Behandlung." Pharmazie in Unserer Zeit **34**: 96.

Huang, Y.-y., Qi, M., Zhang, M., Liu, H.-z. and Yang, D.-z. (2006). "Degradation mechanisms of poly (lactic-co-glycolic acid) films in vitro under static and dynamic environment." Transactions of Nonferrous Metals Society of China **16**: s293-s297.

Huggins, C., Grand, L. C. and Brillantes, F. P. (1961). "Mammary cancer induced by a single feeding of polynuclear hydrocarbons, and its suppression." Nature **189**: 204-207.

Ibrahim, H., Bindschaedler, C., Doelker, E., Buri, P. and Gurny, R. (1992). "Aqueous nanodispersions prepared by a salting-out process." Int. J. Pharm. **87**: 239-246.

Ishihara, T. and Mizushima, T. (2010). "Techniques for efficient entrapment of pharmaceuticals in biodegradable solid micro/nanoparticles." Expert Opinion on Drug Delivery **7**: 565-575.

Jacques, F. (2000). "Analysis of the tangled relationships between P-glycoprotein-mediated multidrug resistance and the lipid phase of the cell membrane." European Journal of Biochemistry **267**: 277-294.

Jain, R. A. (2000). "The manufacturing techniques of various drug loaded biodegradable poly(lactide-co-glycolide) (PLGA) devices." Biomaterials **21**: 2475-2490.

Jiaher, T. and Valentino, J. S. (2009). "Degradation of paclitaxel and related compounds in aqueous solutions III: Degradation under acidic pH

conditions and overall kinetics." Journal of Pharmaceutical Sciences **99**: 1288-1298.

Jiang, Q., Yan, Z. and Feng, J. (2006). "Neurotrophic factors stabilize microtubules and protect against rotenone toxicity on dopaminergic neurons." Journal of Biological Chemistry **281**: 29391-29400.

Jonkers, J. and Berns, A. (2005). Animal models of cancer. Introduction to the cellular and molecular biology of cancer. Eds. M. A. Knowles and P. J. Selby. Oxford, Oxford University Press**:** 317-336.

Kabanov, A. V., Batrakova, E. V. and Alakhov, V. Y. (2002). "Pluronic® block copolymers for overcoming drug resistance in cancer." Advanced Drug Delivery Reviews **54**: 759-779.

Kante, B., Couvreur, P., Lenaerts, V., Guiot, P., Roland, M., Baudhuin, P. and Speiser, P. (1980). "Tissue distribution of [3H]actinomycin D adsorbed on polybutylcyanoacrylate nanoparticles." International Journal of Pharmaceutics **7**: 45-53.

Khandavilli, S. and Panchagnula, R. (2007). "Nanoemulsions as versatile formulations for paclitaxel delivery: Peroral and dermal delivery studies in rats." Journal of Investigative Dermatology **127**: 154-162.

Khanna, S. C., Jecklin, T. and Speiser, P. (1970). "Bead polymerization technique for sustained-release dosage form." Journal of Pharmaceutical Sciences **59**: 614-618.

Khanna, S. C. and Speiser, P. (1969). "Epoxy resin beads as a pharmaceutical dosage form I: Method of preparation." Journal of Pharmaceutical Sciences **58**: 1114-1117.

Kim, S. W., Lee, S. J., Cho, Y. H., Yoon, M. S. and Lee, C. H. (2005). Abstract 328: The anticancer efficacy and toxicity of oral paclitaxel-loaded lipid nanoparticle in a C3H2 bladder cancer mice. European Urology

Supplements, XXth Congress of the European Association of Urology **4:** 84.

Koolen, S. L. W., Beijnen, J. H. and Schellens, J. H. M. (2009). "Intravenous-to-oral switch in anticancer chemotherapy: A focus on docetaxel and paclitaxel." Clinical Pharmacology & Therapeutics **87**: 126-129.

Kramer, P. A. (1974). "Albumin microspheres as vehicles for achieving specificity in drug delivery." Journal of Pharmaceutical Sciences **63**: 1646-1647.

Kreuter, J. (1994). Nanoparticles. Encyclopedia of Pharmaceutical Technology. J. Swarbrick and J. C. Boylan. New York, M. Dekker. **10:** 165-190.

Kreuter, J. (2004). "Influence of the surface properties on nanoparticle-mediated transport of drugs to the brain." Journal of Nanoscience and Nanotechnology **4**: 484-488.

Kreuter, J., Petrov, V. E., Kharkevich, D. A. and Alyautdin, R. N. (1997). "Influence of the type of surfactant on the analgesic effects induced by the peptide dalargin after its delivery across the blood-brain barrier using surfactant-coated nanoparticles." Journal of Controlled Release **49**: 81-87.

Kumar, M. N. V. R., Bakowsky, U. and Lehr, C. M. (2004). "Preparation and characterization of cationic PLGA nanospheres as DNA carriers." Biomaterials **25**: 1771-1777.

Kumar, M. N. V. R., Vadhanam, M. V., Horn, J., Flesher, J. W. and Gupta, R. C. (2005). "Formation of benzylic-DNA adducts resulting from 7,12-dimethylbenz[a]anthracene in vivo." Chemical Research in Toxicology **18**: 686-691.

Kumar, N. (1981). "Taxol-induced polymerization of purified tubulin. Mechanism of action." Journal of Biological Chemistry **256**: 10435-10441.

Lehr, C. M. and Lee, V. H. L. (1993). "Binding and transport of some bioadhesive plant lectins across Caco-2 cell monolayers." Pharmaceutical Research **10**: 1796-1799.

Lesser, G. J., Grossman, S. A., Eller, S. and Rowinsky, E. K. (1995). "The distribution of systemically administered [3H]-paclitaxel in rats: a quantitative autoradiographic study." Cancer Chemotherapy and Pharmacology **37**: 173-8.

Liggins, R. T., Cruz, T., Min, W., Liang, L., Hunter, W. L. and Burt, H. M. (2004). "Intra-articular treatment of arthritis with microsphere formulations of paclitaxel: Biocompatibility and efficacy determinations in rabbits." Inflammation Research **53**: 363-372.

Lipinski, C. A., Lombardo, F., Dominy, B. W. and Feeney, P. J. (1997). "Experimental and computational approaches to estimate solubility and permeability in drug discovery and development settings." Advanced Drug Delivery Reviews **23**: 3-25.

Liu, G., Franssen, E., Fitch, M. I. and Warner, E. (1997). "Patient preferences for oral versus intravenous palliative chemotherapy." Journal of Clinical Oncology **15**: 110-115.

Lopes, N. M., Adams, E. G., Pitts, T. W. and Bhuyan, B. K. (1993). "Cell kill kinetics and cell cycle effects of taxol on human and hamster ovarian cell lines." Cancer Chemotherapy and Pharmacology **32**: 235-242.

Lunberg, B. B. J. (1997). "A submicron lipid emulsion coated with amphipathic polyethylene glycol for parenteral administration of paclitaxel (Taxol)." Journal of Pharmacy and Pharmacology **49**: 16-21.

Maeda, H. (1992). "The tumor blood vessel as an ideal target for macromolecular anticancer agents." J Control Rel **19**: 315-324.

Malingré, M. M., Beijnen, J. H., Rosing, H., Koopman, F. J., van Tellingen, O., Duchin, K., ten Bokkel Huinink, W. W., Swart, M., Lieverst, J. and Schellens, J. H. M. (2001). "The effect of different doses of cyclosporin A on the systemic exposure of orally administered paclitaxel." Anti-Cancer Drugs **12**: 351-358.

Malingre, M. M., Schellens, J. H. M., Van Tellingen, O., Ouwehand, M., Bardelmeijer, H. A., Rosing, H., Jansen, S. E., Koopman, F. J., Schot, M. E., Ten Bokkel Huinink, W. W. and Beijnen, J. H. (2001). "The co-solvent Cremophor EL limits absorption of orally administered paclitaxel in cancer patients." British Journal of Cancer **85**: 1472-1477.

Mass, B., Huber, C. and Kramer, I. (1996). "Plasticizer extraction of Taxol infusion solution from various infusion devices." Pharmacy World and Science **18**: 78-82.

Mathiowitz, E., Jacob, J. S., Jong, Y. S., Carino, G. P., Chickering, D. E., Chaturvedi, P., Santos, C. A., Vijayraghavan, K., Montgomery, S., Bassett, M. and Morrell, C. (1997). "Biologically erodable microspheres as potential oral drug delivery systems." Nature **386**: 410-414.

Matsumura, Y. and Maeda, H. (1986). "A new concept for macromolecular therapeutics in cancer chemotherapy: Mechanism of tumoritropic accumulation of proteins and the antitumor agent smancs." Cancer Research **46**: 6387-6392.

Matulka, L. A. and Wagner, K.-U. (2005). "Models of breast cancer." Drug Discovery Today: Disease Models **2**: 1-6.

Meaney, C. and O'Driscoll, C. (1999). "Mucus as a barrier to the permeability of hydrophilic and lipophilic compounds in the absence and presence of

sodium taurocholate micellar systems using cell culture models." European Journal of Pharmaceutical Sciences **8**: 167-175.

Meerum Terwogt, J. M., Malingré, M. M., Beijnen, J. H., ten Bokkel Huinink, W. W., Rosing, H., Koopman, F. J., van Tellingen, O., Swart, M. and Schellens, J. H. M. (1999). "Coadministration of oral Cyclosporin A enables oral therapy with paclitaxel." Clinical Cancer Research **5**: 3379-3384.

Merkle, H. P. and Speiser, P. (1973). "Preparation and *in vitro* evaluation of cellulose acetate phthalate coacervate microcapsules." Journal of Pharmaceutical Sciences **62**: 1444-1448.

Mistry, P., Stewart, A. J., Dangerfield, W., Okiji, S., Liddle, C., Bootle, D., Plumb, J. A., Templeton, D. and Charlton, P. (2001). "In vitro and in vivo reversal of P-glycoprotein-mediated multidrug resistance by a novel potent modulator, XR9576." Cancer Research **61**: 749-758.

Mittal, G. and Kumar, M. R. (2009). "Impact of polymeric nanoparticles on oral pharmacokinetics: A dose-dependent case study with estradiol." Journal of Pharmaceutical Sciences **98**: 3730-3734.

Mittal, G., Sahana, D. K., Bhardwaj, V. and Kumar, M. N. V. R. (2007). "Estradiol loaded PLGA nanoparticles for oral administration: Effect of polymer molecular weight and copolymer composition on release behavior in vitro and in vivo." Journal of Controlled Release **119**: 77-85.

Moghimi, S. M. and Kissel, T. (2006). "Particulate nanomedicines." Advanced Drug Delivery Reviews **58**: 1451-1455.

Mosmann, T. (1983). "Rapid colorimetric assay for cellular growth and survival: Application to proliferation and cytotoxicity assays." Journal of Immunological Methods **65**: 55-63.

Panchagnula, R. (1998). "Pharmaceutical aspects of paclitaxel." International Journal of Pharmaceutics **172**: 1-15.

Panchagnula, R., Dhanikula, R. S. and Dhanikula, A. B. (2006). "An *ex vivo* characterization of paclitaxel loaded chitosan films after implantation in mice." Current Drug Delivery **3**: 287-297.

Panyam, J., Williams, D., Dash, A., Leslie-Pelecky, D. and Labhasetwar, V. (2004). "Solid-state solubility influences encapsulation and release of hydrophobic drugs from PLGA/PLA nanoparticles." Journal of Pharmaceutical Sciences **93**: 1804-1814.

Parness, J. and Horwitz, S. B. (1981). "Taxol binds to polymerized tubulin in vitro." The Journal of Cell Biology **91**: 479-487.

Partridge, A. H., Avorn, J., Wang, P. S. and Winer, E. P. (2002). "Adherence to therapy with oral antineoplastic agents." Journal of the National Cancer Institute **94**: 652-661.

Patton, J. (2008). "Increased use of oral chemotherapy drugs spurs increased attention to patient compliance." Journal of Oncology Practice **4**: 175-177.

Peetla, C. and Labhasetwar, V. (2009). "Effect of molecular structure of cationic surfactants on biophysical interactions of surfactant-modified nanoparticles with a model membrane and cellular uptake." Langmuir **25**: 2369-2377.

Peltier, S., Oger, J.-M., Lagarce, F., Couet, W. and Benoît, J.-P. (2006). "Enhanced oral paclitaxel bioavailability after administration of paclitaxel-loaded lipid nanocapsules." Pharmaceutical Research **23**: 1243-1250.

Pillai, O., Dhanikula, A. B. and Panchagnula, R. (2001). "Drug delivery: An odyssey of 100 years." Current Opinion in Chemical Biology **5**: 439-446.

Plumb, J. A., Milroy, R. & Kaye, S.B. (1990). "The activity of verapamil as a resistance modifier *in vitro* in drug resistant human tumour cell lines is not stereospecific." Biochemical Pharmacology **39**: 787-792.

Pubchem. (2009). "Paclitaxel - substance summary." Retrieved 30 Dec, 2009, from

http://pubchem.ncbi.nlm.nih.gov/summary/summary.cgi?sid=7847557.

Rehm, S. (1990). "Chemically induced mammary gland adenomyoepitheliomas and myoepithelial carcinomas of mice. Immunohistochemical and ultrastructural features " American Journal of Pathology **136**: 575-584.

Renn, J. (2005). "Einstein's invention of Brownian motion." Annalen der Physik **14**: 23-37.

Romsicki, Y. and Sharom, F. J. (1999). "The membrane lipid environment modulates drug interactions with the P-glycoprotein multidrug transporters." Biochemistry **38**: 6887-6896.

Rosenthal, S. J., Tomlinson, I., Adkins, E. M., Schroeter, S., Adams, S., Swafford, L., McBride, J., Wang, Y., DeFelice, L. J. and Blakely, R. D. (2002). "Targeting cell surface receptors with ligand-conjugated nanocrystals." Journal of the American Chemical Society **124**: 4586-4594.

Rowinsky, E. K., Cazenave, L. A. and Donehower, R. C. (1990). "Taxol: A novel investigational antimicrotubule agent." JNCI Journal of the National Cancer Institute **82**: 1247-1259.

Roy, S. N. and Horwitz, S. B. (1985). "A phosphoglycoprotein associated with Taxol resistance in J774.2 cells." Cancer Research **45**: 3856-3863.

Saez, A., Guzman, M., Molpeceres, J. and Aberturas, M. R. (2000). "Freeze-drying of polycaprolactone and poly(-lactic-glycolic) nanoparticles induce minor particle size changes affecting the oral pharmacokinetics

of loaded drugs." European Journal of Pharmaceutics & Biopharmaceutics **50**: 379-387.

Sahana, D., Mittal, G., Bhardwaj, V. and Kumar, M. N. V. R. (2008). "PLGA nanoparticles for oral administration of hydrophobic drugs: Influence of organic solvent on nanoparticle formation and release behavior in vitro and in vivo using estradiol as a model drug." Journal of Pharmaceutical Sciences **97**: 1530-1542.

Sakuma, S., Hayashi, M. and Akashi, M. (2001). "Design of nanoparticles composed of graft copolymers for oral peptide delivery." Advanced Drug Delivery Reviews **47**: 21-37.

Schaffer, W. and Terminology Committee Chair Tissue Culture, A. (1990). "Terminology associated with cell, tissue and organ culture, molecular biology and molecular genetics." In Vitro Cellular & Developmental Biology - Plant **26**: 97-101.

Scheffel, U., Rhodes, B. A., Natarajan, T. K. and Wagner(Jr.), H. N. (1973). "Albumin Microspheres for Study of the Reticuloendothelial System " Journal of Nuclear Medicine **13**: 498-503.

Schiff, P. B., Fant, J. and Horwitz, S. B. (1979). "Promotion of microtubule assembly in vitro by taxol." Nature **277**: 665-667.

Schiff, P. B. and Horwitz, S. B. (1980). "Taxol stabilizes microtubules in mouse fibroblast cells." Proceedings of the National Academy of Sciences of the United States of America **77**: 1561-1565.

Schnitzer, J. E. (1992). "gp60 is an albumin-binding glycoprotein expressed by continuous endothelium involved in albumin transcytosis." AJP - Heart and Circulatory Physiology **262**: H246-254.

Singh, A. T., Jaggi, M., Khattar, D., Awasthi, A., Mishra, S. K., Tyagi, S. and Burman, A. C. (2008). "A novel nanopolymer based tumor targeted delivery system for paclitaxel." ASCO Meeting Abstracts **26**: 11095.

Skipper, H. E., Schabel Jr, F. M. and Wilcox, W. S. (1964). "Experimental evaluation of potential anti-cancer agents. XIII. On the criteria and kinetics associated with 'curability' of experimental leukemia." Cancer Chemotherapy Reports **35**: 1-111.

Smoluchowski, M. v. (1906). "Zur kinetischen Theorie der Brownschen Molekularbewegung und der Suspensionen." Annalen der Physik **326**: 756-780.

Soepenberg, O., Sparreboom, A., de Jonge, M. J. A., Planting, A. S. T., de Heus, G., Loos, W. J., Hartman, C. M., Bowden, C. and Verweij, J. (2004). "Real-time pharmacokinetics guiding clinical decisions: phase I study of a weekly schedule of liposome encapsulated paclitaxel in patients with solid tumours." European Journal of Cancer **40**: 681-688.

Soma, C. E., Dubernet, C., Barratt, G., Nemati, F., Appel, M., Benita, S. and Couvreur, P. (1999). "Ability of doxorubicin-loaded nanoparticles to overcome multidrug resistance of tumor cells after their capture by macrophages." Pharmaceutical Research **16**: 1710-1716.

Sparreboom, A., van Asperen, J., Mayer, U., Schinkel, A. H., Smit, J. W., Meijer, D. K. F., Borst, P., Nooijen, W. J., Beijnen, J. H. and van Tellingen, O. (1997). "Limited oral bioavailability and active epithelial excretion of paclitaxel (Taxol) caused by P-glycoprotein in the intestine." Proceedings of the National Academy of Sciences of the United States of America **94**: 2031-2035.

Strachan, E. B. (1981). "Case report--suspected anaphylactic reaction to Cremophor EL." Society for the Advancement of Anaesthesia in Dentistry (Great Britain) SAAD digest **4**: 209.

Tarr, B. D. and Yalkowsky, S. H. (1987). "A new parenteral vehicle for the administration of some poorly water soluble anti-cancer drugs." Journal of Parenteral Science & Technology **41**: 31.

Thierry, A. R., Vige, D., Coughlin, S. S., Belli, J. A., Dritschilo, A. and Rahman, A. (1993). "Modulation of doxorubicin resistance in multidrug-resistant cells by liposomes." The FASEB Journal **7**: 572-579.

Thompson, H. J. (2000). Methods for the induction of mammary carcinogenesis in the rat using either 7,12 dimethyl-benz[α]anthracene or 1-methyl-1-nitrosourea. Methods in mammary gland biology and breast cancer research Eds. M. M. Ip and B. B. Asch. New York, Kluwer Academic**:** 19-29.

Tiwari, S. B. and Amiji, M. M. (2006). "Improved oral delivery of paclitaxel following administration in nanoemulsion formulations." Journal of Nanoscience and Nanotechnology **6**: 3215-21.

Treat, J. A., Huang, C., Damjanov, N., Walker, S., Drobins, P., Gokhale, P., Kopreski, M., Massimini, G. and Rahman, A. (2000). "Phase I trial in advanced malignancies with Liposome Encapsulated Paclitaxel (LEP)." Lung Cancer **29**: 64-688.

Valle, J., Armstrong, A., Newman, C., Alakhov, V., Pietrzynski, G., Brewer, J., Campbell, S., Corrie, P., Rowinsky, E. and Ranson, M. (In press). "A phase 2 study of SP1049C, doxorubicin in P-glycoprotein-targeting pluronics, in patients with advanced adenocarcinoma of the esophagus and gastroesophageal junction." Investigational New Drugs.

Varma, M. V. S. and Panchagnula, R. (2005). "Enhanced oral paclitaxel absorption with vitamin E-TPGS: Effect on solubility and permeability *in vitro, in situ* and *in vivo*." European Journal of Pharmaceutical Sciences **25**: 445-453.

Vauthier, C. and Bouchemal, K. (2009). "Methods for the preparation and manufacture of polymeric nanoparticles." Pharmaceutical Research **26**: 1025-1058.

Verdière, A. C. d., Dubernet, C., Némati, F., Soma, E., Appel, M., Ferté, J., Bernard, S., Puisieux, F. and Couvreur, P. (1997). "Reversion of multidrug resistance with polyalkylcyanoacrylate nanoparticles: towards a mechanism of action." British Journal of Cancer **76**: 198–205.

Verwey, E. J. W. (1947). "Theory of the stability of lyophobic colloids." The Journal of Physical and Colloid Chemistry **51**: 631-636.

Visscher, G. E., Robison, R. L., Maulding, H. V., Fong, J. W., Pearson, J. E. and Argentieri, G. J. (1985). "Biodegradation of and tissue reaction to 50:50 poly(DL-lactide-co-glycolide) microcapsules." Journal of Biomedical Materials Research **19**: 349-365.

Walter, K. A., Cahan, M. A., Gur, A., Tyler, B., Hilton, J., Colvin, O. M., Burger, P. C., Domb, A. and Brem, H. (1994). "Interstitial Taxol delivered from a biodegradable polymer implant against experimental malignant glioma." Cancer Research **54**: 2207-2212.

Wani, M. C., Taylor, H. L., Wall, M. E., Coggon, P. and McPhail, A. T. (1971). "Plant antitumor agents. VI. Isolation and structure of taxol, a novel antileukemic and antitumor agent from *Taxus brevifolia*." Journal of the American Chemical Society **93**: 2325-2327.

Warren, L., Jardillier, J.-C., Malarska, A. and Akeli, M.-G. (1992). "Increased accumulation of drugs in multidrug-resistant cells induced by liposomes." Cancer Research **52**: 3241-3245.

Waugh, W. N., Trissel, L. A. and Stella, V. J. (1991). "Stability, compatibility, and plasticizer extraction of taxol (NSC-125973) injection diluted in infusion solutions and stored in various containers." American Journal of Health-System Pharmacy **48**: 1520-1524.

Weingart, S. N., Brown, E., Bach, P. B., Eng, K., Johnson, S. A., Kuzel, T. M., Langbaum, T. S., Leedy, D., Muller, R. J., Newcomer, L. N., O'Brien, S., Reinke, D., Rubino, M., Saltz, L. and Walters, R. S. (2008). "NCCN task force report: Oral chemotherapy." Journal of the National Comprehensive Cancer Network Task Force **6 (Supplement 3)**.

Weir, N., Buchanan, F., Orr, J. and Dickson, G. (2004). "Degradation of poly-L-lactide. Part 1: in vitro and in vivo physiological temperature degradation." Proceedings of the Institution of Mechanical Engineers, Part H: Journal of Engineering in Medicine **218**: 307-319.

Weiss, R. B., Donehower, R. C., Wiernik, P. H., Ohnuma, T., Gralla, R. J., Trump, D. L., Baker, J. R., Jr., Van Echo, D. A., Von Hoff, D. D. and Leyland-Jones, B. (1990). "Hypersensitivity reactions from taxol." Journal of Clinical Oncology **8**: 1263-1268.

Welsch, C. W. (1985). "Host factors affecting the growth of carcinogen-induced rat mammary carcinomas: A review and tribute to Charles Brenton Huggins." Cancer Research **45**: 3415-3443.

Wiernik, P. H., Schwartz, E. L. and Strauman, J. J. (1987). "Phase I clinical and pharmacokinetic study of taxol." Cancer Research **47**: 2486-2493.

Winternitz, C. I., Jackson, J. K., Oktaba, A. M. and Burt, H. M. (1996). "Development of a polymeric surgical paste formulation for Taxol." Pharmaceutical Research **13**: 368-375.

Wong, H. L., Bendayan, R., Rauth, A. M., Xue, H. Y., Babakhanian, K. and Wu, X. Y. (2006). "A mechanistic study of enhanced doxorubicin uptake and retention in multidrug resistant breast cancer cells using a polymer-lipid hybrid nanoparticle system." Journal of Pharmacology and Experimental Therapeutics **317**: 1372-1381.

Woo, D. D. L., Jr, A. P. T. and Wang, C. J. N. (1997). "Microtubule active taxanes inhibit polycystic kidney disease progression in cpk mice." Kidney International **51**: 1613-1618.

Woo, J. S., Lee, C. H., Shim, C. K. and Hwang, S.-J. (2003). "Enhanced oral bioavailability of paclitaxel by coadministration of the P-glycoprotein inhibitor KR30031." Pharmaceutical Research **20**: 24-30.

Yang, S., Gursoy, R. N., Lambert, G. and Benita, S. (2004). "Enhanced oral absorption of paclitaxel in a novel self-microemulsifying drug delivery system with or without concomitant use of P-glycoprotein inhibitors." Pharmaceutical Research **21**: 261-270.

Zhang, B., Maiti, A., Shively, S., Lakhani, F., McDonald-Jones, G., Bruce, J., Lee, E. B., Xie, S. X., Joyce, S., Li, C., Toleikis, P. M., Lee, V. M. Y. and Trojanowski, J. Q. (2005). "Microtubule-binding drugs offset tau sequestration by stabilizing microtubules and reversing fast axonal transport deficits in a tauopathy model." Proceedings of the National Academy of Sciences of the United States of America **102**: 227-231.

Zhang, X., Jackson, J. K., Wong, W., Min, W., Cruz, T., Hunter, W. L. and Burt, H. M. (1996). "Development of biodegradable polymeric paste

formulations for taxol: An *in vitro* and *in vivo* study." International Journal of Pharmaceutics **137**: 199-208.

Zhang, Z. and Feng, S.-S. (2006). "The drug encapsulation efficiency, in vitro drug release, cellular uptake and cytotoxicity of paclitaxel-loaded poly(lactide)-tocopheryl polyethylene glycol succinate nanoparticles." Biomaterials **27**: 4025-4033.

Appendices

Appendix A.   Theory of Brownian motion

In 1827, Robert Brown, a botanist described the random movement of pollen grains in water when viewed under the microscope. It is a result of the imbalance of forces acting on the dispersed molecule due to the collisions with the molecules of the medium. This random movement was termed the "Brownian motion" and was explained mathematically in the beginning of 20th century (Einstein 1905; Smoluchowski 1906). Interestingly, Brownian motion contributes to both aggregation and separation of the particles.

Though the other two major theories of Einstein- quantum mechanics and relativity were quickly picked up and became immediate hits, the work of colloidal stability is turning out to be equally important and today explains a wide range of phenomena ranging from population genetics to economics theories on movement of stocks. Einstein correctly believed that micrometer-sized particles are both big enough to be viewed under the optical microscope and small enough that their Brownian motion keeps them suspended indefinitely against gravity. He argued under the commonly held view at that time that thermodynamic considerations do not apply and can not explain the behaviour of suspended particles.

According to his assumption, n particles of arbitrary volume v suspended in a solvent at small number density $n \ll v^{-1}$ represent an ideal gas and thereby exert an osmotic pressure p. This force was postulated to be existing even without the presence of any physical semi-permeable membrane (a prerequisite as per definition of osmotic pressure). As a result these particles exert, a howsoever small, thermodynamic force on the walls of the container. Mathematically,

$$p = nk_BT \text{ (in modern notation)}$$

$$\text{where } k_B = R/N_0$$

The concept of Boltzmann constant (k_B) had not been established at that time; R is the gas constant and N_0 is Avogadro number.

This force was postulated to be in a dynamic equilibrium with a position-related force. Thus, in presence of this 'constant volume force' **K** acting on the particles, an isothermal force balance exists at equilibrium, which can be denoted by

$$\nabla p(\boldsymbol{r}) + n(\boldsymbol{r})\boldsymbol{K} = 0$$

$$\text{or } p(\boldsymbol{r}) = k_BTn(\boldsymbol{r})$$

$$\text{where } k_BTn(\boldsymbol{r}) \propto \exp(-\boldsymbol{K}\cdot\boldsymbol{r}/k_BT)$$

The most notable interpretation of this equation is that the force acting on the individual particles is related to the bulk (colligative) property of osmotic pressure (Renn 2005).

Further, Einstein combined this 'stationary balance' with a 'dynamic equilibrium' existing between a diffusion component $-D\nabla n$ and a drift component $n\boldsymbol{K}/\zeta$ (derived by Stokes' law for flow of small particles in a liquid). Here ζ is the coefficient of friction and D *is* the coefficient of diffusion of the Brownian particles in the solvent.

Combining the relation between balance of forces and that between diffusion and viscous drag, the Stokes–Einstein relation is derived

$$D \propto k_BT/\zeta$$

$$\text{or } D \propto RT/rN_0\zeta$$

Most interestingly, this relation established a connection between the macroscopic kinetic coefficients D and ζ to the microscopic, molecular phenomena (Frey and Kroy 2005).

Appendix B. Interfacial forces

In mixtures of differing states of matter, the generated interface creates many phenomena under the so called interfacial forces. While covalent bonds also give rise to certain forces that are rather strong in magnitude (usually more than 40 kJ/mol and typically between 300 and 700 kJ/mol), they are limited to distances over a few bond lengths. In comparison, the interfacial forces are weaker but active over long ranges. These forces are broadly classified as (i) Coulombic and (ii) van der Waals interactions. The former arise due to the accumulation of charge on a surface due to ionization. Depending on the charges, the interaction can be attractive or repulsive. Like charges will result in repulsion and opposites will attract.

A surface (including that of a particle) in a liquid may get charged due to the dissociation of chemical groups or by adsorption of charged moieties from the solution. As a result, a wall surface potential is developed. These ions then attract oppositely charged ions which balance the wall surface charge. These loci of counter ions create an electrical double layer composed of two slightly varying potentials. Ions in immediate vicinity of the charged wall surface are held strongly giving rise to the Stern or Helmholtz layer. The outer region composed of comparatively loosely held ions is called the diffuse layer. However, these potentials are not exactly the same and there is always some shielding of the wall surface charge, and is proportional to the distance from the particle surface (Figure Apx B.1). It should be noted here that the intensity of the electrostatic forces falls exponentially as a function of the distance separating the interacting surfaces. This has implication in the balancing of forces that depend differently on the distance where one might be dominant over a given range only.

The van der Waals interactions arise due to the imbalance of charge across

the structure of molecules and are of three types: (a) dipole, (b) induced dipole, and (c) induced dipole-induced dipole or Dispersion (or London, after Fritz London) forces.
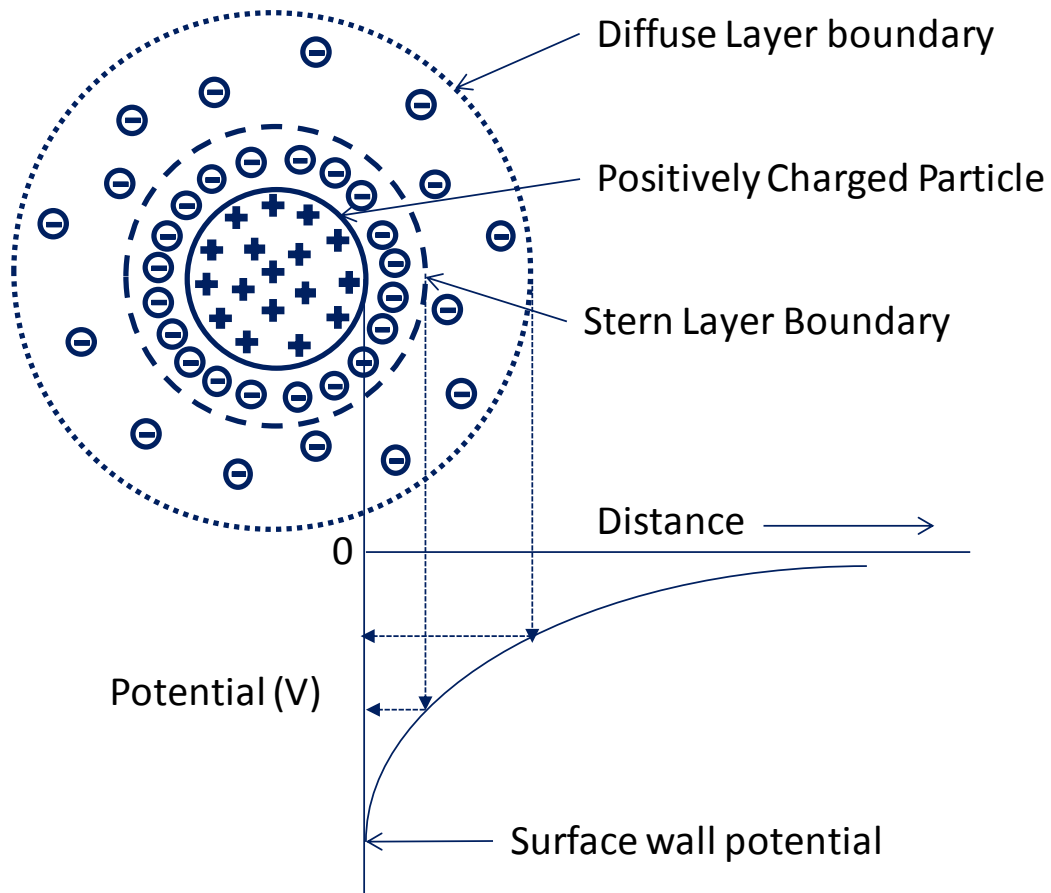
Figure Apx B.1: Surface charge distribution around a charged particle

Asymmetric distribution of electron clouds around a molecule results in a sustained directional bias of charge. For example in a water molecule, the strongly electronegative oxygen atom leaves a slight positive charge on the hydrogen atoms creating a *dipole* that makes the molecule act as if it was composed of bar magnets. Hydrogen bonding is a result of such dipole moments and is typically of the order of 10-40 kJ/mol. However, all molecules that bear strong electronegative centres do not exhibit dipoles, but that is due to a directional neutralization of opposing dipole moments

(example carbon dioxide). If such molecules come in influence of dipole moments from a molecule bearing permanent dipoles, the existing equilibrium is disturbed and then a dipole will be induced in them also (*induced dipole*). The effect of dipole moment and van der Waals interactions in general on colloids can be imagined from the fact that water, which has strong hydrogen bonding exhibits a considerably higher melting point and boiling point compared to those that do not show hydrogen bonding. The third type—*induced dipole-induced dipole* interactions are comparatively weaker forces. As such there is no actual persisting dipole moment in the non-polar molecules. However, the movement of electrons around the atoms or their bonds creates transient polarization of charges. Naturally, the resulting dipole strength is much weaker than the dipole or induced dipole. However, the combined strength of these interactions is much greater and their contribution to total interaction energy most significant in non-polar compounds. The London forces are typically of the energy range of 1 kJ/mol and exert their effect to quite long range, sometimes up to 10 nm (Buckton 1995).

The intensity of forces from van der Waals interactions fall proportionally to the square of the distance between interacting surfaces.

Appendix C.DLVO theory

The phenomena responsible for stability of colloids are explained by the DLVO theory named after Boris Vladimirovich *D*erjaguin, Lev Davidovich *L*andau, Evert Johannes Willem *V*erwey, and Theo *O*verbeek (Derjaguin and Landau 1941; Verwey 1947). Dispersions are mixtures in which the free energy of the system is increased and the stability of such colloids depends on the imbalance of the attractive and repulsive forces towards the latter (Derjaguin 1993). At short distances between particles, attraction forces promote aggregation, and may even lead to coalescence. However, at still shorter range, the repulsion forces become dominant and oppose aggregation. The attractive forces arise from van der Waals interactions. These attraction forces are countered by repulsive forces arising due to the double layer.

This theory is the summation of the interfacial forces; resulting (usually) in net attractive forces (negative energies) at small and large distances of separation and net repulsive forces (positive energies) at intermediate ranges (Figure Apx C.1). This general statement is amenable to influence by the magnitude of the forces and is the basis of interventions to control the stability of suspensions. As shown in Figure Apx C.2, this is achieved by attaining a net attraction beyond a particular distance that is reflected by a secondary energy minima (Buckton 1995).

The surface free energy is directly proportional to the surface area. Since reduction in size of internal phase in a non-miscible biphasic system is associated with increase in specific surface area, the interfacial tension increases. To decrease the interfacial tension and surface free energy, the individual globules of an emulsion or particles of a suspension try to agglomerate. However, the thermodynamic instability in emulsions is higher

than the suspensions. Another important difference is that in suspensions, it may be desirable to have the particles clump together (loosely); but in emulsions, the globules should be kept separate.
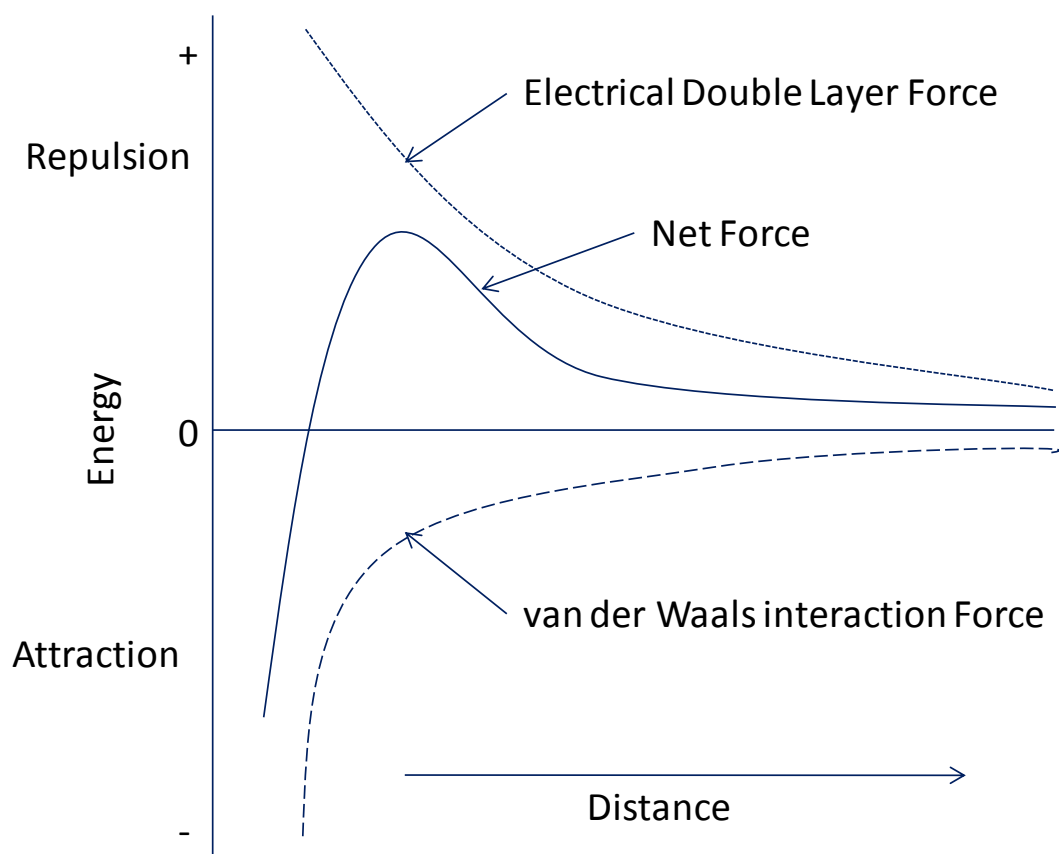
Figure Apx C.1: Interfacial forces acting between particles as a function of separating distance

As per the DLVO theory, to maintain the system in dispersed state, the particles have to be kept sufficiently separated, failing which they will agglomerate. This can be achieved by either increasing the repulsion between the particles or globules (by increasing the surface charge) or by introducing a physical means to prevent the particles from coming too close (steric stabilization). For colloids, since all the particles are expected to be of same type, the result of a charged surface is Coulombic repulsion between the particles.
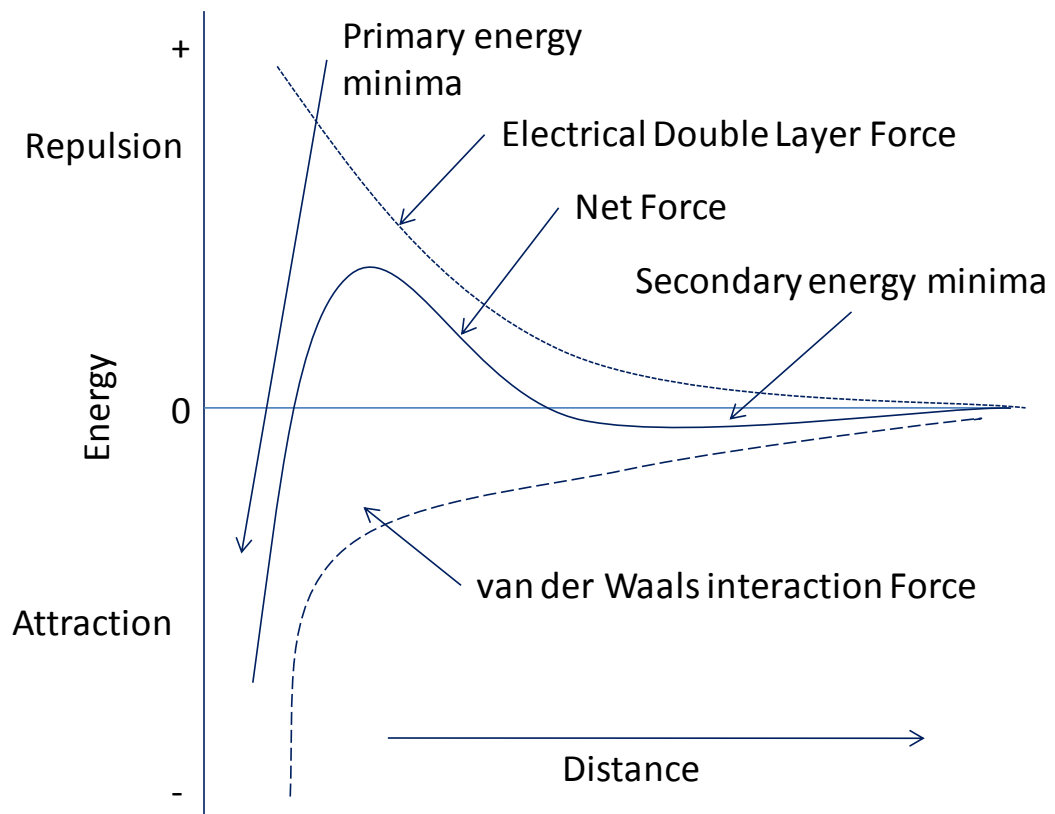
Figure Apx C.2: Interfacial forces acting between particles in solution of high salt concentration

As mentioned earlier, for the stability of suspensions, it is the secondary minima that is of primary interest. It causes a net feeble attraction between the particles that makes them flocculate. The flocculated suspension is easy to disperse and also prevents dense caking which is a much more undesirable instability. Caking in unflocculated suspensions is slower, but the resulting slug is difficult to disperse.

Appendix D.   Zetasizer theory and settings

Table Apx D.1: Measurement settings for zetasizer

Parameter	Value/Specification
Material (type)	Polystyrene latex
Dispersant	Water
Temperature	25°C
Equilibration time	1 min
Cumulants fit	single exponential
Number of runs per measurements	automatic
Time per measurement	automatic
Dilution	none for Nano-ZS and with distilled water q.s. to bring kilo counts per second (kcps) to between 250-500 for Mastersizer (Malvern, UK).

The instrument images the position of particles of a colloidal dispersion using a laser beam by collecting the signal from diffracted light. This image is then compared with a second image after a very small time interval. Since the particles are in constant motion due to the Brownian motion, there is a certain element of dissimilarity in the two images. Such images are taken and analyzed till the similarity decreases from an initial score of 1 (perfect similarity) to 0 (no similarity). The correlation so obtained takes a sigmoidal shape on log scale of time (Figure Apx D.1). Due to their relatively slower motion, bigger particles take longer than the small particles to reach the state of high randomness. This correlation function (Y axis in Figure Apx D.1) is fitted in either single or multiple exponentials (depending on whether samples consists of single peak or multiple narrow peaks, respectively) to calculate the average particle size and width of particle size distribution by cumulants analysis. The raw data obtained is size distribution plot based on light intensity. It can then be converted to size distribution based on volume by using refractive index as per Mie theory.
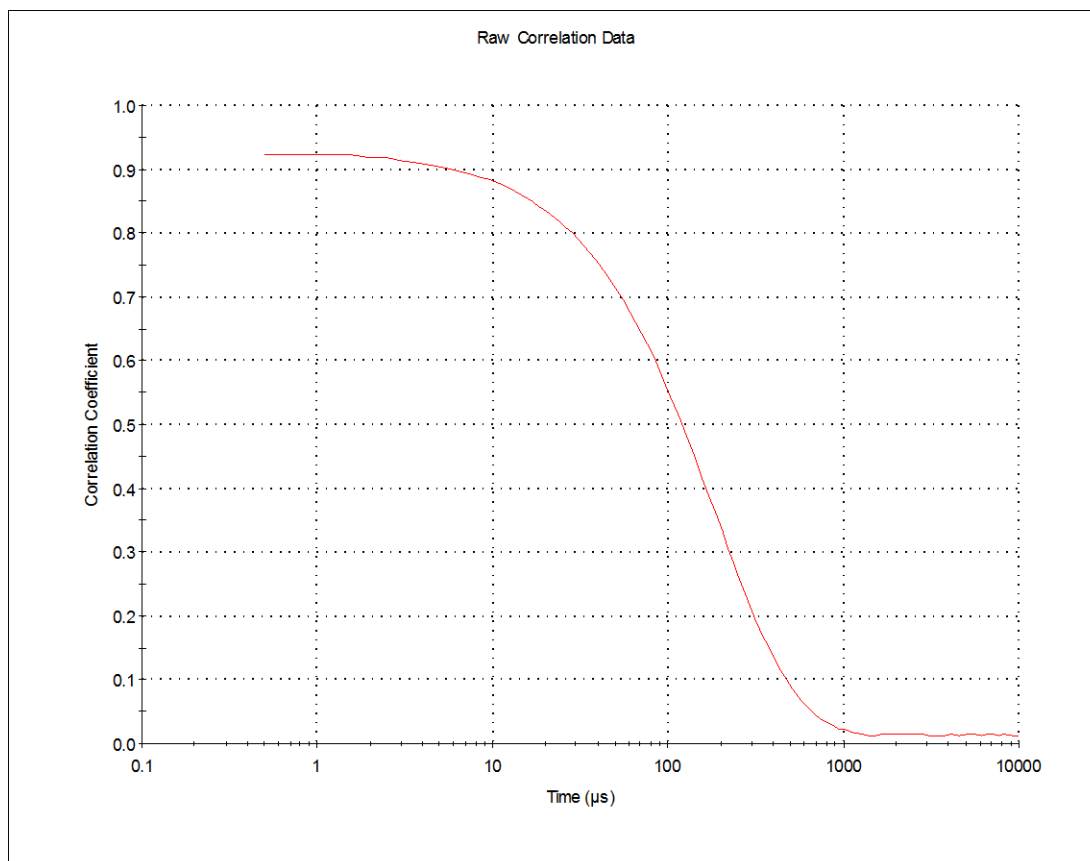
Figure Apx D.1: Sample Correlogram

Note on particle size:

The size mentioned in the thesis refers to z-average size calculated from the hydrodynamic diameter as measured by the DLS. The hydrodynamic diameter is defined as "the size of a hypothetical hard sphere that diffuses in the same fashion as that of the particle being measured". Molecules can however assume any shape in solution/suspension, these shapes can keep presenting different faces due to free rotation (dynamic property) and will always exhibit a weak association with solvent (water in most cases). Thus the size estimation based on diffusion of these molecules represents an apparent size rather than actual one and is referred to as the hydrodynamic diameter. The z-average size is a number used for quality control purposes, and the sample itself is composed of particles of various sizes. It can give a

174

credible indication of particle size only when the sample is monomodal, particles and spherical and are monodisperse.

Note on PDI:

The particle size distribution is represented by polydispersity index (PDI), which is an arbitrary scale from 0 (monodisperse sample) to 1 (high polydispersity). The value of PDI is calculated mathematically from the cumulants analysis as described in the ISO standard document 13321:1996 E and 22412.

For drug delivery systems, a PDI under 0.2 is desirable.
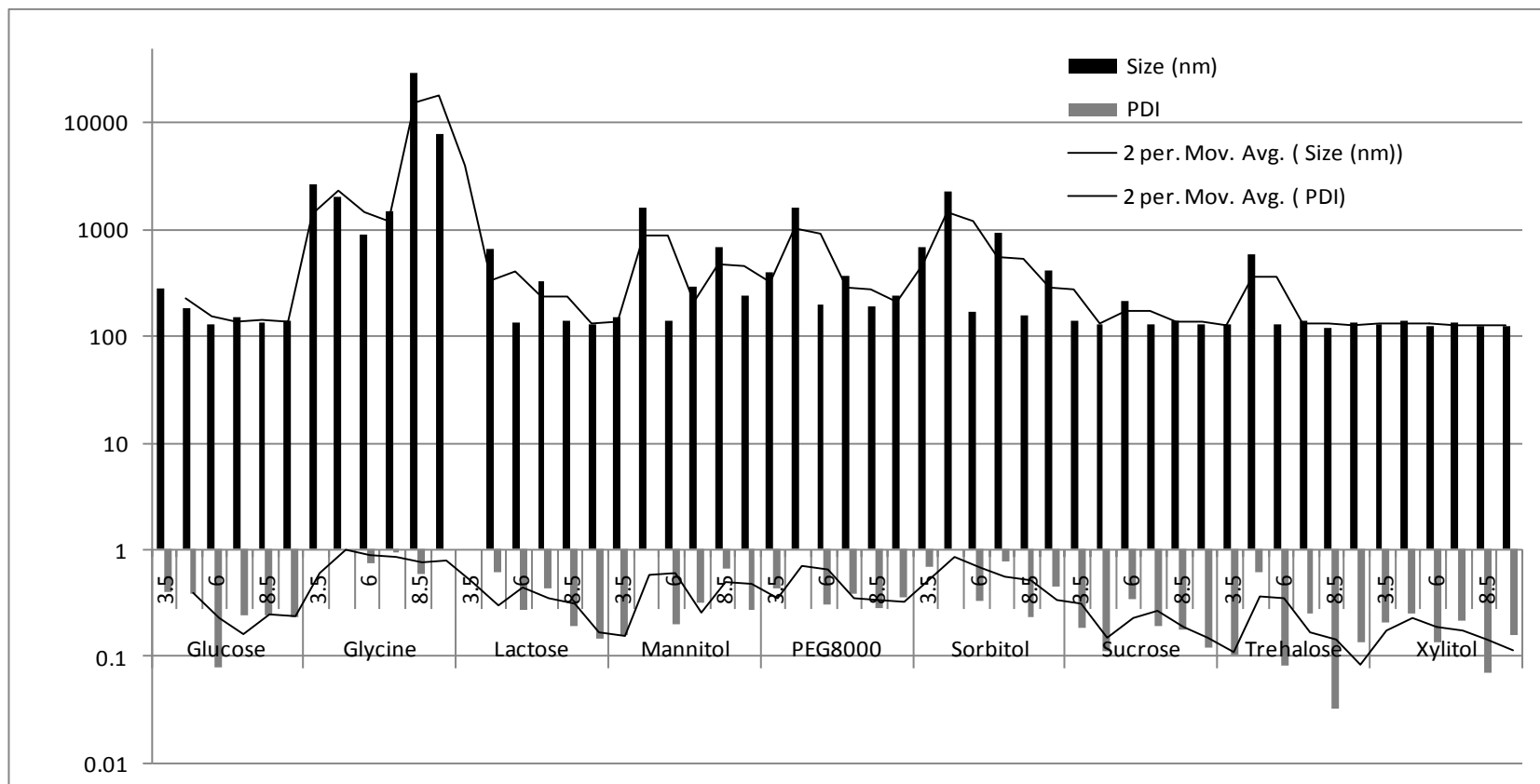
Figure Apx E.1: Particle size of freeze-dried nanoparticles (experiment 3) plotted against percentage of total solid content
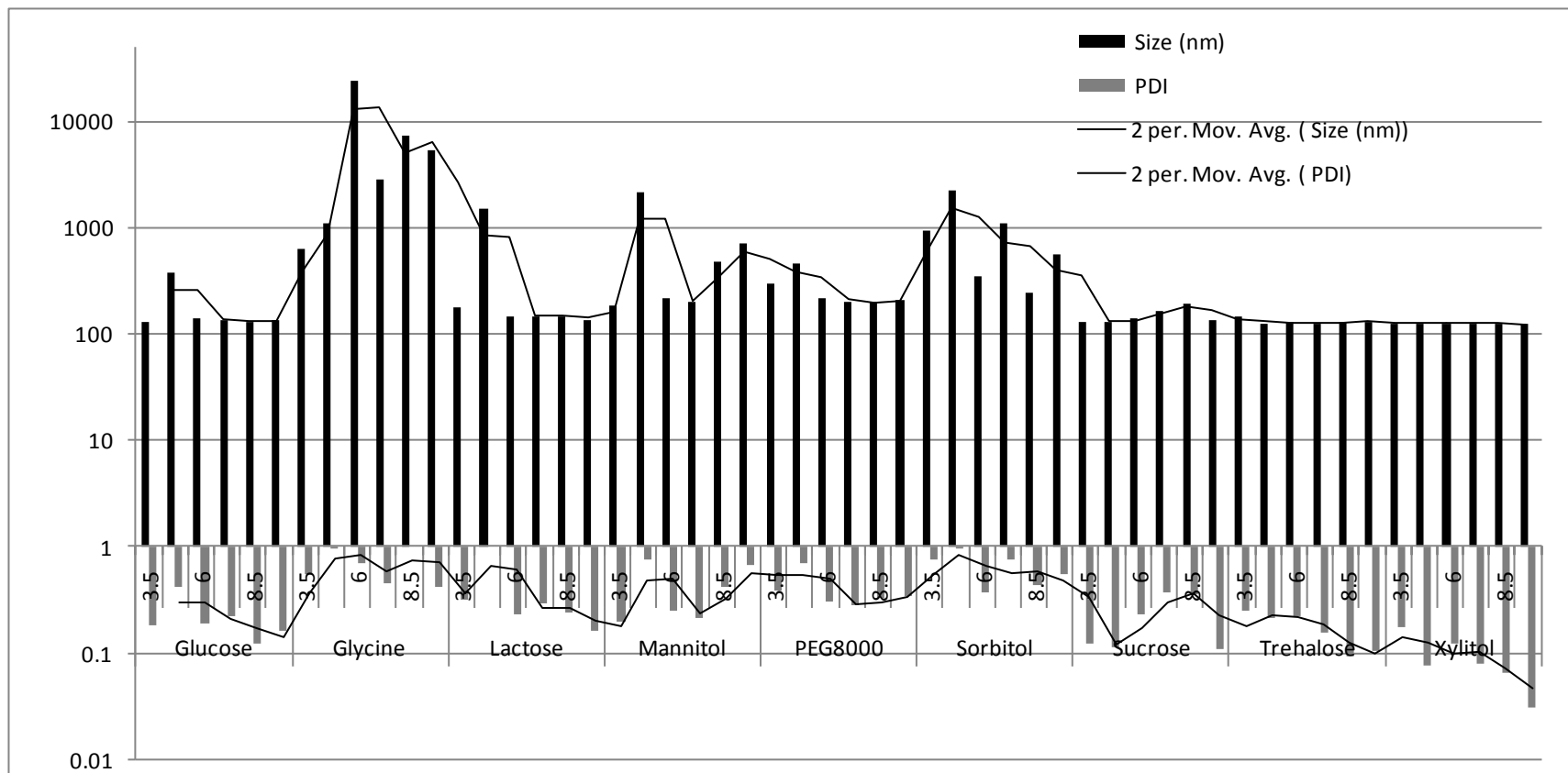
Figure Apx E.2: Particle size of freeze-dried nanoparticles (experiment 4) plotted against percentage of total solid content

Appendix F. Calculations of AlamarBlue® assay

The absorbance is read at 600 nm for the oxidized form and at 570 nm for the reduced form. However, there is a significant degree of overlap in the absorption spectra of these two forms. For this reason, the quantitative estimation is carried out by incorporating the molar absorptivity coefficients (ε) in the calculations. The absorption can be defined, as per Beer-Lambert's law as the product of molar absorptivity coefficient, concentration (C) and path length (l). Since all the measurements are made in the same instrumental set up using similar cell culture plates, the effect of path length is normalized.

The absorption at 570 nm can hence be expressed as

$$A_{570} = C_{RZR}.\varepsilon_{570}^{RZR} + C_{RRF}.\varepsilon_{570}^{RRF}$$

And at 600 nm as

$$A_{600} = C_{RZR}.\varepsilon_{600}^{RZR} + C_{RRF}.\varepsilon_{600}^{RRF}$$

Where

C_{RZR} = Concentration of resazurin (oxidized form)

C_{RZR} = Concentration of resorufin (reduced form)

ε_{570}^{RZR} = Molar absorptivity coefficient for resazurin (oxidized form) at 570 nm

ε_{570}^{RRF} = Molar absorptivity coefficient for resorufin (reduced form) at 570 nm

ε_{600}^{RZR} = Molar absorptivity coefficient for resazurin (oxidized form) at 600 nm

ε_{600}^{RRF} = Molar absorptivity coefficient for resorufin (reduced form) at 600 nm

Solving the two equations, we can find the concentrations of the oxidized and reduced forms.

$$C_{RZR} = \frac{(A_{600}.\varepsilon_{570}^{RRF}) - (A_{570}.\varepsilon_{600}^{RRF})}{(\varepsilon_{600}^{RZR}.\varepsilon_{570}^{RRF}) - (\varepsilon_{570}^{RZR}.\varepsilon_{600}^{RRF})}$$

$$C_{RRF} = \frac{(A_{570}.\mathcal{E}_{600}^{RZR}) - (A_{600}.\mathcal{E}_{570}^{RZR})}{(\mathcal{E}_{600}^{RZR}.\mathcal{E}_{570}^{RRF}) - (\mathcal{E}_{570}^{RZR}.\mathcal{E}_{600}^{RRF})}$$

Estimation of Cell proliferation

The metabolic activity can be defined as the percent reduction of RZR to RRF, and it has to be compared against a negative control (a control set up that doesn't have the converting system like cells). Then

% reduction of alamar blue or RZR = $\frac{C_{RRF}^{test}}{C_{RZR}^{negative\ control}} \times 100$

% Cell Proliferation = $\frac{(A_{570}^{test}.\mathcal{E}_{600}^{RZR}) - (A_{600}^{test}.\mathcal{E}_{570}^{RZR})}{(A_{600}^{negative\ control}.\mathcal{E}_{570}^{RRF}) - (A_{570}^{negative\ control}.\mathcal{E}_{600}^{RRF})} \times 100$

where

C_{RRF}^{test} = concentration of resorufin in wells containing cells

$C_{RZR}^{negative\ control}$ = concentration of resazurin in control well without cells

A_{570}^{test} = absorbance at 570 nm of wells containing the cells

$A_{570}^{negative\ control}$ = average absorbance at 570 nm of control wells without cells

Estimation of cytotoxicity

Similarly, the percentage relative difference in reduction between test substance and growth control can be calculated as

$$\frac{(fraction\ reduced\ in\ control\ cell - fraction\ reduced\ in\ sample\ cell)}{fraction\ reduced\ in\ control\ cell} \times 100$$

or % relative difference in growth = $\dfrac{\left(\dfrac{C_{RRF}^{growth\ control}}{C_{RZR}^{negative\ control}}\right) - \left(\dfrac{C_{RRF}^{sample}}{C_{RZR}^{negative\ control}}\right)}{\dfrac{C_{RRF}^{growth\ control}}{C_{RZR}^{negative\ control}}} \times 100$

where

$C_{RRF}^{growth\ control}$ = concentration of resorufin in positive control wells containing cells but no test substance (representing maximum reduction).

C_{RRF}^{sample} = concentration of resorufin in wells containing cells and the test substance.

The expression can be derived to

$$= \frac{(\varepsilon_{570}^{RZR}.(A_{600}^{growth\ control} - A_{600}^{sample})) - (\varepsilon_{600}^{RZR}.(A_{570}^{growth\ control} - A_{570}^{sample}))}{\left(A_{600}^{sample}.\varepsilon_{570}^{RZR}\right) - (A_{570}^{sample}.\varepsilon_{600}^{RZR})} \times 100$$

The molar absorptivity constants used for calculations are mentioned in Table Apx F.1 (Supplier information).

Table Apx F.1: Molar absorptivity constants of AlamarBlue® assay

molar extinction coefficient of oxidized AlamarBlue® at 570nm	80586
molar extinction coefficient of oxidized AlamarBlue® at 600nm	117216
molar extinction coefficient (E) of reduced AlamarBlue® at 570nm	155677
molar extinction coefficient (E) of reduced AlamarBlue® at 600nm	14652

Appendix G.   Publications from the thesis

1. Bhardwaj V., Plumb J., Cassidy J., & Ravi Kumar M.N.V. "Evaluating the potential of polymer nanoparticles for oral delivery of paclitaxel in drug resistant cancer." Cancer Nanotechnology (In press)

ABSTRACT:

The present study was designed to explore the ability of polymeric nanoparticles to restore drug sensitivity to P-glycoprotein over-expressing cancer cells. A multidrug-resistant cell line 2780 AD and its sensitive parent cell line A2780 were studied in cell culture and as a xenografted tumour model. Paclitaxel was incorporated in poly(lactide-co-glycolide) nanoparticles of average diameter 125 nm stabilised by a positively charged surfactant. The nanoparticulate formulation was shown to be about sevenfold more potent than free paclitaxel against cell line A2780 and the poly(lactic-co-glycolic acid)(PLGA) nanoparticles alone were nontoxic to the cells at the concentrations required to deliver the drug. Whilst the oral formulation of paclitaxel was not as potent as the free drug in the A2780 xenografts, it showed significant activity against 2780 AD tumours, which are resistant to the maximum tolerated intravenous dose of paclitaxel. The efficacy of orally delivered paclitaxel in this drug-resistant model supports the concept of exploring nanoparticles for improved drug delivery.

2. Bhardwaj, V., Ankola, D., Gupta, S., Schneider, M., Lehr, C. M. and Kumar, MNV. (2009). "PLGA nanoparticles stabilized with cationic surfactant: Safety studies and application in oral delivery of paclitaxel to treat chemical-induced breast cancer in rat." Pharmaceutical Research **26**: 2495-2503

ABSTRACT:

Purpose: This study was carried out to formulate poly(lactide-co-glycolide) (PLGA) nanoparticles using a quaternary ammonium salt didodecyl dimethylammonium bromide (DMAB) and checking their utility to deliver paclitaxel by oral route.

Methods: Particles were prepared by emulsion solvent diffusion evaporation method. DMAB and particles stabilized with it were evaluated by MTT and LDH cytotoxicity assays. Paclitaxel was encapsulated in these nanoparticles and evaluated in a chemical carcinogenesis model in Sprague Dawley rats.

Results: MTT and LDH assays showed the surfactant to be safe to *in vitro* cell cultures at concentrations <33 μM. PLGA nanoparticles prepared using this stabilizer were also found to be non-toxic to cell lines for the duration of the study. When administered orally to rats bearing chemically induced breast cancer, nanoparticles were equally effective/better than intravenous paclitaxel in cremophor EL at 50% lower dose.

Conclusions: This study proves the safety and utility of DMAB in stabilizing preformed polymers like PLGA resulting in nanoparticles. This preliminary data provides a proof of concept of enabling oral chemotherapy by efficacy enhancement for paclitaxel.